OPTIMIZATION OF ULTRASONIC REACTORS FOR BACTERIAL AND ORGANIC MATTER DECAY

by

RANA KIDAK

B. S. in Environmental Engineering, Istanbul Technical University, 1993
M. S. in Environmental Engineering, Marmara University, 1997

Submitted to the Institute of Environmental Sciences
In partial fulfillment of the requirements for the degree of

Doctor of Philosophy

Graduate Program in Environmental Technology
Boğaziçi University
2005

OPTIMIZATION OF ULTRASONIC REACTORS FOR BACTERIAL AND ORGANIC MATTER DECAY

APPROVED BY:

Prof. Dr. Nilsun H. İnce.....
(Thesis Supervisor)

Prof. Dr. Işıl Balcıoğlu.....

Prof. Dr. Ayşen Erdinçler.....

Prof. Dr. Ahmet Mete Saatçi.....

Prof. Dr. Orhan Yenigün.....

DATE OF APPROVAL.....

ACKNOWLEDGMENTS

I would like to express my heartfelt gratitude to my thesis supervisor, Prof. Dr. Nilsun H. Ince, who guided, supported and encouraged me throughout this study. She has not only been a supervisor to me, but a patient and supportive role-model. I acknowledge her help to me in every step of my life during the progress of this dissertation.

I am thankful to my jury members Prof. Dr. Işıl Balcıoğlu, Assoc. Prof. Ayşen Erdinçler, Prof. Dr. Ahmet Mete Saatçi and Prof. Dr. Orhan Yenigün for their valuable criticism.

I would like to thank my friends Yonca Ercümen, Gökçe Tezcanli Güyer, Özgür Aktaş, Işıl Gültekin and Altan Süphandağ for their friendship and help throughout the development of this work.

Last but not least, I am grateful to my mother and father, Şengül Kıdak and Ali Kıdak for their love and support throughout my life.

ABSTRACT

Public concern for the environment has taken on a new prominence with waste management becoming a priority. As a consequence, new and environmental friendly methods for pollutant degradation are vastly investigated. Advanced Oxidation Processes, involving ozonolysis, photolysis, electron beams and ultrasonic irradiation have been identified as viable alternatives to such research. In recent years, chemistry with ultrasound waves has become a method of interest among other Advanced Oxidation Processes, owing to the extreme conditions generated during acoustic cavitation. These extremes are such that water molecules are fragmented into radical species, such as the hydroxyl radical, which is the most powerful chemical oxidant ever known.

The dissertation presented herein is about the investigation of advanced oxidation techniques particularly, ultrasound for the remediation of water contaminated with bacterial and organic constituents. The method of study involved the application of three ultrasonic frequencies under various ambient conditions on infected water samples and synthetic effluents containing phenol and phenolic derivatives. Reactor effluents were monitored for assessing the reduction in bacterial density and phenolic concentration.

The results were evaluated with the aim of optimizing process parameters and determining the reaction kinetics. Moreover, the study with phenol covered comparison of ultrasonic decay with that of ozonolysis and assessing impacts of combined ultrasound, ozone and UV applications.

It was found that the efficiency of bacterial decay under 20 kHz ultrasonic irradiation could be enhanced by the addition of solid catalysts such as activated carbon, metallic zinc, ceramic beads. The reaction kinetics was found to represent that of chemical disinfection with chlorine.

The degradation of phenol was found to proceed with maximum efficiency under 300 kHz irradiation at acidic pH and ultrasound rendered detoxification of water samples

along with phenol degradation, although mineralization was not effective. Combination of ultrasound with ozone and UV irradiation was found to induce synergistic effects as a consequence of the enhancement in the mass transfer rate of ozone and photolysis of ultrasound-induced hydrogen peroxide to generate excess hydroxyl radicals.

ÖZET

Günümüzde çevre koruması, endüstriyel atık yönetimi konusu başta olmak üzere üzerinde en çok durulan konulardan biri haline gelmiştir. Bunun yanı sıra, kirleticilerin zararsız hale getirilmesi konusunda yeni ve çevre dostu yöntemler araştırılmaktadır. Bu amaçla geliştirilen İleri Oksidasyon Prosesleri arasında Ozonlama, Fotoliz, Elektron Işını Prosesi ve Sonoliz sayılabilir. Son yıllarda, diğer İleri Oksidasyon Proseslerinin yanı sıra Ses Ötesi Dalgaların kullanıldığı kimyasal metodlar, akustik kavitasyon sonucu meydana gelen sıradışı çevresel koşullar sebebiyle, dikkate değer bir kullanım olanağı bulmaktadır. Bu sıradışı çevresel koşullar, bilinen en kuvvetli yükseltgeyici olan hidroksil radikalinin oluşmasına sebep olan su moleküllerinin parçalanması durumudur.

Bu doktora tezi çalışmasında bakteriyel olarak veya fenol gibi organik kirleticilerle kirletilmiş olan suların arıtılması konusunda ileri oksidasyon teknikleri ve özellikle Ses Ötesi Dalgalarının kullanım olanakları araştırılmıştır. Çalışmalar sırasında biyolojik olarak kirlenmiş sular ile fenol ve fenol türevlerini içeren sentetik atıksuların farklı ortam şartları altında üç değişik Ses Ötesi frekansındaki arıtılabilirlik uygulamaları incelenmiştir.

Reaktörlerin etkisi bakteri sayısındaki ve fenol konsantrasyonundaki azalma bakımından değerlendirilmiştir. Sonuçlar işletim parametrelerinin optimizasyonu ve reaksiyon kinetiği açısından ele alınmıştır.

Fenolle ilgili olan çalışmalarda Ses Ötesi Dalgalarla sağlanan giderim, ozon verimi ile karşılaştırılmış ve Ses Ötesi Dalgalarının ozon ve UV uygulamaları ile birlikte kullanıldığı durumlar değerlendirilmiştir. 20 kHz frekanslı Ses Ötesi Dalgaları kullanılması durumunda aktif karbon, metalik çinko ve seramik parçacıkları gibi katı katalizörlerin kullanımının bakteriyel giderim verimini artırdığı ve işletim kinetiğinin klorlama kinetiğine benzer bir yapıda olduğu gözlemlenmiştir.

Fenol gideriminde en iyi verim 300 kHz frekanslı Ses Ötesi Dalgalarının asidik pH değerlerinde uygulanması sonucu elde edilmiştir ve mineralizasyon sağlanmamasına rağmen fenol gideriminin yanısıra zehirlilik düzeyinde azalma sonucuna ulaşılmıştır.

Ozonun kütle transferinde artış sağlanması ve Ses Ötesi Dalgaların fotolize uğramış hidrojen peroksitle reaksiyonu sonucunda fazla hidroksil radikali oluşumu sebebiyle, Ses Ötesi dalgalarının ozon ve UV ışınlarıyla beraber kullanımı, fenol gideriminde sinerjistik bir etki göstermektedir.

TABLE OF CONTENTS

LIST OF FIGURES

LIST OF TABLES

1 . INTRODUCTION

Advanced treatment of water and bio-treated effluents to remove pathogenic organisms and refractory organic compounds is of significant challenge to water scientists and environmental engineers. “Advanced Oxidation Processes” (AOP) have recently emerged as potential alternatives to the solution of these problems, owing to their potential to generate a variety of highly oxidative radical species, particularly the hydroxyl radical. Among a vast variety of methods employed in AOP, the most common are ozonation, photolysis, dark and light Fenton processes, heterotrophic photocatalysis and combinations thereof. During the last decade, high energy chemistry with ultrasonic pressure waves have appeared as effective tools of AOP, owing to the extreme conditions generated upon the formation, growth and implosive collapse of acoustic cavities in the surrounding liquid.

Sonochemistry is a terminology to define chemical effects in a liquid created by cavitational collapse, which within extremely short cycles (e.g. several microseconds) results in temperatures as high as 5000 K and pressures in the range of 1000-2000 atm. At such conditions, microreactors as “local hot spots” are generated, in which entrapped gases undergo pyroltic decomposition to dissociate into atomic and radicalar species. Consequently, in the water environment cavitational collapse renders molecules of water vapor in the gaseous bubble interiors to be fragmented into hydroxyl and hydrogen radicals. While some of these radicals recombine in the cooler interface, others may be ejected out and diffuse into the bulk liquid, where they initiate a series of oxidation reactions.

The purpose of this Ph.D. research was to investigate the potential of ultrasonic cavitation for inactivating bacterial cells in infected water bodies and for destroying organic matter in aqueous solutions. Hence, the research is composed of two independent studies: The first one encompasses a thorough investigation of bacterial disinfection using Escherichia Coli as indicators of pathogenic infection; the second one is about organic matter decay, using phenol as a model compound. In both, samples were prepared in the laboratory with ultrapure deionized water to isolate interferences of water or effluent components other than the target species.

The research is composed of three parts:

(1) Literature Review and Publication of two Review Papers: A thorough review of the literature that covers principles of ultrasonic processes and lab-scale applications to environmental remediation was carried out. The study was published in *Applied Catalysis-B* in 2001 as a review paper titled "**Ultrasound as a Catalyzer of Aqueous Reaction Systems: the State of the Art and Environmental Applications**". Moreover, a review of the literature on the decomposition of phenol and substituted phenols by ultrasound with title "**Ultrasonic Destruction of Phenol and Substituted Phenols: a Review of Current Research**" has been recently submitted to *Ultrasonics & Sonochemistry* (August 2005), and is currently in press.

(2) Ultrasonic Disinfection: A 20 kHz ultrasonic probe was used to sonicate water samples with varying concentrations of *E. coli* in the absence and presence of solid particles such as granules of ceramic, zinc and activated carbon. Bacterial density of reactor effluents was periodically analyzed throughout the contact time to depict kinetics of inactivation and to assess individual impacts of the solids on the rate of kill. The results of this study were published in *Environmental Science & Technology* in 2001 under the title: "**Aqueous Phase Disinfection with Power Ultrasound: Process Kinetics and Effects of Solid Catalysts".**

(3) Organic Matter Destruction: Phenol was exposed to 20 kHz, 300 kHz and 520 kHz ultrasound under various ambient conditions to optimize the operating parameters and to assess the effects of frequency, pH, solute concentration, and sparge gas. Concentration of residual phenol in reactor effluents was monitored either by spectrophotometry or Gas Chromatograph (GC). The capacity of ultrasound for total mineralization and detoxification were determined by a Total Organic Carbon Analyzer (TOC) and a Microtox® Toxicity Analyzer, respectively. Finally, the decomposition of phenol was monitored in combined operations such ultrasound/ozone, ultrasound/UV-irradiation, and

ultrasound/ozone/UV-irradiation to see if the effects are additive or synergistic. The results related to detoxification of effluents were presented in ULTRASONICS INTERNATIONAL-2003 in Granada-Spain; those related to parametric effects and optimization of operating conditions have been recently submitted as a full paper "**Effects of Operating Conditions on Sonochemical Decomposition of Phenol**" to *Journal of Hazardous Materials*, and is currently under review.

Financial support for research on ultrasonic disinfection was partly provided by DPT, through project DPT98K120900, and that for organic matter decay was supplied by Boğaziçi University BAP, through Project BAP01Y104.

2. BACKGROUND ON THE RESEARCH TOPICS

2.1. Bacterial Disinfection

Disinfection has become a challenging aspect of water treatment due to rapid elevation of health standards and the growing concern in pollution-free water resources. It is the general name of the processes which are applied to water to destroy disease-causing organisms (pathogens), as an essential step in ensuring safety. Disinfection is differentiated from sterilization, which is the destruction of all organisms. Disinfection is useful to virtually eliminate waterborne diseases such as cholera, typhoid and dysentery.

There are four mechanisms that have been proposed to explain the action of disinfectants (1) damage to the cell wall, (2) alteration of cell permeability, (3) alteration of the colloidal nature of the protoplasm, and (4) inhibition of enzyme activity (Pelczar and Chan, 1986).

2.1.1. Methods of Disinfection

Disinfection of water and wastewaters is possible using chemical and/or physical methods.

2.1.1.1. Chemical. The chemical methods of disinfection are listed below:

Chlorination

The principle chlorine compounds used at water disinfection are chlorine (Cl_2), chlorine dioxide (ClO_2), calcium hypochlorite (CaOCl) and sodium hypochlorite (NaOCl). When the latter two forms are used, chlorination process is known as “hypochlorination”. Chlorination of drinking water has been one of the most effective public health measures ever undertaken. Although chlorine is the most commonly used disinfectant, due to the fact that it leaves residuals in the distribution system to obtain further protection, chlorine reacts with natural organic matter present in surface waters to produce disinfection by-

products (DBP). Concern focused initially on the formation of trihalomethanes (THM), but a wide variety of DBPs are now known to result from chlorination (Bull et al., 1995).

Chlorine kills pathogens such as bacteria and viruses by breaking the chemical bonds in their molecules. Disinfectants that are used for this purpose consist of chlorine compounds which can exchange atoms with other compounds, such as enzymes in bacteria and other cells. When enzymes come in contact with chlorine, one or more of the hydrogen atoms in the molecule are replaced by chlorine. This causes the entire molecule to change shape or fall apart. When enzymes do not function properly, a cell or bacterium will die. When chlorine is added to water, following acids are formed (Morris, 1975):

$$Cl_2 + 2H_2O \rightarrow HOCl + H_3O + Cl^- \quad (2.1)$$

$$HOCl + H_2O \rightarrow H_3O^+ + OCl^- \quad (2.2)$$

$$OCl^- \rightarrow Cl^- + O \quad (2.3)$$

Both hypochlorous acid (HOCl, which is electrically neutral) and hypochlorite ions (OCl^-, electrically negative) have very distinctive behavior. Hypochlorous acid is more reactive and is a stronger disinfectant than hypochlorite. Hypochlorite ions split into chloride ion (Cl^-) and atomic oxygen (O). The oxygen atom is a powerful disinfectant. The disinfecting properties of chlorine in water are based on the oxidising power of the free oxygen atoms and on chlorine substitution reactions.

At pH 7.2 approximately 60 percent of dissolved chlorine exists as hypochlorous acid. As pH values increase, the amount of HOCl decreases and the amount of hypochlorite ion increases. At pH 8.5, the dissolved chlorine exists as 90 percent OCl^- and only 10 percent HOCl. Thus, it can be seen that the disinfection and oxidation properties of chlorinated water are six times greater at pH 7.2 than at 8.5. For this reason, a pH of 7.8 is generally the upper limit for disinfection process.

When chlorine reacts with ammonia the resulting compounds are called chloramines, and the chlorine becomes “combined” rather than “free” residual. Chloramines are undesirable because like hypochlorite ion, their oxidizing and germicidal power is greatly reduced. The extent to which chlorine reactions produce chloramines

rather than hypochlorous acid is governed largely by the amount of ammonia present. Chlorine prefers to chemically react with ammonia rather than with bacteria and soil. Thus, a large amount of ammonia in water causes the chlorine to exist largely as combined residual chloramine, greatly reducing the oxidation and disinfection activity (Morris, 1975).

Breakpoint chlorination is accomplished by increasing chlorine dosage to a point at which all ammonia compounds in the water are completely oxidized and removed by chlorine reaction, after which point all dissolved chlorine exists as free available hypochlorous acid or hypochlorite ion. Amount of chlorine required to reach breakpoint depends upon the amount of ammonia present.

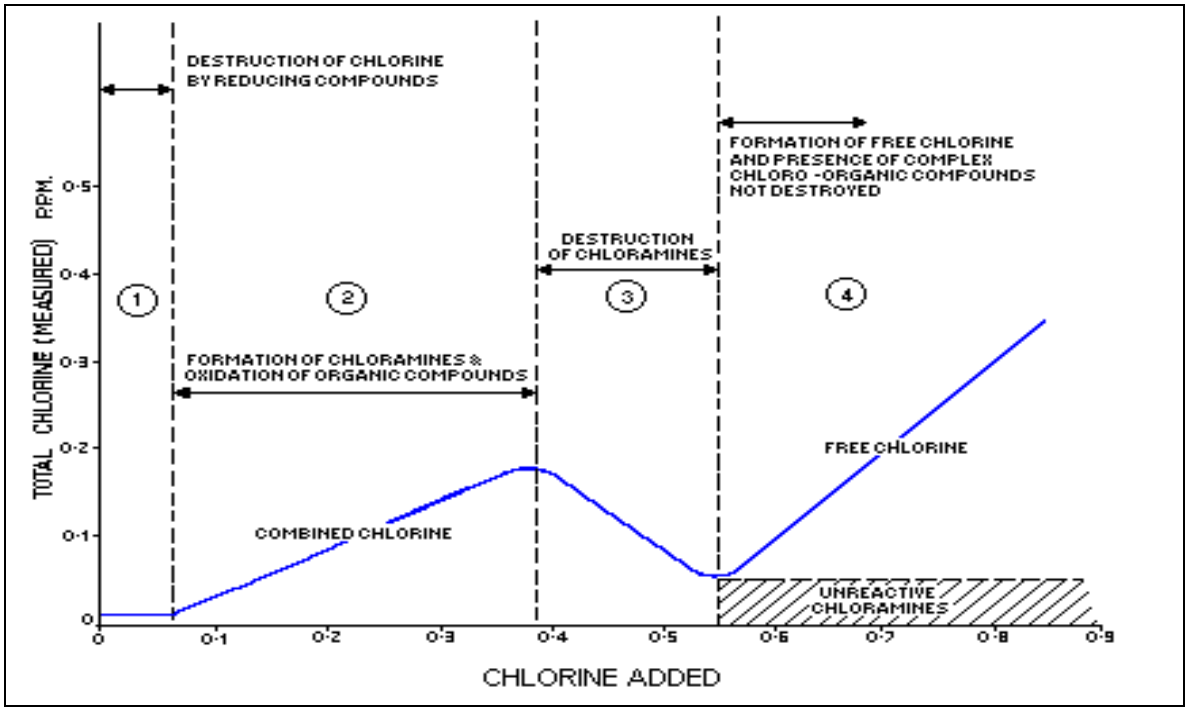

Figure 2.1. Breakpoint chlorination curve
(http://education.qld.gov.au/corporate/doem/forms/am-02b.doc)

Ozonation

Ozone is a very effective disinfectant, which can be produced on-site while eliminating the transportation needs of chemicals. Ozonation has lately emerged as a viable alternative for disinfection by virtue of its non-residual effect, but more research is required

to lower its operational costs and to protect the water from re-infection in the distribution system. It is a viable solution in case of higher requirements for water quality including virus and protozoa removal (Lazarova et al., 1999).

Studies were undertaken to separate, identify, and quantify the successive individual reactions that control the overall rate of ozone decomposition in drinking water and other aqueous solution. The results will allow better predictions of how the rates will be influenced by changes in water composition. The kinetics by which the decomposition of ozone in water is initiated by water itself is described under conditions where secondary radical-type chain reactions are excluded by •OH radical scavengers. Such situations resemble those encountered when natural waters are ozonated. The findings suggest that reactions of OH^- and HO_2^- with ozone can initiate radical chain reactions. The kinetic chain length of such reactions depends on the relative rate by which the radicals formed react with ozone compared with other solutes present in the solution. Therefore such chain reactions can be more important in pure water than in real drinking water or in some types of wastewaters where bicarbonate and organic impurities may significantly scavenge •OH radicals. (Staehelin and Holgne, 1982).

$$O_3 + H_2O \rightarrow 2HOO\bullet \quad (2.4)$$

$$O_3 + HOO\bullet \rightarrow \bullet OH + 2O_2 \quad (2.5)$$

Bromination

Most bromine compounds, especially bromine chloride, are corrosive chemicals, but because of their lower vaporization rate than chlorine, they are less hazardous. In disinfection, bromine chloride is dispensed as liquified gas. Bromine compounds are disinfectants and can be used as an alternative for chlorine. In swimming pools, bromine is used against the formation and growth of algae, bacteria and odors in swimming water. In the United States, bromine has been used since 1936 to treat swimming water. During World War II, chlorine became scarce and many swimming pools started to use bromine for disinfection instead. Bromine can be applied in fluid form or in a mixture. When bromine is applied in fluid form, the following equilibrium is established:

$$Br_2 + 2H_2O \leftrightarrow HOBr + H_3O^+ + Br^- \quad (2.6)$$

$$HOBr + H_2O \leftrightarrow OBr^- + H_3O^- \quad (2.7)$$

This equilibrium strongly depends on the pH value. At the pH value that is usually found in swimming pools, bromine is mainly present as hypobromous acid (HOBr). Bromine has to be used combined with an oxidizing agent (for example chlorine or ozone) (Plewa et al., 2004).

Other Methods

Chloramination is the subject of renewed investigation by the water treatment industry as an alternative to chlorination. The advantages of using chloramines for disinfection include: increased stability of residuals; a reduction in certain odor problems caused by chlorination; and relative chemical inertness towards trihalomethane precursors. Chloramines are the least expensive of the major alternative drinking water disinfectants. Potential disadvantages of chloramines include: interference by certain nitrogenous organic compounds and toxicity to aquatic organisms (Wolfe et al., 1984).

Chloramines are frequently produced by adding ammonia to water containing free chlorine (HOCl or OCl^-, depending on the pH). The ideal pH value for this reaction is 8.4. Reaction mechanism is:

$$NH_{3\,(aq)} + HOCI \rightarrow NH_2Cl + H_2O \quad (2.8)$$

When the reaction takes place three kinds of inorganic chloramines can be formed. The pH value determines which kind of chloramines is formed. They are namely NH_2Cl (monochloramine), $NHCl_2$ (dichloroamine), NCl_3 (trichloramine). Trichloramines mainly form when the pH value is 3 or below. When the pH value is 7 or above, dichloramine concentrations are highest. When chloramines are used as a disinfectant, ammonia is added to chlorine treated water. Chloramines are as effective as chlorine for the deactivation of bacteria and other microorganisms; however the reaction mechanism is slower. Chloramines, like chlorine, are oxidants. Chloramines can kill bacteria by penetration of the cell wall and blockage of the metabolism. Monochloramine is the most effective

disinfectant. It reacts directly with amino acids in the bacterial DNA. During deactivation of microorganisms chloramines destroy the shell which protects a virus. When the pH value is 7 or higher, monochloramine is the most abundant chloramine. The pH value does not interfere with the effectiveness of chloramines.

Among other applications, hydrogen peroxide is also used as a disinfectant. Hydrogen peroxide eliminates proteins through oxidation. Peroxides such as hydrogen peroxide (H_2O_2), perborate, peroxiphosphate and persulphate, are good disinfectants and oxidisers. In general these can adequately remove micro-organisms. However, these peroxides are very unstable. It is used to treat inflammation of the gums and to disinfect (drinking) water. It is also used to combat excessive microbial growth in water systems and cooling towers. In the United States, hydrogen peroxide is used more and more frequently to treat individual water supplies. It is used to prevent the formation of colors, tastes, corrosion and scaling by pollution degradation (iron, manganese, sulphates) and micro-organism degradation. Hydrogen peroxide reacts very fast. It will than disintegrate into hydrogen and water, without the formation of by-products. This increases the amount of oxygen in water (Wolfe et al., 1984).

The disinfection mechanism of hydrogen peroxide is based on the release of free oxygen:

$$H_2O_2 \rightarrow H_2O + \tfrac{1}{2} O_2 \qquad (2.9)$$

Pollutions are decomposed by free oxygen radicals, and only water remains. Free radicals have both oxidising and disinfecting abilities. Among other applications, hydrogen peroxide is used as a disinfectant. Hydrogen peroxide reacts very fast. It will than disintegrate into hydrogen and water, without the formation of by-products. This increases the amount of oxygen in water. However, peroxides are very unstable, and they must be used only for small quantities of water, where residual disinfectants are not required.

2.1.1.2. Physical. The physical methods of disinfection are listed below:

Ultraviolet irradiation

Special lamps that emit ultraviolet rays have been used successfully to sterilize small quantities of water. The efficiency of the process depends on the penetration of the rays into water. The contact geometry between the ultraviolet light source and water is extremely important because suspended matter, dissolved organic molecules and water itself, as well as the microorganisms, will absorb the radiation. It is therefore difficult to use ultraviolet irradiation in aqueous systems, especially when large amounts of particulate matter are present (Qualls and Johnson, 1983).

Disinfection of drinking water by ultraviolet radiation does not produce toxic chlorinated organic chemicals as does chlorination. The germicidal effectiveness of UV radiation is in the 180-320 nm region, optimum 265 nm. A low-pressure mercury arc is effective for germicidal applications because 95% of the energy radiated by this source is at the 253.7 nm line. When microorganisms are subjected to UV radiation, they are not all inactivated at once, but a constant fraction of the present living number dies in each increment of time. With viruses activation usually occurs with one hit. However, with bacteria a shouldered survival curve is seen; this means that more than one hit is necessary for inactivation or that reactivation mechanisms are opposing the UV inactivation. Destruction of a microorganism is the result of UV radiation hitting one or more targets such as DNA, RNA, or enzymes. Those microorganisms which are more resistant to inactivation are algae, gram-positive bacteria, and spore-forming bacteria. A microorganism may be spared if it is shaded by another particle during UV exposure. UV radiation can act as a catalyst in oxidation reactions with ozone or hydrogen peroxide to decrease the total inorganic carbon. The more turbid the water to be treated, the more radiation intensity is required. Lamps should not be immersed in the water. The decrease of radiation intensity with lamp age must be considered. One disadvantage of UV disinfection is that the destroyed organisms are not removed from the treated water. (Meulemans, 1987).

γ-Irradiation

Because of their high penetration, power gamma rays have been used to disinfect both water and wastewater. A high power-energy electron beam device, which generates the irradiation, disinfects the water while the stream of water is passing in a stream from through slim pathway.

In the literature, it was found that the effect of an alternative disinfectant, gamma radiation, was important on three major waterborne microorganisms. *Escherichia coli*, coliphage MS-2, and *Cryptosporidium parvum* were chosen for this investigation as representative bacterial, viral, and protozoan microorganisms, respectively. A ^{60}Co irradiator was used to expose test microorganisms to a controlled radiation dose. Experiments were performed for each of the test microorganisms to evaluate the effect of dissolved oxygen concentration and carbonate alkalinity on inactivation efficiency. For each microorganism, a strong effect of dissolved oxygen was observed, regardless of alkalinity. A subtle effect of alkalinity was observed for *E. coli* and coliphage MS-2, but only in air-saturated solutions. No significant alkalinity effect was observed for *Cryptosporidium parvum*. Inactivation kinetics was modeled for *E. coli* and coliphage MS-2 using single-target theory to calculate an inactivation rate constant. Multitarget theory was used to represent the inactivation response of *Cryptosporidium parvum*. The inactivation models based on target theory were found to provide suitable representations of experimental observations (Thompson and Blatchley, 2000).

Thermal disinfection

Thermal disinfection of water is obtained by heating water to very high temperatures. It is mostly used in the beverage and dairy industry, but it is not a feasible means of disinfecting large quantities of wastewater because of the high cost. Water temperatures with a threshold of approximately 50^{o}C considerably increase the inactivation rate of bacteria induced by thermal ways whereas the inactivation rate of viruses steadily increases with temperatures in the range of 20-50^{o}C. The recorded synergetic effects of solar radiation and thermal water treatment favour a combined use of these two water-treatment processes (Wegelin et al., 1994)

Ultrasonic Irradiation

Recent studies with power ultrasound in aqueous systems have shown that such frequencies are capable of inactivating bacteria, viruses and fungi in water, but long contact or high intensities are required for accomplishing high rates of kill (Mason et al., 1990). It was further shown that bacterial survival under ultrasonic effects exhibits an exponential behavior, while the shear forces set up by cavitation bubbles are insufficient to rupture the cells (unless by prolonged contact), although they disengage the more delicate attachment sites of the DNA to the membrane (Singh, 1995). The results of a novel study on the effects of discrete frequencies and dissolved gases have shown that germicidal effectiveness of ultrasound depends strongly on the frequency (highest at 205 kHz), but moderately on the power intensity and gas properties, being highest in argon-oxygen mixtures (Hua and Thompson, 2000).

2.2. Phenols and Methods of Phenol Removal from Aqueous Media

2.2.1 Properties of Phenol

Many of the benzene-like compounds discovered had pleasant odors and hence acquired the name aromatic. Phenol is an aromatic compound. In chemistry an aromatic compound refers to a substance with a ring structure and with bonding characteristics and properties related to those of benzene. The schematic structure of phenol is given below:

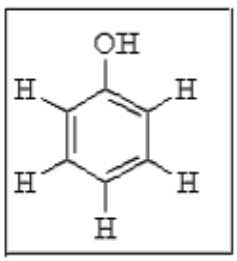

Figure 2.2. The chemical structure of phenol.

Phenol is a colorless or white solid when it is pure; however, it is usually sold and used as a liquid. The odor threshold for phenol is 0.04 ppm, with a strong very sweet odor. It is very soluble in water (approximately 8 g phenol/100 g water) and is quite flammable.

The vapor pressure for phenol is 0.41 mm Hg at 25 ^{o}C, and it has a log octanol/water partition coefficient (Log K_{ow}) of 1.46. Log K_{ow} is a parameter which indicates the solubility of a compound in water. A small Log K_{ow} tells us that the compound is soluble in water (Hua and Hoffmann, 1997).

When substituted phenols are considered, chlorinated phenol compounds are solids at room temperature, except 2-monochlorophenol which melts at 8^{o}C. It is a toxic compound. But the toxic property accounts for many of its uses. It is used as bactericide, fungicide and preservative. The water solubility of chlorophenols is low and it is weakly acidic. The octanol/water partition coefficients increase as chlorination increases. The taste and odour thresholds are quite low. Chlorophenols are prepared by the alkaline hydrolysis of the appropriate chlorobenzenes or by the direct stepwise chlorination reaction of phenol or lower chlorinated phenols at a high temperature. Generally, higher chlorinated phenols and their salt forms are used in wood preservation industry and in surface treatments for fresh-cut logs and lumber against sapstain fungi and mould. 4-nitrophenol is a colorless to light yellow solid with no odor. The vapor pressure for 4-nitrophenol is 0.0003 mm Hg at 30 ^{o}C, and it has an octanol/water partition coefficient (Log K_{ow}) of 1.91. It is moderately soluble in cold water (Amoore and Hautala, 1983). .

The polar nature of the O-H bond (due to the electronegativity difference of the atoms) results in the formation of hydrogen bonds with other phenol molecules or other H-bonding systems. The implications of this include high melting and boiling points compared to analogous ones and high solubility in aqueous media. Phenols are more acidic (pK_a>>10) than alcohols (pK_a>>16 - 20), but less acidic than carboxylic acids (pK_a>>5). The acidity difference means that it is possible to separate phenols from alcohols and/or carboxylic acids (Amoore and Hautala, 1983).

2.2.2. Industrial Consumption of Phenols

Many different processes used in the chemical manufacturing industry result in a large number of specific wastes. Typical wastes from chemical manufacturing plants

include spent solvents, distillation bottoms and side-cuts, off specification or unused chemicals, wastewater, wastewater treatment sludge, emission control sludges, filter cake, spent catalysts, by-products, reactor clean out wastes, and container residues. Many wastes from chemical manufacturing (e.g., spent solvents and off-specification chemicals) include phenol and phenolic compounds (Kim et al., 2002).

Phenol and phenolic compounds are widely used in industrial operations for the production of resins, preservatives of paint, leather, textile goods and antimicrobial agents. Many of these products are highly toxic to living organisms, and some are classified as suspected carcinogens (Kim et al., 2002).

Among these industries; urea and phenolic resins manufacturing produces large phenolic resin particles. Application of preventive measures such as recycle/reuse of wastewater, use of filters, rinsing of resins and other process modifications would effectively result in the reduction of the volume of phenolic waste.

The furniture/wood manufacturing and refinishing industry uses many solvents. The many waste types generated from the use of paints, wood treatments, stains, varnishes, polishes, and adhesives may include phenol and other phenolics. Spent solvents and solvent still bottoms are usually hazardous ignitable or toxic wastes.

Basic laboratory studies on the phenolic wastewater from a typical pharmaceutical plant were found to produce waste streams containing phenol, up to 12 g/L (9.33 g/L 4-nitrophenol and 3.11 g/L phenol) (Tukac and Hanika, 1995).

In an EPA ranking of the 20 chemicals whose production generates the most total hazardous waste, five of the top six are chemicals commonly used by the plastics industry. These include propylene (ranked first), phenol (third), ethylene (fourth), polystyrene (fifth), benzene (sixth).

2.2.3. Treatment Methods for Phenol Removal

2.2.3.1. Biological. Bioreactors including activated sludge systems and trickling filters, with acclimated phenol bacteria, have been used for the treatment of phenol containing wastewater. In the petroleum refining process activated-sludge systems have been employed for the conventional treatment of wastewater, containing highly concentrated phenol which is discharged from the bottom oil cracking furnace. The wastewater treatment systems used today, have the disadvantages such as increased plant area, excess sludge and foul odors.

The trickling filter process for removal of phenol, has exhibited certain practical characteristics which have made it a popular secondary waste treatment method. Simplicity, operational economy, ability to give good effluents under wide variations of load, and quick recovery from pH variations and shock loads of toxic substances are factors which frequently result in choice of trickling filtration over the activated sludge process. On the other hand there are some deficiencies which are observed in the operation of activated sludge systems are poor ventilation, plugging, pending and channeling caused usually by excessive accumulation of bacterial growths. Materials tried as trickling filter media with limited success included: corn cobs, wood chips and slabs, coke, cinders, broken tile, broken brick etc (Bevilaqua et al., 2002).

Phenol is also removed through combined biological and enzymatic treatments (Bevilaqua, et al., 2002). The systems operated were conventional batch aerobic biological systems followed or proceeded by enzymatic treatment. Tyrosinase extracted from the mushroom *Agaricus bispora* was employed. Biological treatment efficiently degraded effluents containing up to 420 mg/L of phenol, removing 97% of the COD and 99% of the phenol in 48-hour batches. Such systems have disadvantages of reduction in removal efficiency when phenol concentration changes significantly.

2.2.3.2. Physicochemical. The physicochemical methods of phenol removal are described in details below:

Adsorption

Adsorption is one of the most effective processes of wastewater treatment. Use of activated carbon as an adsorbent for industrial wastewater treatment is capital-intensive and has some problems such as (i) regeneration of activated carbon; (ii) intraparticle resistance in adsorption; (iii) high cost of manufacture. There is nowadays tendency for developing adsorbents from low-cost materials. In a study by Kumar et al. (1987), adsorption of phenol from aqueous solutions on activated carbon and fly ash has been investigated. The effects of contact time and initial solute concentration have been studied and isotherm parameters are evaluated. The Freundlich isotherm has been found to be more suitable for all the systems investigated.

Experimental investigations were conducted on the adsorption characteristics of phenol and *m*-chlorophenol by organobentonites. The organobentonites were prepared by modifying the natural bentonite by various quaternary amines including tetramethylammonium bromide (TMAB), hexadecyltrimethylammonium bromide (HDTMAB), benzyltriethylammonium bromide (BTEAB), tetraethylammonium bromide (TEAB) and cetylpyridinium bromide (CPB), all surfactants. The empirical Freundlich isotherm was found to describe well the equilibrium adsorption data. Multistage adsorption of phenol or chlorophenol by organobentonites was investigated both theoretically and experimentally. Theoretical equations were found to predict reasonably well the observed data. Preliminary regeneration of the exhausted organobentonites was also attempted. Results from several test runs showed the potential of regeneration by a simple thermal method (Lin and Cheng, 2000). Other materials such as fertilizer wastes, wood and rice husk are subjected to be adsorbents for phenol treatment (Abdom et al., 1997).

Membrane Techniques

Another application for the removal of phenol is application of membrane systems for wastewater treatment in chemical industry. A membrane can be viewed as a semi-permeable barrier between two phases, which can restrict the movement of molecules across it in a very specific manner. Phenol can be removed from about 1000 ppm to 0.5

ppm with an extraction efficiency of greater than 99.95 per cent. The internal reagent NaOH converts the phenol to sodium phenolate and the phenolate is trapped into the internal phase. However use of permeable membranes and semi-permeable membranes in microfilters, ultrafilters, osmosis, reverse osmosis, dialysis (which are comparatively newer methods of separation processes) have the problems like high capital costs, low mass transfer rate, low selectivity, large equipment size etc. (Cahn et al., 1974).

Chemical Oxidation. Chemical oxidation, such as with hydrogen peroxide or chlorine dioxide, has a low capital cost but a high operating cost. Bio-oxidation has a high capital cost and a low operating cost. Removal must be accomplished with chemical oxidants, the most commonly used being chlorine dioxide, hydrogen peroxide and potassium permanganate. Chlorine dioxide is very effective at oxidizing phenols and substituted phenols in industrial wastewaters. Its reaction with phenol is much faster and more complete at neutral and alkaline pHs than achieved by hydrogen peroxide or potassium permanganate (Rivas et al., 1995).

Advanced Oxidation Processes (AOP). Advanced oxidation processes involving hydroxyl radicals have shown their potential to destroy toxic organic compounds in wastewater. The main interesting characteristics of the hydroxyl radical is that it has a very high oxidation potential (larger than ozone) and can be generated by a variety of methods. It may be produced by combining ozone with ultraviolet light (Glaze et al., 1982; Gurol and Vatistas, 1987; Esplugas et al., 1994; Prado et al., 1994), ozone with hydrogen peroxide (Trancart, 1990), hydrogen peroxide with ultraviolet light, hydrogen peroxide with ferrous or ferric ion (David et al., 1991) and by photocatalysis, which uses a semi conductor in combination with visible and UV radiation and molecular oxygen (Weir et al., 1993). Ultrasonically-induced cavitation is being investigated as an AOP, and chemical effects of ultrasound are due to the phenomenon of acoustic cavitation. It is the formation, growth and violent collapse of bubbles formed by coupling the pressure waves of ultrasound with a liquid (Hua and Hoffmann, 1996; Mason, 1990). Upon ultrasonic irradiation, organic compounds in water are degraded via several mechanisms, due to the extreme conditions. Three main pathways of pollutant degradation are •OH oxidation, pyrolytic degradation, and the existence of supercritical water oxidation.

3. LITERATURE REVIEW ON ADVANCED OXIDATION AND ULTRASOUND TECHNIQUES FOR ENVIRONMENTAL REMEDIATION

3.1. Overview of Advanced Oxidation Processes

In the developing world, the environment has been exposed to extravagant use of complex organic compounds as a result of industrialization and most of these complex organic compounds are discharged into conventionally operated wastewater treatment systems. Although chemical oxidation processes are widely used to treat drinking water, wastewater and groundwater contaminated with organic compounds, remediation of these waters with conventional oxidants is not always feasible due to very long reaction times (Wu et al., 2001). Research and development in innovative technologies during last decade have shown that advanced oxidation processes (AOPs) are highly promising for the remediation of such contaminated water/effluent systems without generating any sludge or solid material of hazardous character (Ince et. al., 2001).

AOPs are the oxidation processes at mild conditions by highly reactive species called free radicals (Ince, 1998). The efficiency of AOPs are based on the presence and beneficial reaction capacity of radicals, especially the hydroxyl radical (•OH), which is ultimately capable of mineralizing organic contaminants. Direct oxidation of aqueous solutions containing organic contaminants can be performed under a variety of conditions ranging from ambient conditions to supercritical water oxidation at very high temperatures and pressures. AOPs are studied in different combinations; ozone with ultraviolet radiation; ozone with hydrogen peroxide; ozone/hydrogen peroxide with ultraviolet radiation; hydrogen peroxide with ultraviolet radiation and ultrasound alone or with other oxidants (Alnaizy et al., 2000).

The reaction rates of hydroxyl radicals with organic compounds are extremely fast, leading to reduced plant size and treatment costs in water and wastewater treatment. The observed rate constant of the reaction of phenol with hydroxyl radical is in the range of 10^9

to 10^{10} L/mol.s, while it is 10^{3} L/mol.s with ozone. This fast oxidation of organic compounds may occur via one of these pathways: (i) hydrogen abstraction; (ii) electron transfer; and (iii) radical addition (Hoffmann et al., 1995).

The most commonly used AOP involve photochemical, ozonation, electron beam, radiolysis, ionizing radiation and ultrasonic irradiation processes. There are also a number of practical applications of AOPs in combinations with chemical reagents such as H_2O_2, O_3 and Fenton's Reagent.

3.1.1. Photochemical Processes

These are processes, which involve the use of ultraviolet (UV) irradiation in the presence of an oxidant and/or a catalyst. There are four very common types of photochemical AOPs (Legrini et al., 1993):

(1) photolysis of hydrogen peroxide,
(2) photolysis of ozone,
(3) ozone/hydrogen peroxide/ultraviolet irradiation,
(4) the photo Fenton's reaction

The mechanism most commonly accepted for the photolysis of H_2O_2 is the cleavage of the molecule into hydroxyl radicals and other reactive species that attack the organic molecules (Legrini et al., 1993):

$$H_2O_2 + h\nu \rightarrow 2\ \bullet OH \qquad (\lambda=200\ \text{nm radiation}) \qquad (3.1)$$

If an excess of H_2O_2 is used, •OH will produce hydroperoxyl radicals, •OOH, which are much less reactive. Unfortunately, the molar extinction coefficient of H_2O_2 at 254 nm is only 19.6 L/mol.cm, which is significantly lower than that of ozone, 3300 L/mol.cm. This means that higher concentration of H_2O_2 is needed to yield the same amount of •OH (Glaze et al., 1987).

The O_3 / UV process seems at present to be the most frequently applied AOP for a wide range of compounds. This is due to the fact that ozonation is a well-known procedure for water and wastewater technology. For the photolytic oxidation by ultraviolet light combined with ozone, hydroxyl radicals are generated as active species.

$$O_3 + h\nu \rightarrow O_2 + O(^1D) \qquad (\lambda=254 \text{ nm radiation}) \qquad (3.2)$$

$$O(^1D) + H_2O \rightarrow \bullet OH + \bullet OH \qquad (3.3)$$

$$O_3 + H_2O \rightarrow \rightarrow H_2O_2 + O_2 \qquad (3.4)$$

Hydrogen peroxide is produced after photolysis of ozone, and that is photolyzed to •OH radical. Addition of hydrogen peroxide results in a net enhancement due to the dominant production of •OH radicals.

$$H_2O_2 \leftrightarrow HOO^- + H^+ \qquad (3.5)$$

$$O_3 + HOO^- \rightarrow \bullet OH + O_2^{\cdot -} + O_2 \qquad (3.6)$$

$$O_3 + O_2^{\cdot -} \rightarrow O_3^{\cdot -} + O_2 \qquad (3.7)$$

$$O_3^{\cdot -} + H_2O \rightarrow \bullet OH + HO^- + O_2^{\cdot} \qquad (3.8)$$

The reaction is based on the catalytic effect of the ferrous ions on the decomposition of H_2O_2 (Ruppert et al., 1993):

$$Fe^{2+} + H_2O_2 \rightarrow Fe^{3+} + OH^- + \bullet OH \qquad (3.9)$$

The primary step is oxidation of ferrous ions to ferric ones (Equation (3.9)) and the formation of •OH. In the dark, the reaction is retarted after complete conversion of Fe^{2+} to Fe^{3+}. After the complete disappearance of the oxidant, no more Fe (II) can be consumed. In the presence of UV or near-UV light, ferric ions are photo-reduced and ferrous iron can be regenerated and feedback reaction takes place. The following reaction occurs at acidic conditions, especially at pH 3-5 (Tezcanli, 1998).

$$Fe^{3+} + H_2O_2 + h\nu \rightarrow Fe^{2+} + \bullet OH + H^+ \ (\lambda > 300 \text{ nm}) \qquad (3.10)$$

3.1.2. Ozonation

The use of chemicals for the removal of organic compounds is not suggested, because toxic or less biodegradable by-products may be formed. On the other hand, ozone is a noble process for the following reasons (Wu, 2001):

- No chemical sludge is left in the treated effluent
- Less space is required, and it is easily installed on site
- There is less danger, since no stock hydrogenperoxide or other chemical is required on site
- It is easily operated
- All residual ozone can easily be decomposed to oxygen and water

The oxidation potential of ozone (2.08 Volt) is much higher than that of many other oxidants as shown in Table 3.1.

Table 3.1. Oxidation potentials of some important oxidizing agents (http://hyperphysics.phy-astr.gsu.edu/hbase/chemical/electrode2.html#c1)

Oxidizing agent	Symbol	electrical-chem. potential (V)	potential relative to Chlorine (%)
Fluorine	F_2	3.06	2.25
Hydroxyl radical	●OH	2.80	2.05
Atomic oxygen	●O	2.42	1.78
Ozone	O_3	2.08	1.52
Hydrogenperoxide	H_2O_2	1.78	1.30
Hypochlorous acid	HClO	1.49	1.10
Chlorine	Cl_2	1.36	1.00
Chlorine dioxide	ClO_2	1.27	0.93
Oxygen	O_2	1.23	0.90

In an aqueous solution, ozone reacts with various organic compounds via two different pathways namely direct molecular and indirect radical chain type reaction

depending upon pH of water. Molecular O_3 is the major oxidant at acidic pH and reacts directly by electrophilic attack, where as less selective and faster radical reaction oxidation (mainly •OH) becomes predominant at pH>7 as a consequence of OH^- accelerated O_3 decomposition (Glaze et al., 1987). The net reaction of ozone with OH^- ions is given below (Calgon Carbon Oxidation Technologies):

$$2O_3 + H_2O \xrightarrow{OH^-} \bullet OH + 2O_2 + HO_2 \qquad (3.11)$$

Staehelin and Hoigne (1982) showed that the mechanism of reaction of ozone with another substrate M may involve both direct reaction of ozone and indirect •OH chain type reaction with M, even at neutral pH the relative proportions of which will depend on various contaminants present or added. It was also reported that at pH>10.3 where carbonate ion is a more prevalent species than bicarbonate ion, its scavenging effect is 20 times greater than that of bicarbonate ion.

The high oxidation potential of ozone allows it to degrade most organic compounds. In an aqueous solution ozone reacts with organic contaminants via two different pathways; direct molecular reaction and indirect radical reaction. These two ways depend on the pH of the solution. At acidic mediums ozone is the molecular oxidant, while at high pH values the hydroxyl radical takes the oxidants place (Glaze et al., 1987).

The ozone reactions in aqueous media which produce radicals are listed below:

$$O_3 + H_2O \rightarrow 2HOO\bullet \qquad (3.12)$$

$$O_3 + HOO\bullet \rightarrow \bullet OH + 2O_2 \qquad (3.13)$$

3.1.3. Electron Beam Processes

The ability of high-energy electrons to alter the chemical structure of molecules is well known and this phenomenon has led to the establishment of several developments. Recently there has been interest in using the ability of high-energy electrons to alter molecular structure to either modify or destroy hazardous or polluting molecular species, particularly organic molecules present in aqueous solutions. The advantage of the electron

beam radiation process in destruction of pollutants is connected to its high efficiency and possibility to transfer of high amounts of energy directly into the object under treatment. It may be applied to a variety of wastes including, water, sewage sludge and silt. A disadvantage is related mostly to high investment cost of accelerator. Traditional electron injection processing facilities capable of processing bulk materials employ accelerators with electron energies in excess of 0.5 MeV (Schuets and Vroom, 1998).

3.1.4. γ - Irradiation Processes

γ - Irradiation treatment of dissolved organic substances in water is a promising method for the treatment of wastewater and the destruction of chemical waste. It has the potential for reductive and oxidative degradation of hazardous waste. The ^{60}Co γ-irradiation has a much higher potential and it appears to involve hydroxyl radical generation as the main oxidant in the degradation process (O'Shea et al., 1998).

3.1.5. Ultrasonic Processes

Ultrasound is a rarely used tool in wastewater treatment, despite the very unique and extreme conditions generated by ultrasound waves in liquid media, resulting in a remarkably suitable medium for high energy chemistry, which is called "sonochemistry". Under well-established conditions, these extremes not only promote the oxidative destruction of target contaminants via free radical reactions, but also provide an excellent medium for their thermal decomposition in the gas phase. Hence, the production of free radical species by sonochemical irradiation extends the goals of AOP beyond aqueous phase oxidative destruction to gaseous decomposition, owing to very special effects generated by the formation and collapse of acoustic cavities in sonicated water (Ince et al., 2001).

Sonochemistry derives principally from acoustic cavitation; the formation, growth and implosive collapse of bubbles in a liquid. Cavitation serves as a means of concentrating the diffuse energy of sound. It is the underlying phenomenon responsible for sonochemistry. Bubble collapse induced by cavitation produces intense local heating, high pressures at micro scales and they are called "hot spots". These hot spots have

temperatures of roughly 5000^{o}C, pressures of about 500 atmospheres and heating/cooling rates greater than 10^{9} K/s.

3.2. Ultrasound and Its Uses in Water Remediation

The history of ultrasound dates back 100 years to the work of F. Galton, who was interested in establishing the threshold of frequencies of hearing both for animals and human beings. He produced a whistle with an adjustable resonance cavity which was capable of generating sound of known frequencies. With the aid of this instrument he was able to determine that the limit of human hearing is normally around 16000 cycles/s (16 kiloHertz (kHz)). The whistle is an example of transducer - a device which converts one form of energy (gas motion) into another (sound).

The recent rapid growth in interest in sonochemistry is due in part to the availability of ultrasonic laboratory equipments. The equipments are usually of disk type or a sonic probe (or horn). Disk type sonicators and probes have the same basic arrangement in that they contain an electrical generator and an ultrasonic transducer. The generator provides high-voltage pulses of energy at the desired frequency to the transducer. The transducer is the most important component in the system and in virtually all pieces of modern ultrasonic equipment operates on the piezoelectric principle. A transducer is defined as a device that is actuated by power from one system supply power to a second system; piezoelectric transducers convert electrical energy to ultrasonic energy.

3.2.1. Sonochemistry

The chemical applications of ultrasound, “sonochemistry”, have become an exciting new field of research during the past decade. The history of sonochemistry, however, begins in the late 1800s. During field tests of the first high-speed torpedo boats in 1894, Sir John I. Thornycroft and Sydney W. Barnaby discovered severe vibrations from and rapid erosion of the ship's propeller. They observed the formation of large bubbles (or cavities) formed on the spinning propeller and postulated that the formation and collapse of these bubbles were the source of their problems. By increasing the propeller size and

reducing its rate of rotation, they could minimize this difficulty of cavitation. As ship speeds increased, however, this became a serious concern and the Royal Navy commissioned Lord Rayleigh to investigate. He confirmed that the effects were due to the enormous turbulence, heat, and pressure produced when c avitation bubbles imploded on the propeller surface. In the same work, he explained that cavitation was also the origin of tea kettle noise!

This phenomenon of cavitation occurs in liquids not only during turbulent flow but also under high-intensity ultrasonic irradiation. It is responsible for both propeller erosion and for the chemical consequences of ultrasound. Alfred L. Loomis noticed the first chemical effects of ultrasound in 1927, but the field of sonochemistry lay fallow for nearly 60 years. The renaissance of sonochemistry occurred in the 1980's, soon after the advent of inexpensive and reliable laboratory generators of high-intensity ultrasound (Suslick, 1994).

Scientists now know that the chemical effects of ultrasound are diverse and include substantial improvements in both stoichiometric and catalytic chemical reactions. In some cases, ultrasonic irradiation can increase reactivities by nearly a millionfold. The chemical effects of ultrasound fall into three areas:

- homogeneous sonochemistry of liquids,
- heterogeneous sonochemistry of liquid-liquid or liquid-solid systems,
- sonocatalysis (which overlaps the first two).

Because cavitation can take place only in liquids, chemical reactions do not generally occur during the ultrasonic irradiation of solids or solid-gas systems.

Nonetheless, the ultrasonic irradiation of liquids produces excessive energy for chemical reactions. This occurs because ultrasound causes other physical phenomena in liquids that create the conditions necessary to drive chemical reactions. The most important of these is cavitation, which is composed of:

- formation
- growth
- implosive collapse

of bubbles in a liquid. The dynamics of cavity growth and collapse are strikingly dependent on the local environment. Cavity collapse in a homogeneous liquid is very different from cavitation near a liquid-solid interface.

As ultrasound passes through a liquid, the expansion cycles exert negative pressure on the liquid, pulling the molecules away from one another. If the ultrasound is sufficiently intense, the expansion cycle can create cavities in the liquid. This will occur when the negative pressure exceeds the local tensile strength of the liquid, which varies according to the type and purity of liquid. (Tensile strength is the maximum stress that a material can withstand from a stretching load without tearing).

Normally, cavitation is a nucleated process; that is, it occurs at pre-existing weak points in the liquid, such as gas-filled crevices in suspended particulate matter or transient microbubbles from prior cavitation events. Most liquids are sufficiently contaminated by small particles that cavitation can be readily initiated at moderate negative pressures (Suslick, 1994).

Once formed, small gas bubbles irradiated with ultrasound will absorb energy from the sound waves and grow. Cavity growth depends on the intensity of the sound. At high intensities, a small cavity may grow rapidly through inertial effects. If cavity expansion is sufficiently rapid during the expansion half of a single cycle, it will not have time to recompress during the compression half of the acoustic cycle.

At lower acoustic intensities cavity growth can also occur by a slower process called rectified diffusion. Under these conditions a cavity will oscillate in size over many expansion and compression cycles. During such oscillations the amount of gas or vapor that diffuses in or out of the cavity depends on the surface area, which is slightly larger during expansion than during compression. Cavity growth during each expansion is, therefore, slightly larger than shrinkage during the compression. Thus, over many acoustic cycles, the cavity will grow. The growing cavity can eventually reach a critical size where it can efficiently absorb energy from the ultrasonic irradiation. Called the resonant size, this critical size depends on the liquid and the frequency of sound; at 20 kHz, for example, it is roughly 170 micrometers. At this point the cavity can grow rapidly during a single cycle of sound.

Once the cavity has overgrown, either at high or low sonic intensities, it can no longer absorb energy as efficiently. Without the energy input the cavity can no longer sustain itself. The surrounding liquid rushes in, and the cavity implodes (catastrophic collapse). This collapse occurs only if the intensity of the ultrasound wave exceeds that of the acoustic cavitational threshold (typically a few Watts/cm^2 for ordinary liquids exposed to 20 kHz). It is the implosion of the cavity that creates an unusual environment for chemical reactions (Ince et al., 2001; Mason, 1990; Suslick et al., 1990).

There are some theories to describe how the energy to cause chemical reactions. The mostly favoured theory is the 'Hot Spot Theory'. Compression of a gas generates heat. The compression of cavities when they implode in irradiated liquids is so rapid than little heat can escape from the cavity during collapse. The surrounding liquid, however, is still cold and will quickly quench the heated cavity. Thus, one generates a short-lived, localized hot spot in an otherwise cold liquid.

Such a hot spot is the source of homogeneous sonochemistry; it has a temperature of roughly 5000 °C, a pressure of about 1000 atmospheres, a lifetime considerably less than a microsecond, and heating and cooling rates above 10 billion °C per second (Dahlem et al., 1998; Suslick, 1990).

For a rough comparison, these are, respectively, the temperature of the surface of the sun, the pressure at the bottom of the ocean, the lifetime of a lightning strike, and a million times faster cooling that a red hot iron rod plunged into water. Thus, cavitation serves as a means of concentrating the diffuse energy of sound into a chemically useful form.

The second most accepted theory is 'Electrical Theory' by Margulis (Margulis, 1995). This theory suggests that during bubble formation and collapse, enormous electrical field gradients are generated and these are sufficiently high to cause bond breakage and chemical activity.

The 'Plasma Theory' by Lepoint and Muille (1994) also suggests the extreme conditions associated with the fragmentative collapse is due to intense electrical fields and seems not to involve a true implosion. They compared the origin of cavitation chemistry to

corona-like discharge caused by a fragmentation process and supported and indicated the formation of micro plasmas inside the bubble.

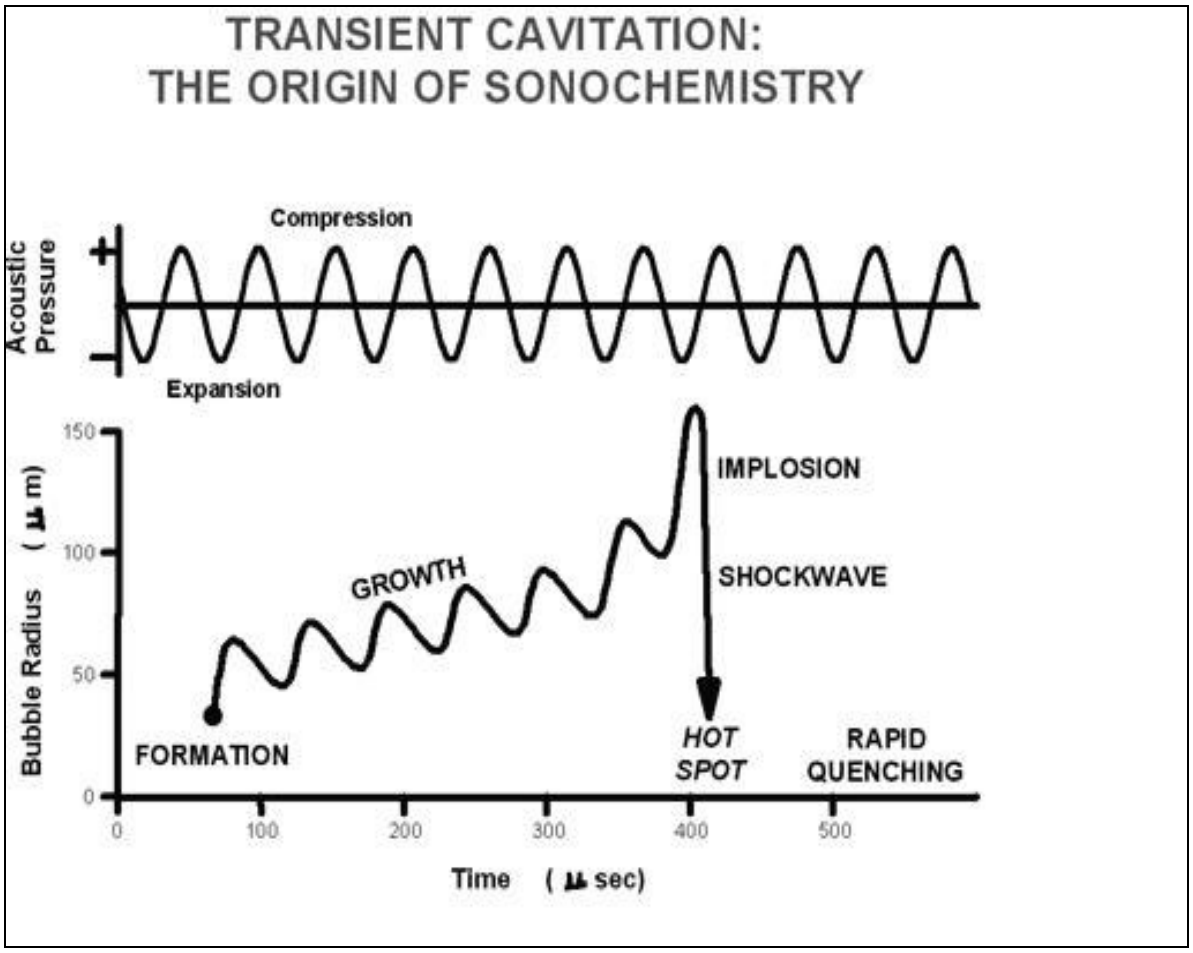

Figure 3.1. Formation, growth and implosion of a cavitation bubble (Suslick, 1994).

The 'Supercritical Theory' recently proposed by Hoffmann (Hua et al., 1995) suggests the existence of a layer in the bubble-solution interface where temperature and pressure may be beyond the critical conditions of water (647 K, 22.1 MPa) and showed that supercritical water is obtained during the collapse of cavitation bubbles generated sonolytically.

Determination of the temperatures reached in a cavitating bubble has remained a difficult experimental problem. The transient nature of the cavitation event precludes direct measurement of the conditions generated during bubble collapse. Chemical reactions themselves, however, can be used to probe reaction conditions. The effective temperature of a system can be determined with the use of competing unimolecular reactions whose rate dependencies on temperature have already been measured. This technique of "comparative-rate chemical thermometry" was used by Suslick et al., 1986, to determine the effective temperature reached during cavity collapse. For a series of organometallic reactions, the relative sonochemical rates were measured. In combination with the known temperature behavior of these reactions, the conditions present during cavity collapse could then be determined. The effective temperature of these hot spots was 5200 K. Of course, the comparative rate data represent only a composite temperature: during the collapse, the temperature has a highly dynamic profile, as well as a spatial gradient in the surrounding liquid.

When a liquid is subjected to ultrasound, not only does chemistry occur, but light is also produced. Such "sonoluminescence" provides an alternate measure of the temperature of the high-energy species produced during cavitation. From a comparison of synthetic to observed spectra, the effective cavitation temperature of the emitting species is 5100 K. The agreement between this spectroscopic determination of the cavitation temperature and that made by comparative rate thermometry of sonochemical reactions is surprisingly close.

It is reported that a great majority of sonochemical systems, having potential industrial applications involve heterogeneous reactions, where enhancement of chemical reactivity is associated with the physical effects of ultrasound such as heat and mass transfer, surface activation, and phase mixing (Suslick, 1990; Reisse, 1995; Leighton, 1994; Serpone et al., 1994). Sonocatalysis of liquid-liquid heterogeneous reactions is based on the mixing effect of acoustic streaming, which promotes the emulsification of non-miscible liquids by enhancing reaction rates upon increased interfaces. When the heterogeneous system is made of a solid-liquid biphasic medium, catalysis of reactions is a consequence of the disruption of the solid by the jetting phenomenon associated with the collapse of cavitation bubbles. All together, it was found that the most effective frequency

range for catalyzing heterogeneous reaction systems by the mechanical effects of ultrasound is the 20-100 kHz range, i.e. the region of power ultrasound (Reisse, 1995).

On the other hand, homogeneous sonochemistry induced by ultrasonic irradiation of homogeneous fluids is a direct outcome of the extreme conditions generated in collapsing microbubbles (Ince et al., 2001; Reisse, 1995). Such extremes are reported to produce very unique catalytic effects, arising from inherent advantages of the system such as: (i) the ability to generate high-energy species and (ii) the mimicry of autoclave reaction conditions (i.e. high temperatures and pressures) on a microscopic scale (Suslick, 1990). These effects start in the cavities, which are made of microbubbles filled with vapour of the liquid medium and/or dissolved solutes and gases diffused into them (Mason and Cordemans, 1998). During the collapse of these cavities in pure aqueous systems, gaseous water molecules entrapped in expanded microbubbles are fragmented as in pyrolysis to generate highly reactive radical species such as hydroxyl radicals and hydrogen atoms (Riesz and Mason, 1991).

The formation of hydroxyl radicals in sonicated water has been demonstrated in various laboratories, using combined spin trapping and EPR techniques; the Weissler reaction; fluorescence measurements from 2-hydroxy-terephtalate produced by hydroxylation of aqueous terephtalate ion; DMPO trapping; and sonoluminescence measurements based on the oxidative degradation of luminol to aminophtalate under the action of sonochemically produced hydroxyl radicals (Petrier et al., 1992; Mason et al., 1994; Weissler et al., 1950; Negishi, 1961; Hart and Henglein, 1985; Riesz et al., 1990). In non-aqueous organic solvents or aqueous media containing volatile organic gases and solutes, cavitational collapse not only results in hydroxyl and hydrogen radicals, but also in organic radicalar species, as confirmed by experimental studies with ESR spectroscopy (Seghal et al., 1982).

The hydroxyl radicals generated by water sonolysis may either react in the gas phase or recombine at the cooler gas liquid interface and/or in the bulk during cavity collapse to produce hydrogen peroxide and water (Riesz and Mason, 1991; Fischer et al., 1986). The reaction mechanisms are shown below:

$H_2O \rightarrow))) \bullet OH + \bullet H$ (pyrolysis) (3.14)

$\bullet OH + \bullet H \rightarrow H_2O$ (3.15)

$2\bullet OH \rightarrow H_2O + O$ (3.16)

$2\bullet OH \rightarrow H_2O_2$ (3.17)

$2\bullet H \rightarrow H_2$ (3.18)

If the solution is saturated with oxygen, peroxyl and additional hydroxyl radicals are formed in the gas phase (due to the decomposition of molecular oxygen), and the recombination of the former at the cooler sites (interface or the solution bulk) produces more hydrogen peroxide, as shown (Ince et al., 2001; Makino et al., 1982; Petrier et al., 1994):

$O_2 + \bullet H \rightarrow \bullet O_2H$ (3.19)

$O_2 \rightarrow))) O + O$ (3.20)

$O + H_2O \rightarrow \bullet OH + \bullet OH$ (3.21)

$\bullet O_2H + \bullet O_2H \rightarrow H_2O_2 + O_2$ (3.22)

3.2.2. Sonochemical Reaction Sites

Experiences in homogeneous sonochemistry have shown that there are three reaction sites in ultrasonically irradiated liquids (Weavers et al., 1998):

- the cavitation bubble itself
- the interfacial sheath between the gaseous bubble and the surrounding liquid
- the solution bulk.

In water or effluent treatment practices, organic pollutants may be destroyed either at the first two sites upon combined effects of pyrolytic decomposition and hydroxylation, or in the solution bulk via oxidative degradation by hydroxyl radicals and hydrogen peroxide (Weavers et al., 1998). The intensity of oxidation reactions in the latter site is directly and exclusively related to the quantity of available uncombined hydroxyl radicals, as they migrate into the aqueous phase during collapse of cavity bubbles.

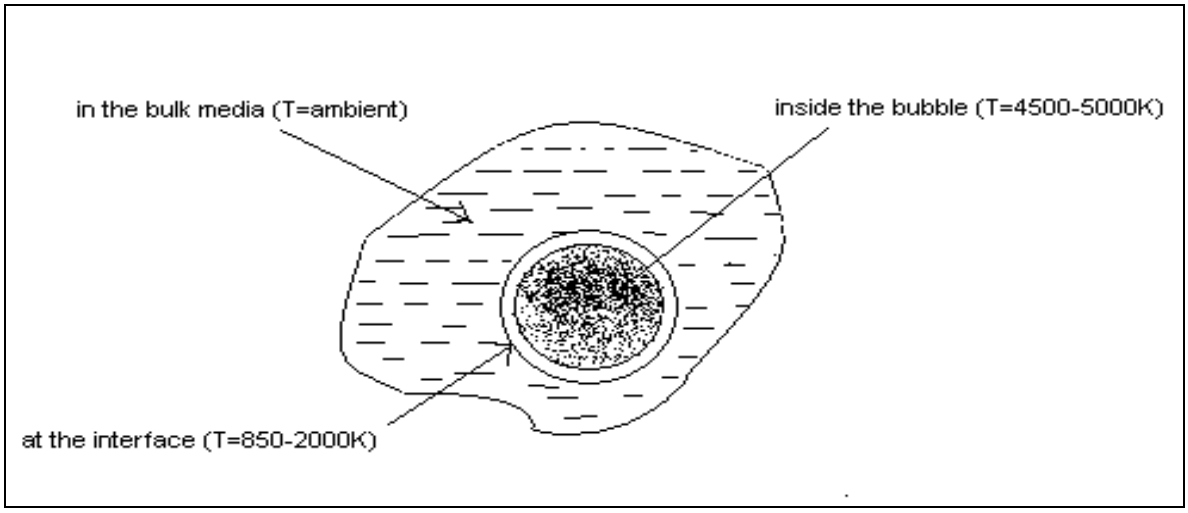

Figure 3.2. Possible sites of chemical reactions in homogeneous reaction media (Ince et al., 2001).

3.2.3. Parameters Affecting Sonochemical Reaction Systems

The main parameters affecting the degradation reaction efficiencies are the frequency of ultrasonic waves, properties of the target solute, the properties of the solvent used, the power intensity applied to the system, properties of the applied bubbling gas and addition of solids as catalysts to the system.

3.2.3.1. Frequency. The rate of free radical transfer from the bubble interior (and its interfacial sheath) into the solution bulk depends on the lifetime and collapse duration of the cavities, and therefore, to the intensity of the ultrasonic pressure, the geometry of the reactor and the frequency of the applied ultrasound waves. The more important cavity effects are reported to occur when the frequency of the ultrasonic wave is equal to the resonating frequency of the bubbles (Mason and Lorimer, 1990). The resonance radius of a bubble excited by low frequency waves is reported to be ~170 μm (at 20 kHz), and the cavities entrapping such bubbles are said to be "stable" or long-lived, with average life times of ~10 μs (Petrier et al., 1994; Colarusso and Serpone, 1996). In this kind of cavitation, the collapse stage is delayed till after the elapse of a number of compression and rarefaction cycles, during which sufficient volumes of volatile solutes and solvent vapours within the liquid may flow into the gas phase. The delayed growth and elongated collapse

of such gas-filled bubbles will allow radical scavenging and recombination reactions at the interfacial sheath, thus inhibiting the mass transfer of hydroxyl radicals into the solution (Barbier and Petrier, 1996). Hence, low frequency ultrasound is expected to induce effects only for hydrophobic solutes, which easily diffuse into the cavity bubbles to undergo pyrolytic destruction inside the collapsing bubble, or hydoxylation and thermal decomposition at its interfacial sheath, where pressure gradients and temperatures are still high enough to induce thermolytic fragmentation.

On the contrary, the resonance radii of bubbles excited by medium frequency (300-1000 kHz) ultrasound waves are extremely small (4.6 μm at 500 kHz), giving rise to very short-lived (0.4 μs on the average) and mainly void or vapour-filled "transient" cavitations (Suslick, 1994). The pressures and temperatures developed in such cavities are much higher than found in "stable" cavities, and larger energies are released into the surrounding liquid during their more rapid and violent collapse (Mason and Lorimer, 1990; Henglein, 1987; Suslick, 1990). Furthermore, such cavitations are so short-lived and the collapse is so rapid that the time for appreciable degree of radical scavenging reactions in the hot bubble or at the interfacial region is insufficient. As a consequence, medium frequency ultrasound waves are highly effective for catalyzing advanced oxidation processes, which are aimed to destroy non-volatile organic pollutants in the liquid medium via free radical effects. The destructive effect of ultrasound arises upon the highly probable ejection of uncombined hydroxyl radicals into the surrounding liquid during the collapse of cavity bubbles. (Lepoint and Mullie, 1994; Petrier et al, 1992; Barbier and Petrier, 1996).

3.2.3.2. Properties of Solute. It is obvious, then that the selection of the right frequency range (the region of conventional power ultrasound, or that of "sonochemical effects" ultrasound) is of utmost significance for achieving appreciable degrees of decontamination. The choice is based primarily on the physicochemical properties of the contaminating species, such as vapour pressure (or Henry's constant), solubility and octanol-water partition coefficient (Log K_{ow}) (Suslick, 1990; Hua and Hoffman, 1997). Hydrophobic chemicals with high vapour pressures have a strong tendency to diffuse into the gaseous bubble interior, and the most effective site for destruction, therefore, is the bubble-liquid interface and/or the bubble itself (Alegria et al., 1989; Kotronarou et al., 1991; Drijvers et al., 1999). Hence, aqueous solutions contaminated with volatile pollutants should

preferably be exposed to power ultrasound (whereby long-lived "stable" cavities are generated) for thermal and oxidation effects in the gas phase and the gas-liquid interface (Weavers et al., 1998; Kotronarou et al., 1991; Drijvers et al., 1999; Hung and Hoffmann, 1998). In contrast, hydrophilic compounds with low vapour pressures and low concentrations tend to remain in the bulk liquid during irradiation, due to the repulsive forces exerted to-and-from the slightly hydrophobic bubble surfaces. The major reaction site for these chemicals, therefore, is the liquid medium, where they may be effectively destroyed by oxidative degradation, provided that sufficient quantities of hydroxyl radicals are ejected into the solution during cavity collapse. As stated previously, maximum radical transfer into the bulk medium occurs when the collapse is "transient", or when sonication is carried out via medium frequency ultrasound waves. Moreover, at this frequency and at high concentrations of such solutes, an additional destructive pathway via thermal decomposition was observed, as demonstrated by the formation of pyrolysis products along with hydroxylated intermediates during sonolysis at 300-500 kHz (Vinodgopal et al., 1998a). The extent of destruction by pyrolytic fragmentation of non-volatile contaminants is directly related to their concentration and hydrophobicity, which dictates their ability to migrate towards the bubble and/or to accumulate at the bubble-liquid interface (Serpone et al., 1994). Consequently, the probable site for thermal decomposition of non-volatile solutes is the interfacial bubble sheath, at which solutes may accumulate via adsorptive processes during the formation and growth of acoustic cavities. At appreciable concentrations, the adsorptive tendency of non-volatile solutes on non-polar surfaces of cavity bubbles was verified by the exhibition of saturation type kinetics, typical of Langmuirian behavior, which is commonly proposed for describing photocatalytic process kinetics (Serpone et al., 1994).

3.2.3.3. Properties of Solvent. Each solvent will have its own particular parameters so that the choice of solvent medium becomes very important when considering the reaction conditions to be used for sonochemistry. Consider the solvents water and pentane: The intramolecular forces within these liquids are quite different, in that water has much stronger cohesion via hydrogen bonding than does pentane, which is held by van der Waals forces. Water also has a higher surface tension, giving water a much lower cavitation threshold than pentane (i.e. under otherwise identical conditions a greater intensity is required to cause cavitation in water than in pentane). The vapour pressure of water is

considerably lower than that of pentane, so that it is a better choice of medium for sonochemical reactions than pentane (Mason and Lorimer, 1990).

3.2.3.4. Power Intensity. The intensity (*I*) in sonication is directly proportional to the square of the amplitude of vibration of the ultrasonic source. The direct measurement of the amplitude at the vibrating tip of a probe transducer may be a physical measurement, which is simply achieved by observing the vibration using a metalurgical microscope with a calibrated eyepiece. This measurement will give a parameter that should be directly proportional to the acoustic power, which is being transmitted into the reaction solution where the probe is immersed into. The intensity has the unit W/m^2 and is calculated by the Equation 3.23:

$$I = \frac{P_a^{\,2}}{2\rho c} \tag{3.23}$$

where P_a = acoustic power (W),
r = density of water (g/cm^3)
c = speed of sound in water (1500 m/sec)

In general an increase in intensity will provide an increase in the sonochemical effects, but there are limits to the ultrasonic energy input to the system.

- A minimum intensity for sonication is required to reach the cavitation threshold. This minimum depends upon the frequency.
- When a large amount of ultrasonic power enters a system, a great number of cavitation bubbles are generated in the solution. Many of these will coalesce forming larger, more long lived bubbles. These will certainly act as a barrier to the transfer of acoustic energy through the liquid.
- At high vibrational amplitude the source of ultrasound will not be able to maintain contact with the liquid throughout the complete cycle. Technically this is known as decoupling, and results in a great loss in efficiency of transfer of power from the source to the medium. Decoupling is more effective when large

numbers of cavitation bubbles build up at or near the emitting surface of the transducer.

3.2.3.5. Properties of Saturating Gas. Aqueous media free of impurities are well known with their high cavitation threshold, so that any kind of interference to create "liquid defects" in the structure is reported to favour cavitation events (Mason and Cordemans, 1998). The easiest way of creating impurities in sonicated water is by saturating the solution with a soluble gas, which speeds up the initialization of cavity formation via provision of excess nuclei, while enhancing the collapse conditions by increasing the temperature within the cavity bubbles (Petrier et al., 1992; Riesz et al., 1990). However, since the first effect of cavitation is degassing, the solution will rapidly be free of dissolved gases if gas entrainment is ceased during sonication. It is a common practice, therefore, to bubble the liquid incessantly with a gas throughout the sonication period to maintain a constant gas flow into the bubbles so as to sustain the "extreme" conditions of collapse.

The selection of this gas is also of significance, because the final temperature of a collapsing bubble is closely related (by a power function) to a gas parameter, called the "polytrophic γ ratio", i.e. the ratio of specific heats (C_p/C_v) of ambient gases entrapped in the bubble (Noltingk and Neppiras, 1950; Riesz et al., 1990). The nature of the saturating gas is further important, due to the inverse relationship between thermal conductivity of a gas and the temperature build-up in a cavity bubble (Petrier et al., 1992; Hua and Hoffman, 1997).

Sonoluminescence studies with rare gases have shown that as the thermal conductivity decreases in the order: Xe < Kr < Ar < Ne < He, the amount of the heat loss to the surrounding liquid (due to heat conduction in the gas) also decreases, the collapse approaching perfect adiabatic conditions (Riesz et al., 1990; Hua and Hoffman, 1997). Hence, sonolytic radical yields increase with increasing effective temperature of collapsing bubbles, i.e. with increasing γ ratios, but decrease with increasing thermal conductivities of ambient gases (Hua and Hoffman, 1997). Furthermore, rare gases are more effective than diatomic gases (and air), owing to higher γ ratios obtained with monatomic gases in water (Hung and Hoffman, 1998; Riesz et al., 1990; Hua and Hoffman, 1997). However, despite equal γ ratios of Argon and Helium in water, much higher yields of pyrolysis products

were detected with the former, as attributed to its 10-fold lower thermal conductivity (Colarusso and Serpone, 1996).

Assuming adiabatic bubble collapse, the maximum temperatures and pressures within the collapsed cavitation bubbles are predicted by Noltingk and Neppiras from approximate solutions of Rayleigh-Plesset equations as follows (Noltingk and Neppiras, 1950; Neppiras,1980):

$$T_{\max} = T_o \left\{ \frac{P_a(\gamma - 1)}{P} \right\} \tag{3.24}$$

$$P_{\max} = P \left\{ \frac{P_a(\gamma - 1)}{P} \right\}^{\left[\gamma / \gamma - 1 \right]} \tag{3.25}$$

where T_o = ambient temperature in the solution bulk

P_a = pressure in the bubble at the moment of collapse (acoustic pressure)

P = pressure in the bubble at its maximum size or the vapour pressure of the solution

γ = polytrophic ratio.

3.2.3.6. Solids as Catalysts. The addition of solid catalysts, such as glass beads, ceramic disks, SiO_2, Al_2O_3 and talc into the reaction medium is another common method for enhancing cavitation effects. The presence of such material is reported to be especially useful for micronization of species (in ultrasonic cell disruption), and for the abrasion, activation and alteration of the chemical properties of catalyst surfaces during ultrasonic irradiation of liquid media (Mason and Cordemans, 1998).

3.2.4. Definition of the "Cavitation Threshold"

When very low power ultrasound is passed through a liquid and the power is gradually increased, a point is reached at which the intensity of sonication is sufficient to cause cavitation in the fluid. It is only at powers above the cavitation threshold that sonochemistry can occur because only then can the great energies associated with

cavitational collapse be released into the liquid. In the medical profession, where the use of ultrasonic scanning techniques is widespread, keeping scanning intensities below the cavitation threshold is of vital importance, so as not cause chemical reactions in the body (Mason and Lorimer, 1990).

3.2.5. Physicochemical Aspects of Sonochemistry

The main concern of scientists and engineers working with ultrasonic systems is to accomplish maximum reaction yields and/or maximum pollutant destruction at optimal conditions. Research and development in sonochemical systems exposed to the significance of two basic strategies for maximizing reaction efficiencies:

- Optimization of power and reaction configuration and/or enhancement of cavitation (Mason and Cordemans, 1998; Hua and Hoffman, 1997). The first strategy requires a mechanistic approach with features like:
  a. selection of the transducer (piezoelectric or magnetic material that converts electrical impulses to mechanical vibrations) and generator (probe types for low-frequency, and plate-types for high-frequency effects)
  b. configuration and dimensioning of the reaction cell
  c. optimization of the power efficiency (i.e. the effective power density delivered to the reaction medium).
- The second strategy, i.e. the enhancement of cavitation to maximize chemical reactivity involves the addition of different gases and solids into the system to test and compare their effectiveness in increasing reaction yields and/or reaction yields.

3.2.6. Ultrasonic Destruction of Phenol and Substituted Phenols: A Review of Current Research

The study presented in this section has been recently submitted to *Ultrasonics Sonochemistry* under the title **"Ultrasonic Destruction of Phenol and Substituted**

Phenols: A Review of Current Research" and is currently *in Press*. The following sections are a copy of this manuscript.

Introduction

Phenols are widely consumed in the industry such as in preservers of paint, leather, textile goods, and in the production of phenolic resins, disinfectants, medicine, caprolactam and bisphenol A. Improper handling of these compounds and/or inadequate discharge of their wastes result in long-term deterioration of the water environment and impose considerable risk on all life forms through their suspected carcinogenic properties (Kim et al., 2002).

Sonochemistry is a field, which studies the enhancement of chemical reaction and mass transfer rates under various ultrasonic conditions**.** It is based on the fact that when a liquid is exposed to a sufficiently large acoustic field, the pressure waves lead to the formation of liquid voids or cavitation holes, into which dissolved gases rush to form acoustic microbubbles (Suslick, 1997). As these bubbles expand during the rarefaction cycles of the pressure waves, they ultimately become too large to sustain themselves, thus undergoing violent implosions with release of very extreme temperatures and pressures at "local hot spots" in the liquid (Suslick et al., 1986). At this condition, gas molecules entrapped in gaseous cavity bubbles are thermally fragmented (pyrolysis) to dissociate into a variety of short-lived energetic species as free radicals.

The impact of a collapsing bubble on the contents of the surrounding liquid depends on the vibrational frequency of the applied field: if the frequency is low (20 kHz-100 kHz) mechanical effects overcome, whereas in the medium to high range (300-800 kHz) chemical effects dominate (Suslick, 1990). Environmental remediation by ultrasound involves pollutant destruction either directly via activating thermal decomposition reactions, or indirectly by the production and/or enhancement of oxidative species such as hydroxyl radicals (Ince et al., 2001).

Application of sonochemical techniques to aqueous systems to remove phenol and phenolic compounds has been widely investigated with emphasis on the identification and optimization of operating parameters such as frequency, pH, dissolved gases, reactor

geometry and the type of chemical reagents and catalysts. Many of such studies are focused on parametric and kinetic analyses of contaminant degradation, and comparison of reaction efficiencies with those conducted in the absence of ultrasound. The input concentrations range between 10^{-9}-10^{-3} M as typical of refractory organic compounds found in natural waters and conventionally treated effluents (Goel et al., 2004).

Background

Overview of radical sonochemistry

Implosion of cavity bubbles in sonicated water containing dissolved gases result in hydrogen and hydroxyl radicals by fragmentation of water molecules. These in turn combine and generate other oxidative species such as peroxy and superoxide radicals as well as hydrogen peroxide, the quantity of all depending on the ambient conditions and the operating parameters. A simplified reaction scheme showing the formation and depletion of radical species and hydrogen peroxide in sonicated water is given below (Goel et al., 2004; Riesz, 1991; Hart et al., 1986):

$$H_2O \rightarrow))) \bullet OH + \bullet H \quad (3.26)$$

$$\bullet OH + \bullet H \rightarrow H_2O \quad (3.27)$$

$$2 \bullet OH \rightarrow H_2O \quad (3.28)$$

$$2 \bullet OH \rightarrow H_2O_2 \quad (3.29)$$

$$2 \bullet H \rightarrow H_2 \quad (3.30)$$

If the solution is saturated with oxygen, additional reactions occur as a consequence of combination of molecular oxygen with hydrogen atom and the thermal decomposition of oxygen in the gas phase (Makino et al., 1982; Petrier et al., 1994):

$$O_2 + \bullet H \rightarrow \bullet O_2H \quad (3.31)$$

$$O_2 +))) \rightarrow 2 \bullet O \quad (3.32)$$

$$O + \bullet O_2H \rightarrow \bullet OH + O_2 \quad (3.33)$$

$$O_2 + O \rightarrow O_3 \quad (3.34)$$

$O + H_2O \rightarrow 2\bullet OH$ (3.35)

$\bullet O_2H + \bullet O_2H \rightarrow H_2O_2 + O_2$ (3.36)

In the case of ozone injection into solution, excess hydroxyl radicals are generated by decomposition of ozone in the aqueous (at pH>9.5) and gas phases as shown (Serpone et al., 1994; Kang and Hoffmann, 1998; Weavers et al., 1998; Hart and Henglein, 1985; Berlan et al., 1994):

$O_3 + H_2O \rightarrow 2HOO\bullet$ (3.37)

$O_3 + HOO\bullet \rightarrow \bullet OH + 2O_2$ (3.38)

$H_2O +))) \rightarrow \bullet H + \bullet OH$ (3.39)

$O_3 +))) \rightarrow O_2(g) + O(^3P)\ (g)$ (3.40)

$O(^3P)(g) + H_2O(g) \rightarrow 2\bullet OH$ (3.41)

Reactions of phenol, chlorophenol and nitrophenol in sonicated water

Phenol and its chloro/nitro derivatives are largely soluble in water so that the main reaction site for their destruction during ultrasonic irradiation is the bulk liquid, whereby hydroxyl radical attacks on the ring carbons results in various oxidation intermediates, which after sufficiently long contact undergo mineralization. Sonochemical degradation of phenol and the major intermediates as detected by HPLC analysis is as shown (Teo et al., 2001):

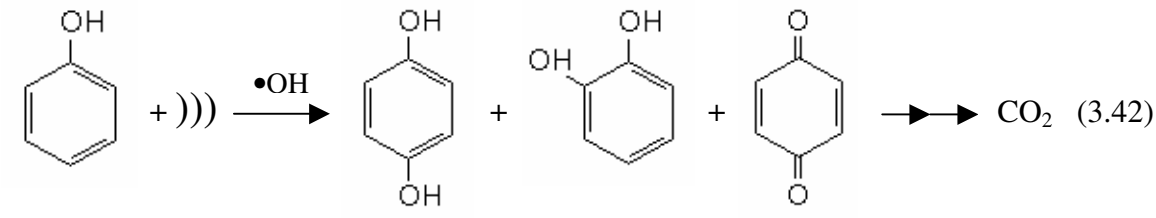

(3.42)

Phenol Hydroquinone Catechol p-benzoquinone

Monochlorophenols are water pollutants of moderate toxicity and are suspected of carcinogenic properties. They originate from natural degradation of chlorinated herbicides, chlorination of phenolic substances and disinfection of water (Serpone et al., 1994). Major

intermediates produced during their sonication are chloro-hydroquinone, hydroquinone, catechol, 4-chlorocatechol and 4-chlorosorcinol, which eventually are converted to acetylene, maleic acid, carbon monoxide and carbon dioxide (Serpone et al., 1994; Teo et al., 2001; Petrier et al., 1998).

Mononitrophenols are water pollutants of high toxicity and they are released into the water environment as a result of the synthesis and use of organo-phosphorus pesticides, azo dyes, and some medical goods (Asmar et al., 2005). Major intermediate products detected during their sonochemical degradation are 4-nitrocatechol (Petrier et al., 1998), benzoquinone, hydroquinone and a number of organic acids (Colarusso and Serpone, 1996; Gogate and Pandit, 2004).

Sonochemical Degradation of Phenol and its Derivatives: Impact of Ambient and Operational Parameters

Phenol

Serpone et al. (1992) have reported that ultrasonic removal of phenol at a concentration range of 30 to 70 μM, irradiated at 20 kHz with power intensities of either 25 or 50 W/cm^2 followed zero-order kinetics with k=0.08 μM/min They observed three principal intermediate products at pH=3 as catechol, hydroquinone and p-benzoquinone, whereas only catechol and hydroquinone were observed at natural pH (5.4-5.7) and no intermediates at pH=12. When the power intensity was increased to 75 W/cm^2 without changing the applied frequency, the decomposition process was found to exhibit pseudo-first order kinetics.

The study of Berlan et al. (1994) with 20 and 541 kHz irradiation in the presence of varying dissolved gases, catalysts and hydrostatic pressure showed that regardless of the reaction conditions 20 kHz was ineffective in phenol decomposition, while they could detect oxidation intermediates such as di-hydroxybenzene and quinone in effluents sonicated at 541 kHz. They have also reported that pyrolytic destruction of phenol in the gas phase is negligible; the degradation occurs mainly in the solution bulk and is accelerated with the addition of Fenton's reagent.

In another study by Petrier and Francony (1997), where relative efficiencies of 20 kHz, 200 kHz and 500 kHz were compared, it was reported that the most effective frequency for destroying phenol in solution was 200 kHz, as explained by the larger potential at this frequency for ejection of radical species to the bulk solution. Moreover, comparison of 487 kHz and 20 kHz by Petrier et al.(1994) have shown that the rate of degradation by the former was 10 times faster owing to the much faster hydroxyl radical transfer from the gas phase to the aqueous at this frequency than at 20 kHz. They reported that the larger efficiency of 487 kHz arises from the fact that at this condition radicals are concentrated at the surface of the solution, whereas at 20 kHz they are located intensely around the tip of the transducer.

Entezari et al. (2003) studied the degradation of phenol in the presence of H_2O_2, $CuSO_4$ and $H_2O_2/CuSO_4$ combination using a cylindrical ultrasonic reactor operated at 35 kHz, and compared their results with those obtained in more classical devices operated at 20 and 500 kHz, all at the same power. They found that the rate of degradation is highest at 500 kHz, but in the presence of H_2O_2 -$CuSO_4$ combination the novel reactor with 35 kHz turned out the most effective device by virtue of its larger surface area that provided more effective hydroxyl radical production in the presence of Fenton type regents.

Entezari and Petrier (2005) have investigated the degradation of phenol and its mixtures with p-cresol, p-chlorophenol and p-nitrophenol in aqueous medium during sonication at 423 kHz in the presence and absence of horseradish peroxidase. They found that in all mixtures the rate of phenol degradation was faster than when it was alone, but maximum enhancement was observed in the case of phenol-p-nitrophenol mixture, owing to the strong e-withdrawing capacity of the $–NO_2$ group. Moreover, whether in a mixture or not, the presence of the enzyme was reported to accelerate the rate of phenol decomposition.

In another study, Petrier and Casadonte (2001) have compared the degradation of phenol in oxygen and air-saturated solutions during sonication at 20 and 500 kHz. They reported that enhanced rates in the presence of air is due the fact that while O_2-saturated solutions involve mainly H_2O_2 and •OH as oxidative species, air-saturated solutions are

enriched with additional radicals such as $\bullet NO_2$ and $\bullet NO_3$, which are comparably strong oxidants if not as strong as the OH radical.

Zheng et al. (2005) studied the effect of carbon tetrachloride addition on the rate of phenol degradation at 20 kHz, reporting that the process was significantly accelerated by H-scavenging reactions of CCl_4 that indirectly increase the availability of uncombined OH radicals in solution.

Papadaki et al. (2004) have found that sonication at 20 kHz in the presence of Fenton's reagent was an inefficient method of phenol degradation for the fact that Fe^{+2} and ultrasound compete for H_2O_2 (by catalytic and thermal decomposition routes, respectively), thus reducing the concentration of Fenton's reagent in solution.

Wu et al. (2001) have studied the effect of UV irradiation on sonochemical degradation of phenol, reporting that while total phenol destruction was possible by this way the degree of mineralization was no more than 20.6%, which however, could be effectively improved by the addition of Fenton's reagent to the solution. Their investigation on the effect of the sparge gas showed that affectivity was in the order: Nitrogen<Air<Oxygen. In a similar study by Naffrechoux et al. (2000), the synergy observed in the degradation of phenol by combined UV irradiation and sonolysis at 500 kHz was explained by simultaneous action of three mechanisms on the overall process: photodecomposition; sonodecomposition and oxidation by ozone, which was produced by photolysis of atmospheric oxygen in solution.

In another study encompassing the combination of Advanced Oxidation with ultrasound at 20 kHz, Chen and Smirniotis (2002) have reported that ultrasound played deagglomeration role by microstreaming and microbubble cruptions caused by surface cleaning of TiO_2 particles. Moreover, they showed that interruption of UV irradiation for some intervals of time enhanced the efficiency of the destruction process. In a similar study by Drijvers et al. (1999), the decomposition of phenol was investigated under combined effects of sonolysis (at 520 kHz), chemical oxidation (with H_2O_2) and solid catalysts (e.g. Al_2O_3, ZnO, Ni_2O_3, CuO) and reported that the degradation was largely enhanced by H_2O_2 and CuO.

Substituted Phenols

Chlorophenols

The study of Serpone et al (1994) on the impact of substrate concentration on 4-chlorophenol degradation at 20 kHz irradiation showed that the reaction was zero order at low concentrations of substrate, but followed a mechanism similar to Langmurian adsorption when substrate concentration exceeded 75 μM. Petrier et al. (1998) reported that dechlorination of 4-chlorophenol was more efficient at 500 kHz than at 20 kHz, and the presence of Cl^- and hydroxylated intermediates in reactor effluents was reported as evidence of a two-step reaction. Hau et al. (2004) studied the degradation of p-chlorophenol under 1.7 MHz and their analysis of reaction by-products by MS and NMR spectroscopy revealed merely the presence of CO_2 and Cl^- as an indication of direct pyrolysis of the parent compound in the gas phase.

Consistently, Ku et al. (1997) claimed that the degradation of chlorophenols involve four different pathways as: free radical attack in the bubble, pyrolysis in the bubble, free radical attack at the bubble liquid interface and pyrolysis at the bubble liquid interface. They also reported that the reactions were not affected by altering the sparge gas between oxygen and air, as a consequence of their very close polytrophic gas ratios.

Lin et al. (1999) investigated the effects of initial solute concentration, pH and $FeSO_4$ on the decomposition and mineralization of 2-chlorophenol in aqueous solutions containing H_2O_2. They found that at a concentration of 100 mg/l, rates of decomposition and mineralization were 6.6-fold and 9.8-fold larger at pH=3 than at pH=11. The effect of was found insignificant when compared with that of H_2O_2 addition.

Moreover, De Visscher et al. (1998) have reported that the degradation of o-chlorophenol under 518 kHz in the presence of hydrogen peroxide was significantly faster than that in the presence of ultrasound or H_2O_2 alone. A study on the degradation of 2-, 3- and 4- chlorophenol at 200 kHz by Nagata et al. (2000) under argon and air media showed that the former was more effective, and the faster degradation of 3-CP was attributed to

three simultaneous points of o- and p- orientation of chlorine substituents, which enhanced addition reactions of electrophilic OH radicals on the ring carbons.

Investigation of the effects of reactor design by Teo et al. (2001) on the degradation of p-chlorophenol revealed that among the three test reactors they used: an 850 kHz plane type sonicator, a 20 kHz cup-horn sonicator and a 20 kHz horn type sonicator, the latter was the most efficient via provision of the highest deposited power in solution. In another study by Tiehm and Neis (2005), the effects of frequency and co-pollutants on dechlorination and toxicity reduction of chlorophenols were investigated. The authors reported that dechlorination was most efficient at 360 kHz, being retarded moderately by the presence of hydrophilic co-pollutants (e.g. acetate and glucose), and significantly by that of t-butanol. The original toxicity of the compounds was reported to be partially reduced by sonication.

Nitrophenols

Kotronarou et al (1991) found that in the presence of ultrasound (20 kHz), p-nitrophenol was denitrated to yield NO_2^- and NO_3^- by two independent mechanisms: gas phase reactions in pure water and the decay of the parent compound. Further, they reported that while the presence of NO_3^- did affect sonochemical degradation of p-nitrophenol, NO_2^- interfered with the process and the formation of the by-product 4- nitrocatechol. On the basis of products formed and the kinetics of the process, it was concluded that the degradation of p-nitrophenol involved high temperature reactions occurring at the gas-liquid interface and the main pathway was carbon-nitrogen bond cleavage with OH reactions providing a secondary reaction channel.

In another study by Cost et al. (1993) the degradation of p-nitrophenol was investigated at 20 kHz using natural waters containing phosphate, bicarbonate and humic acids. It was found that the rate of degradation was not dependent on constituents of natural waters owing to the fact that the mechanism involves thermal reactions at the gas-liquid interface of the cavitation bubbles not oxidation in the bulk solution.

Barbier and Petrier (1996) investigated the degradation and mineralization of p-nitrophenol at 20 kHz and 500 kHz in solutions saturated with oxygen and a mixture of oxygen-ozone. They found that the presence of ozone enhanced the mineralization of the intermediate degradation products. At low pH, where ozone auto-decomposition radical pathway was suppressed, they observed that mineralization at 500 kHz was 1.8 times faster than at 20 kHz to be attributed to increased ozone utilization at the higher frequency.

Finally in a recent study by Tauber et al (2000) conducted at 321 kHz with 4-nitrophenol, it was found that at pH=10 (pK_a=7.1) •OH-induced reactions in the aqueous phase are fully responsible for the degradation process, whereas at pH=4 oxidative pyrolytic degradation is the predominating reaction.

Conclusions

The use ultrasonic pressure waves for destroying phenolic compounds in water and wastewater is a promising approach to environmental remediation, owing to mechanical and chemical effects of ultrasound that produce oxidizing species such as OH radicals and H_2O_2 in the bulk solution, where these compounds undergo oxidative degradation. Operating parameters of main interest are the applied frequency, contact time, injected gas type, reactor configuration and pH, the proper control of which is of utmost significance for best results. In general, the optimum range for the frequency lies within 200-540 kHz, while that for the pH is the acidic region. Injection of mixtures of gases is preferred over injection of a single gas and mixtures containing nitrogen are more favorable due to the formation of nitrite and nitrate radicals. Integration of ultrasonic techniques with classical advanced oxidation tools (e.g. ozonation, UV irradiation, Fenton and photo-Fenton reactions) and heterogeneous catalysis definitely enhances the efficiency of the process.

4. MATERIALS AND METHODS

4.1. Materials

4.1.1. Chemicals

Phenol was purchased from Riedel Häen (97% pure) in solid form, and was dissolved in deionized water. Potassium ferrocyanide ($K_3Fe(CN)_6$), 4-aminoantipyrine, ammonium chloride (NH_4Cl), ammonium hydroxide (NH_4OH), sulfuric acid, methylene chloride and potassium hydrogen phthalate (KHP) and all other reagents were obtained from Fluka and used as received. All of Microtox reagents were purchased from Azur Environment, UK.

All reagents used during cultivation and analysis of bacterial counts were of analytical grade, and materials such as petri dishes, petri pads and filter papers were of Millipore quality. Tryptone (DIFCO), Yeast Extract (DIFCO) and NaCl (Merck) were used without further purification. Air, Argon and Oxygen were purchased from Habaş, with high purities, over 99%.

4.1.2. Apparatus

4.1.2.1. Ultrasonic Generators and Reactors: Definition of Systems as I, II , III. The systems are defined and explained below:

System I- 20 kHz probe-inserted reactor

The system is made of a 100 mL glass cell, which is surrounded by a water-cooling jacket to keep the reactor at constant temperature (20 ± 0.5 ^oC); a Bandelin Sonopuls HD2200 a probe type transducer (probe tip area = 2.5 cm^2), emitting ultrasonic waves at 20 kHz and a 180 W generator. The horn was submerged 1-2 cm from the top of a reaction cell, which had an effective volume of 80 mL. The system was mounted in a polyurethane isolating material to prevent excessive noise. A photographic view of the system is presented in Fig. 4.1.

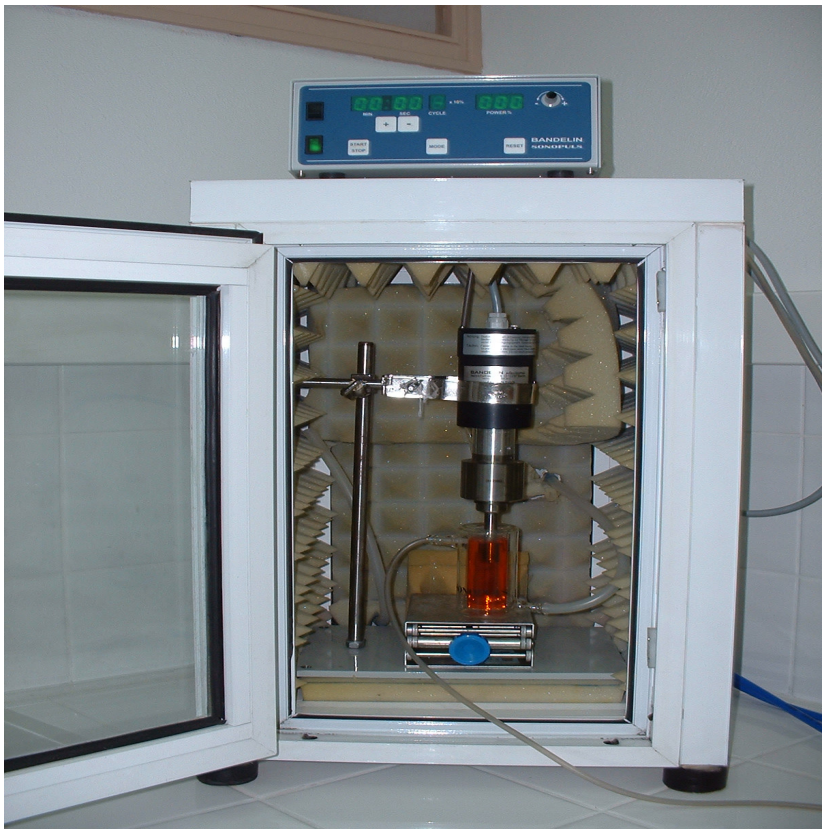

Figure 4.1. Photographic view of system I

System II- 300 kHz-plate type Reactor

The system (Undatim Ultrasonics – Belgium) consists of a 150 mL glass cell equipped with a water cooling jacket, a 300 kHz frequency plate type piezoelectric transducer (vibrational area= 22 cm^2) and a 25 W generator, which converts electrical power into ultrasonic energy. A photographic view of the system is presented in Fig. 4.2.

System III- 520 kHz plate type Reactor

The system (Undatim Ultrasonics-Belgium) consists of a 1200 mL glass cell equipped with a water cooling jacket, a stainless steel top cover, a 520 kHz frequency plate type piezoelectric transducer (vibrational area = 22 cm^2) and a generator with a power capacity of 100W (The generator can operate at 25 W for 300 kHz frequency option). A photographic view of system II is presented in Fig. 4.3.

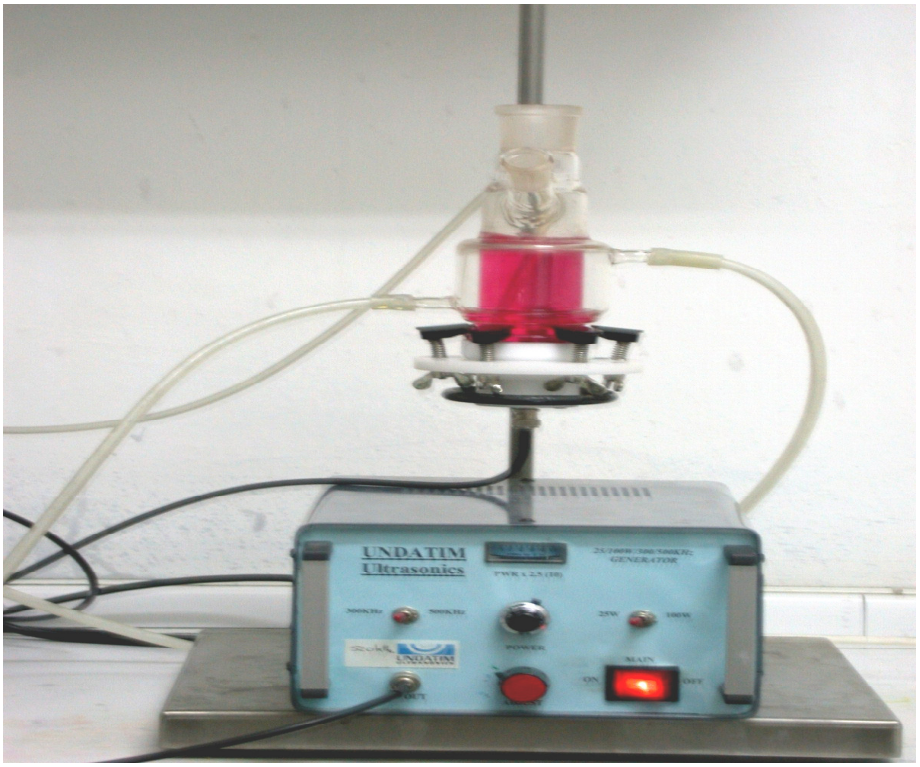

Figure 4.2. Photographic view of system II

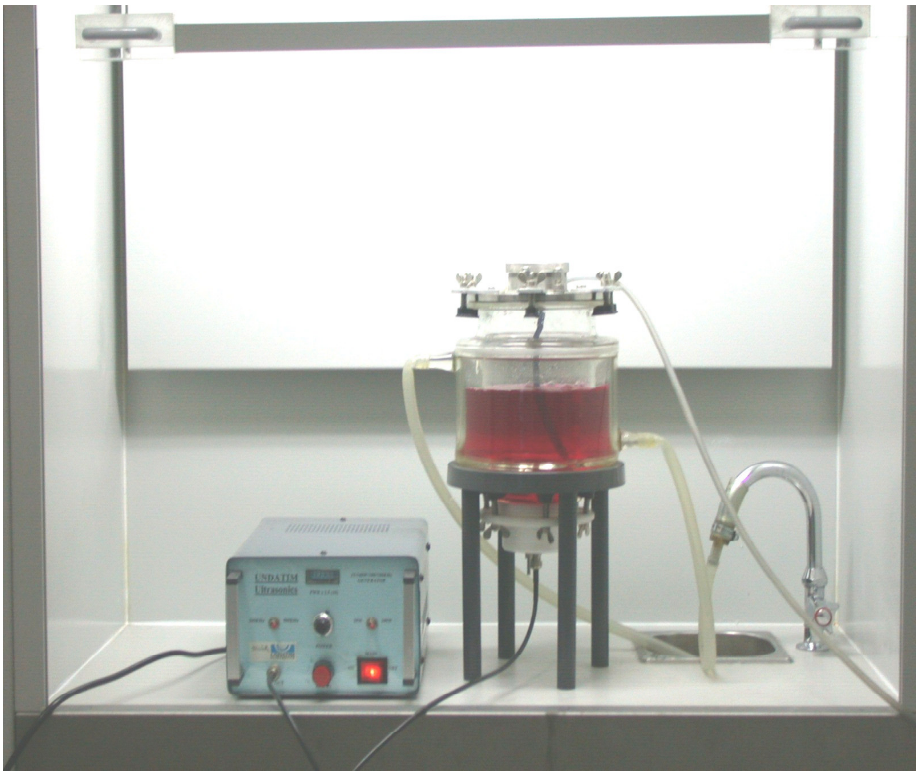

Figure 4.3. Photographic view of system III

4.1.2.2. The Ozone Generator; Ultrasound Systems Combined with Ozone and UV. Ozone was generated onsite from dry pure O_2 through an Ozonelab 100 Model (Ozone Service) generator. In combined operations, System II was integrated with the Ozone generator and/or UV lamp as shown Fig. 4.4.

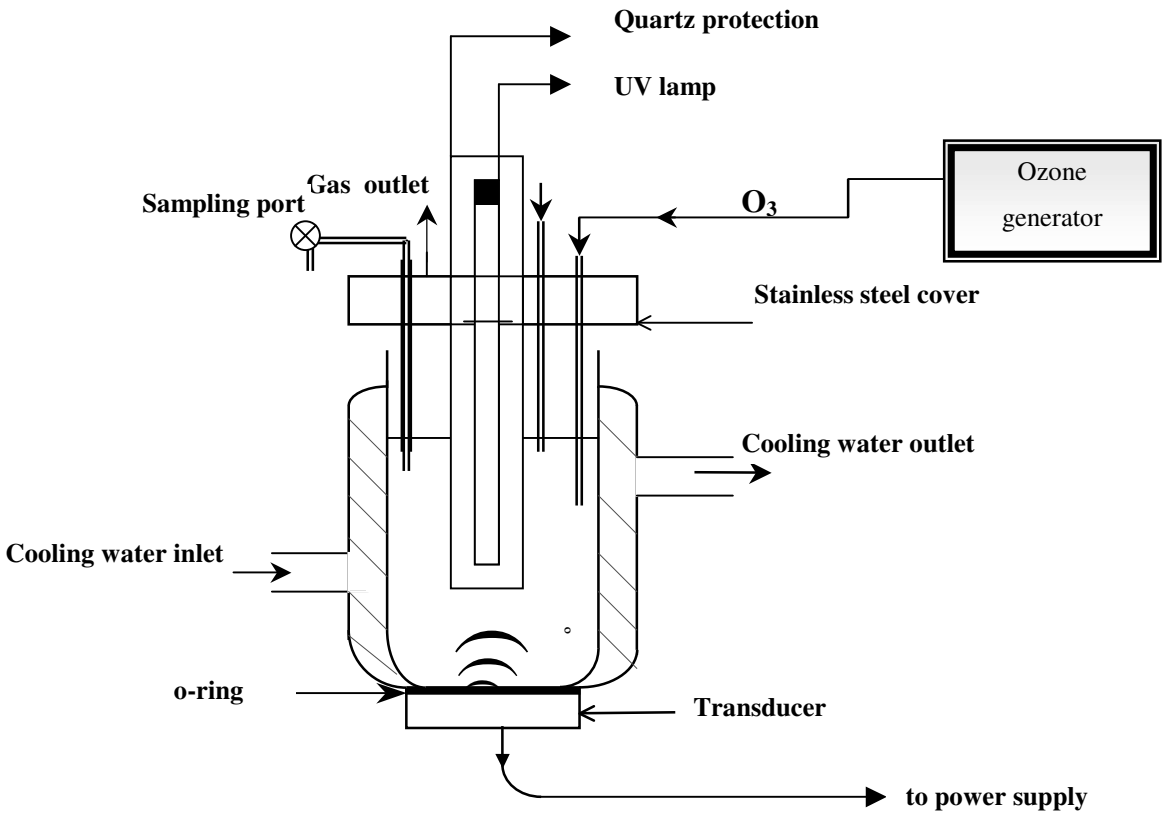

Figure 4.4. Schematic representation of the combined set-up

In the experimental runs with UV light only, ultrasound and ozone generators were shut down, while in O_3/US experiments the UV light was off. All were on in the tests involving UV irradiation, O_3 and ultrasound.

4.2. Methods

4.2.1. Bacterial Disinfection

4.2.1.1.Preparation of the Test Solutions. A pure culture of *E. Coli* was grown in LB (Luria Bertani) medium, prepared by mixing 1 g of Tryptone (DIFCO), 0.5 g of Yeast Extract (DIFCO) and 1 g of NaCl (Merck) in 100 mL of ultra pure deionized water; followed by sterilization in autoclave for 1 h (APHA/AWWA/WPCP, 1992). A clean and healthy colony of *E. Coli* was selected from the culture and placed in the growth medium in a closed container for 24 h to allow incubation at 37 ^{o}C in a shaking bath.

The bacterial concentration in the medium at the end of the incubation period was approximately 10^{10} /mL in accordance with the "Membrane Filter Technique" of coliform count, based on the formation of colonies in standardized Endo-Broth growth medium (Sambrook et al., 1989). The test solutions were prepared by serial dilutions of this stock using ultra pure deionized water and a phosphate buffer to prevent cell damage by osmotic pressure.

4.2.1.2. Experimental Procedure.

Sonolysis of bacterial test solutions with Ultrasound: 80 mL of the test solutions were placed in System I and the generator was activated at 30% of the 180 W power for 20 minutes.

Treatment of bacterial test solutions with the Solid Catalysts: 80 mL of the test solutions were placed in System I and the solutions were mixed continuously for 20 minutes without any ultrasonic power, in the presence of ceramic granules (irregular size) prepared in the laboratory, metallic zinc particles (0.6x0.25mm) of HACH, and granular activated carbon (0.84x0.25 mm) of AQUATECH. In heterogeneous samples, the mass concentration of the solids was 0.12 g/L in each run, irrespective of the solid type.

Treatment of bacterial test solutions with Ultrasound / Solid Catalysts: 80 mL of the test solutions were placed in System I, coupled with the addition of the solid catalysts each of which have the concentration mentioned above and the generator was activated at 30% of the 180 W power for 20 minutes.

The bacterial test was repeated with the spent AC granules in one of the control experiments, where the ultrasonic power was off.

4.2.1.3. Analytical Method. Bacterial count was performed by using the "Membrane Filter Technique". Test samples were filtered through the 1μm pore-size filter papers, by using the vacuum pump and the vacuum filter. The filter papers were placed into the petri dishes which were wetted with the Endo Broth growth medium. 24±4 hours waiting time, at 37^{o}C, is required in order to obtain countable colonies, each of which represent an original *E. coli* in the representative sample solution.

4.2.2. Phenol Removal

4.2.2.1. Preparation of the Test Solutions. A stock phenol solution of 0.5 M was prepared in deionized water and stored at 4 °C in the dark. Test samples of 0.005 M, 0.002 M, 0.001 M, 0.0005 M and 0.00025 M were diluted from the stock using deionized water.

4.2.2.2. Experimental Procedure. Sample volumes in systems I, II and III were 80 mL, 100 mL and 300 mL, respectively. The test solutions were bubbled with air or argon for 30 min prior to sonication, which lasted 90 min, and the same gas used for saturation was continually sparged into the solution throughout exposure. Samples were withdrawn from the reactors every 10 min for duplicate analysis of the antipyrine complex by spectrometry. The molar concentration of phenol was estimated from a calibration curve plotted for five data sets using fixed concentrations of phenol (Appendix A).

4.2.2.3. Analytical Methods.

Spectrophotometric Analysis: Concentration of phenol was monitored using the spectrophotometric method by the 4-aminoantipyrine method (APHA/AWWA/WPCP,

1992) using a UNICAM-Heλios, Alpha/Beta double beam spectrophotometer with an optical pathlength of 1 cm. The method is based on the reaction of phenol with 4-aminoantipyrine in the presence of potassium ferrocyanide at pH=7.9 to form a colored antipyrine complex (AMPH), which is quantified by absorbance measurement at 500 nm. The procedure involved the following steps: After preparing a 100 mL distilled water blank and series of 100 mL phenol standards, they were treat as follows:

- Add 2.5 mL 0.5 N NH_4OH and immediately adjust to pH 7.9 ± 0.1 with phosphate buffer (3 mL).
- Add 1.0 mL 4-aminoantipyrine solution, mix well, add 1.0 mL $K_3Fe(CN)_6$ solution, and mix well.
- After 15 min, transfer to cells and read absorbance of sample and standards against the blank at 500 nm..

Preparation of Reagents for Spectrophotometric Analysis

Ammonium hydroxide solution: NH_4OH, 0.5N. Dilute 35 mL fresh, concentrated NH_4OH to 1I L with water.

Phosphate buffer solution: Dissolve 104.5 g K_2HPO_4 and 72.3 KH_2PO_4, in water and dilute to 1 L. The pH should be 6.8.

4-aminoantipyrine solution: Dissolve 2.0 g 4-aminoantipyrine in water and dilute to 100 mL. Prepare daily.

Potassium ferricyanide solution: Dissolve 8.0 g $K_3Fe(CN)_6$ in water and dilute to 100 mL. Filter if necessary. Store in a brown glass bottle. Prepare fresh weekly.

Formation of the colored antipyrine complex (AMPH) is as follows:

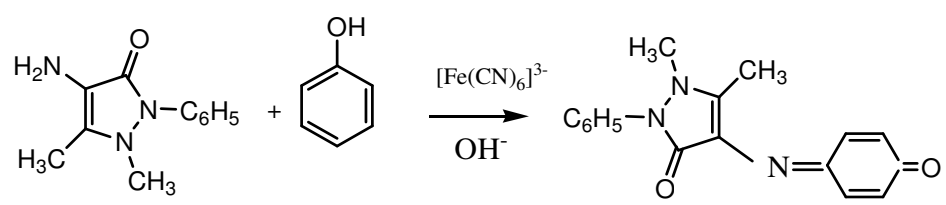

4-aminoantipyrine Phenol AMPH

Gas Chromatography (GC) Analysis: For the determination of intermediates of phenol, some samples were analysed using an Agilent 6890N gas chromatograph. The system was equipped with an auto-injector, which works either in split or splitless mode. Chromatographic separations were achieved on a HP5 capillary column. The column had a length of 30 m, an inner diameter of 250 μm and was coated with a stationary phase film of 0.25 μm. The detector was flame ionization detector (FID) and it was heated to 300^{o}C. The carrier and the make-up gas were Helium. The analysis method was built on Environmental Protection Agency (EPA) methods 604 and 8270, which are proposed for the determination of phenols in water (EPA, 2005a; EPA, 2005b).The applied temperature program was as follows: Oven was heated from 40 ^{o}C (1 min) to 100^{o}C at 10^{o}C/min, subsequently to 260^{o}C at 20^{o}C/min

Samples were prepared by extracting 1.0 mL aqueous phenol solutions into 0.5 mL methylene chloride. The volume of the automatic injection was adjusted at 2 μL and the sample was injected into the 240^{o}C injector inlet. A series of phenol solutions were injected to the GC, to achieve a calibration curve and it was utilized for the quantification of phenol as presented in Appendix A.

Toxicity Analysis: Toxicity of the phenol solutions was determined using a Microtox Model 500 Analyzer, which utilizes freeze-dried luminescent bacteria (*V. fisheri*) as test organisms. The test system is based on the principle that bacterial luminescence is tied directly to cell respiration, so that any inhibition of cellular activity (due to toxicity) results in a reduction in the degree of luminescence. The Microtox analyzer is made of an array of sample wells for holding dilutions of bacterial suspensions, and a photometer to measure the light output of *V. fisheri* at 0, 5 and 15 min after contact with the toxicant. Light readings are compared to those of control bacteria (healthy) to determine the inhibition of light emission, and to estimate the EC_{50} of the sample (EC_{50} is defined as the effective concentration of the toxicant- expressed as percentage relative to the original sample strength- that causes a 50 per cent reduction in the light output of the test organisms during the designated time interval). Sample preparation, osmotic adjustment and serial dilution procedures were carried out by reference to the Basic Protocol of the Microtox assay (Microtox Manual, 1992). A photograph of Microtox Analyzer is given in Figure 4.5.

Figure 4.5. Photographic view of the Microtox toxicity analyzer.

*Total Organic Carbon (TOC) Analysis:*Total organic carbon (TOC) monitored with a Shimadzu TOC-V CSH analyzer. The instrument was calibrated by standard solutions of KHP (5-30 ppm).

Hydrogen Peroxide (H_2O_2) Analysis: Hydrogen peroxide (H_2O_2) determination was carried out following the triiodide method procedure described by Klassen et al., (1994). The triiodide method is based on the reaction of (I^-) with H_2O_2 to form triiodide ion (I_3^-), which has a strong absorbance at 351 nm. The analysis of H_2O_2 at concentrations as low as 1mM is conveniently proceeded by determining the yield of I_3^- formed when H_2O_2 reacts with KI in a buffered solution containing ammonium molybdate tetrahydrate as a catalyst. Two sample solutions (A and B) were prepared as described below and 2.5 mL of each was mixed with one another and 1 mL of sample to record the absorbance at 351 nm.

Solution A: 33 g of KI, 1g of NaOH and 0.1 g of ammonium molybdate tetrahydrate diluted to 500 mL with deionized water. The solution was stirred for 1 h to dissolve the molybdate. It must be kept in dark in order not to cause I^- to oxidize.

Solution B: 10 g of potassium hydrogen phthalate was dissolved in 500 mL to act as the buffer solution.

4.2.3. Phenol Removal with Combined US/ O_3/UV Processes

Test samples of phenol were prepared according to the procedure mentioned in section 4.2.2.1. and they were exposed to 300 kHz ultrasonic irradiation coupled with UV/O_3 exposure in the combined systems.

5. RESULTS AND DISCUSSIONS

5.1. Optimization of Power and Reaction Volumes in Ultrasonic Reactor Systems

An ultrasonic system transforms electrical power to vibrational energy, which is then transmitted into the sonicated reaction medium. Part of it is lost to produce heat, and another part produces cavitation, but not all of the cavitation energy produces chemical and physical effects. Some energy is reflected and some is consumed in sound re-emission. Hence, there can be significant differences between the power supplied from the generator and that delivered into the reactor. In a pure liquid, one might assume that almost all of the mechanical energy is transformed to heat by absorption. Of the methods available to measure the amount of ultrasonic power entering a sonochemical medium, the most common and easiest is calorimetry, which involves a measurement of the initial rate of heating produced when a system is irradiated by ultrasound (Mason, 1999). The method involves the measurement of the temperature rise T against time for about 30 seconds, using a thermocouple placed in the reaction vessel. From T versus t data, the temperature rise dT/dt can be estimated either by curve fitting the data to a polynomial in t, followed by constructing a tangent to the curve at time zero. The ultrasonic power (P_d) actually entering the system can then be calculated by substituting the value of dT/dt into Equation 5.1 (Mason, 1999; Mason and Cordemans, 1998):

$$P_d = (dT/dt)\, C_p\, M \qquad (5.1)$$

where P_d = power dissipated in the system (W)

C_p = specific heat of water (4.184 J/g.^{o}C)

(dT/dt) = the change in temperature at certain time interval (^{o}C/sec)

M = mass of water in the reaction vessel (g)

The power which is calculated by calorimetric method is used to determine the ultrasonic intensity in the reactor. Ultrasonic intensity may have the unit W/cm^2 (power per unit emitting area), or W/mL (power per unit volume of water in the reactor).

5.1.1. Determination of Ultrasonic Power in System I

The ultrasonic generator was operated at any multiples of 10 that is a fraction of the total capacity (180 W). The power input was determined by the calorimetric method using tap water as the sample. The results of calorimetric experiments are listed in Table 5.1.

Table 5.1.Temperature increase in System I during sonication of tap water for 4 min under varying power inputs without cooling

time, sec	Power input %,						
	P= 10%	P=20%	P=30%	P=40%	P=50%	P=60%	P=70%
	Temperature, ^{o}C for 80 mL sample volume						
0	18.00	22.00	21.00	23.00	21.00	22.00	23.00
30	21.00	25.00	25.00	26.50	26.00	27.00	28.50
45	22.00	26.50	26.50	29.00	28.00	29.50	31.00
60	22.00	28.00	28.00	30.50	30.50	32.00	33.00
90	23.00	30.50	31.00	34.00	35.00	37.00	38.00
120	24.50	33.50	34.00	38.00	39.00	42.00	43.50
150	25.00	36.00	37.50	42.00	43.00	47.50	50.50
180	27.50	39.00	40.50	45.50	47.50	51.50	55.00
210	28.00	41.50	43.00	49.00	51.50	55.50	58.00
240	30.50	44.00	47.00	53.50	55.00	59.50	63.00

Plots of T vs. time for all applied power inputs and the fit of the data to the best polynomial or straight line are presented in Figure 5.1. The value of dT/dt for each set was estimated from the slope of the curves or the tangent at the point of inflection, as given in Table 5.1. The reason why the highest applied power is only 70 % of the total is because above that value, there was the threat of overheating, which could seriously damage the probe.

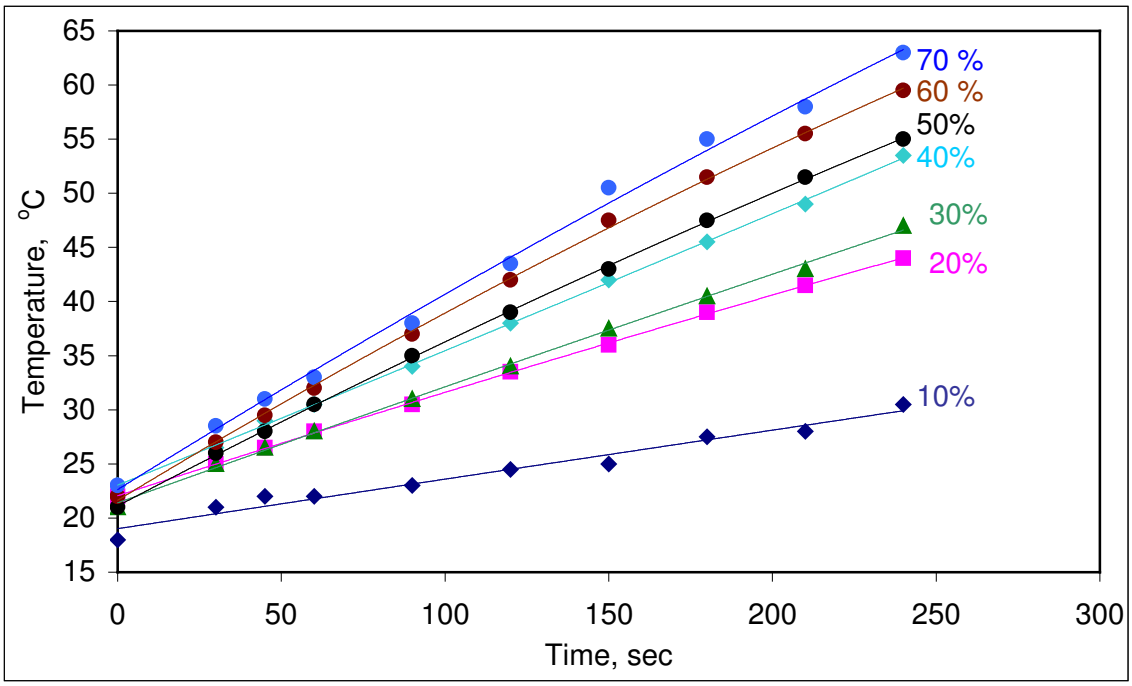

Figure 5.1. Polynomial fits for changes in temperature in 80 mL reaction volume in System I for various generator outputs.

Table 5.2 Estimations of dT/dt from the curves in Figure 5.1

Applied Power (as % of Maximum-180 W)	P=10%	P=20%	**P=30%**	P=40%	P=50%	P=60%	70%
dT/dt (^{o}C/sec)	0.046	0.099	**0.111**	0.126	0.157	0.180	0.184

The values in Table 5.2 were used in Equation 5.1.for calculating the power dissipated in solution, and the results are presented in Table 5.3.

Table 5.3. The dissipated powers in solution at each input power in System I

Applied Power (as % of Maximum-180 W)	P= 10%	P=20%	P=30%	P=40%	P=50%	P=60%	70%
Power in solution (W)	15.4	330	**37.3**	42.1	52.4	60.2	61.6

As obvious in the above table, the higher the applied power the larger is the transferred energy in solution. However, for reasons of economy and prevention of excess heating, the optimum power was selected as 30%, at which the effective power in solution was 37.3 W.

The power densities found by dividing the dissipated powers by the reaction volume (80 mL) at each applied power are presented in Figure 5.2 as bar charts.

$$Power-density=\frac{P_d(W)}{V(mL)} \tag{5.2}$$

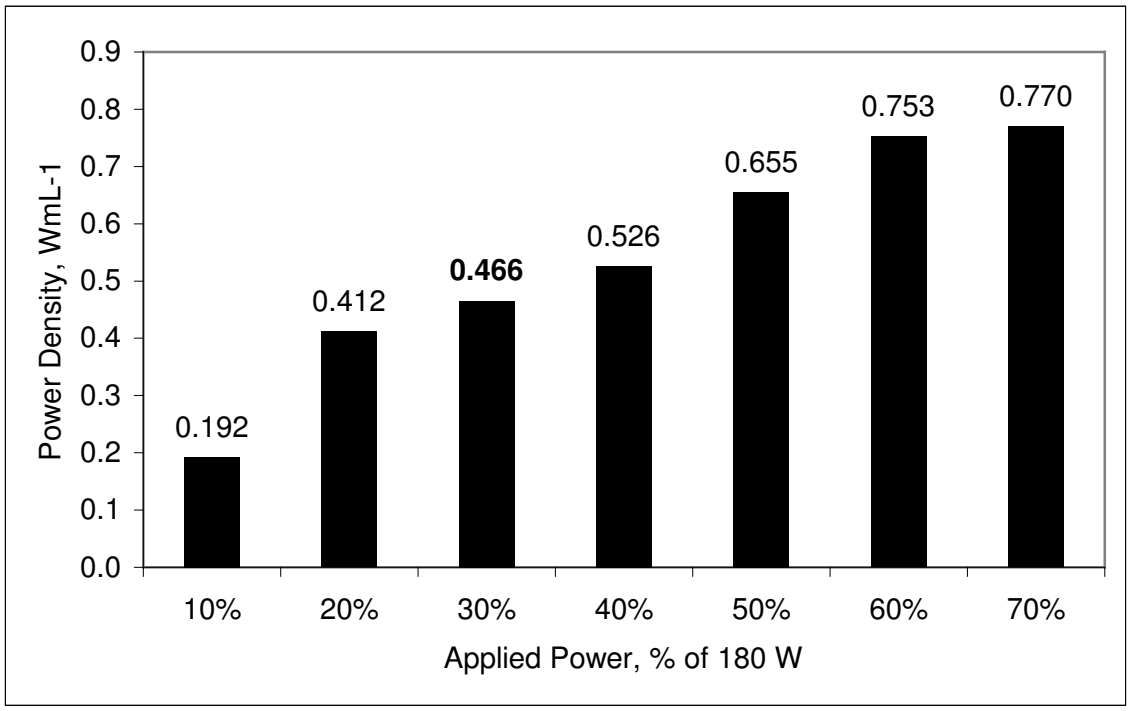

Figure 5.2. Representation of power density as a function of applied power

Calorimetric determination of the dissipated power P_d was repeated for three other volumes (other than 80 mL), and the results are tabulated in Table 5.4. Despite the fact that the smaller the solution volume the better is the power transfer efficiency, selecting any volume smaller than 80 mL resulted in serious drawbacks in continuous sampling to monitor the decay rates. Note that the selected power and volume for the system are 80 mL and 54 W (30%), at which the power in solution is 37.25 W.

Table 5.4. Impact of solution volume on the power dissipated in solution (W)

Generator power (W)	70 mL	80 mL	90 mL	100 mL
18.00 (10%)	14.13	15.40	17.80	19.61
36.00 (20%)	31.59	32.97	33.76	36.51
54.00 (30%)	38.61	37.25	39.78	43.95
72.00 (40%)	44.00	42.07	44.38	47.68
90.00 (50%)	50.21	52.42	53.79	56.67
108.00 (60%)	59.22	60.22	63.65	65.95
126.00 (70%)	63.55	61.59	66.17	69.42

5.1.2. Determination of Ultrasonic Power in System II

The ultrasonic generator was operated at 5, 10, 15, 20, 25 W power inputs upto the maximum power supplied by the generator (25 W). The optimum power input was determined by the calorimetric method using tap water as the sample. Examples of the results of these experiments applied at 25 W are listed in Table 5.5.

Table 5.5. Temperature increase in System II during sonication of tap water for 5 min under 25 W power input without cooling

t (sec)	0	30	60	90	120	150	180	210	240	270	300
T (^{o}C)	16	17.5	18.5	20	21	22	23	24	25	25.5	26.5

The temperature data were plotted against time fitted to a polynomial as shown in Figure 5.3. The value of dT/dt is estimated as 0.0454 from the fitted curve.

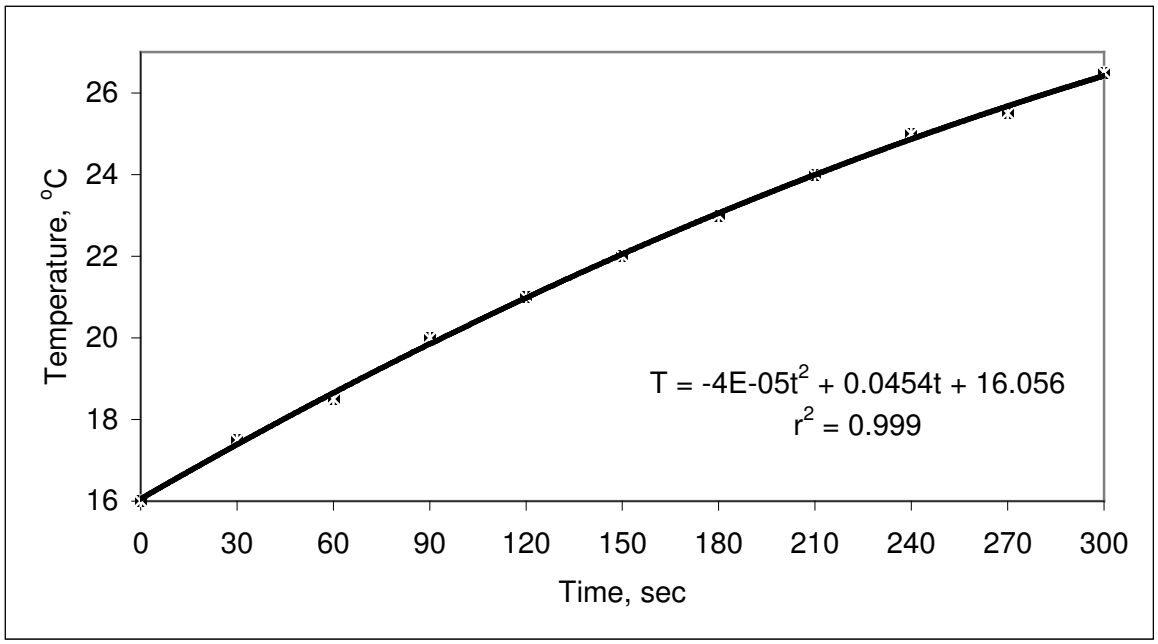

Figure 5.3. Polynomial fit for change in temperature in 100mL reaction volume in System II for 25 W power output.

The dT/dt value was used in Equation 5.1. for calculating the power dissipated in solution and the power density:

$$P_d = 0.0454 \frac{^oC}{\sec} x4.182 \frac{J}{g\,^oC} x100g = 18.986 - W \tag{5.3}$$

$$Power - density = \frac{18.986W}{100mL} \cong 0.190 \frac{W}{mL} \tag{5.4}$$

Calorimetric determination of the dissipated power P_d was repeated for two other volumes (other than 100 mL), and the results are tabulated in Table 5.6. Note that at 80 mL, maximum efficiency is accomplished at an applied power of 25 W as presented in Figure 5.4.

Table 5.6. Impact of Solution volume on the power dissipated in solution (W)

Generator power (W)	100 mL	125 mL	150 mL
5.00	1	-	2
10.00	7	4	4
15.00	9	7	6
20.00	12	13	11
25.00	19	14	12

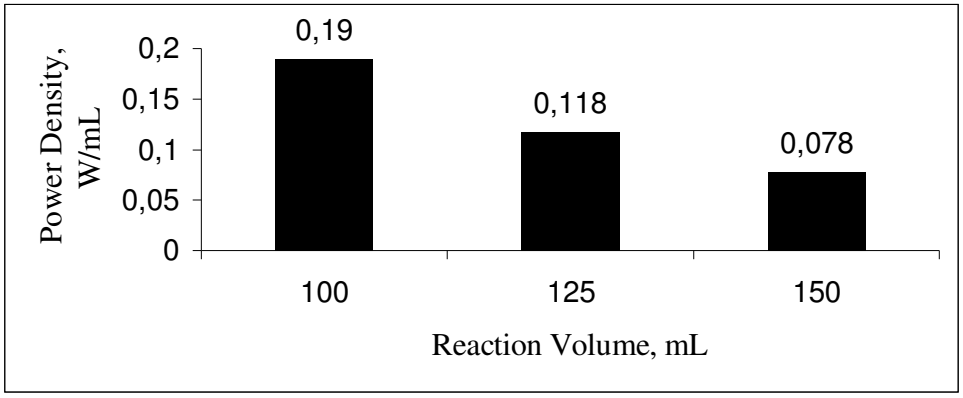

Figure 5.4. Representation of power density as a function of applied power

5.1.3. Determination of Ultrasonic Power in System III

The ultrasonic generator was operated at 20, 40, 60, 80, 100 W power inputs up to the maximum power supplied by the generator (100 W). The optimum power input was determined by the calorimetric method using tap water as the sample. An example of the results of these experiments applied at 40 W are listed in Table 5.7.

Table 5.7. Temperature increase in System III during sonication of 300 mL tap water for 5 min under 40 W power input without cooling

t (sec)	0	30	60	90	120	150	180	210	240	270	300
T (^{o}C)	26.5	27.5	28.5	29	30	31	31.5	32.5	33.5	34	34.5

The temperature data were plotted against time fitted to a polynomial as shown in Figure 5.5. The value of dT/dt is estimated as 0.0312 from the fitted curve.

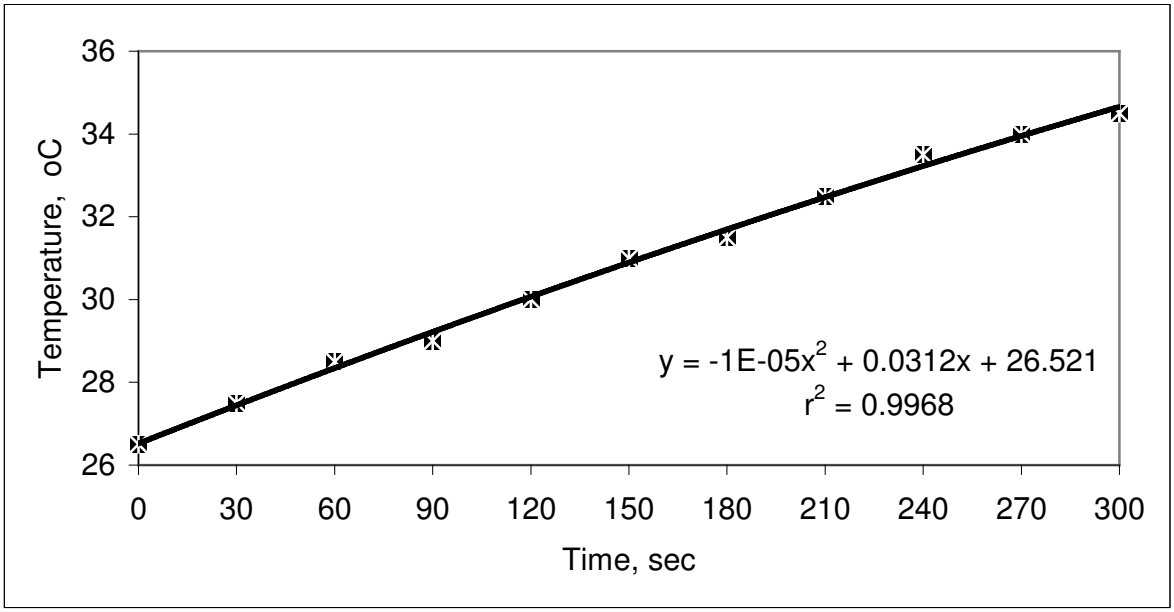

Figure 5.5. Polynomial fit for change in temperature in 300mL reaction volume in System III for 40 W power output.

The dT/dt value was used in Equation 5.1. for calculating the power dissipated in solution and the power density:

$$P_d = 0.0312 \frac{^oC}{\sec} x4.182 \frac{J}{g\,^oC} x300g = 39.144 \cdot W \tag{5.5}$$

$$Power - density = \frac{39.144W}{300mL} \cong 0.130 \frac{W}{mL} \tag{5.6}$$

Calorimetric determination of the dissipated power P_d was repeated for three other volumes (other than 300 mL), and the results are tabulated in Table 5.8. Note that at 300 mL, maximum efficiency is accomplished at an applied power of 40 W as presented in Figure 5.6.

Table 5.8 Change in power density with changing volumes.

Generator power (W)	300 mL	600 mL	900 mL	1200 mL
20.00	31.44	-	28.220	39.100
40.00	39.14	35.86	32.460	36.610
60.00	25.08	29.56	31.260	35.490
80.00	21.12	25.12	26.850	34.140
100.00	20.73	17.53	24.810	-

The maximum power density was obtained when the power of the generator was 40 W. It was found that the power which is transferred into the reaction medium (power input) was increasing upto 40 W, but afterwards there was a declining tendency in power input, despite that the applied power was increased. The increase in acoustic power increases the maximum radius of the cavity bubble, as well as increases its time of collapse (Gogate and Pandit, 2004). When too much power is applied to the solution, excess number of bubbles can be formed and then they coalesce forming larger and more longer lived bubbles and act a barrier to the transfer of acoustic energy through the liquid. Decoupling effect can be the other reason for the loss in energy efficiency of transfer of power from the source to the medium by the formation of large numbers of cavitating bubbles at or near the emitting surface of the transducer (Mason, 1999). So, the working power for the 520 kHz system ultrasound studies was selected as 40 W. The minimum volume of the reaction should not be less than 300 mL, because the depth of the liquid should be at least a couple of centimeters to enable the scientist to take trustable samples without touching the surface of the transducer.

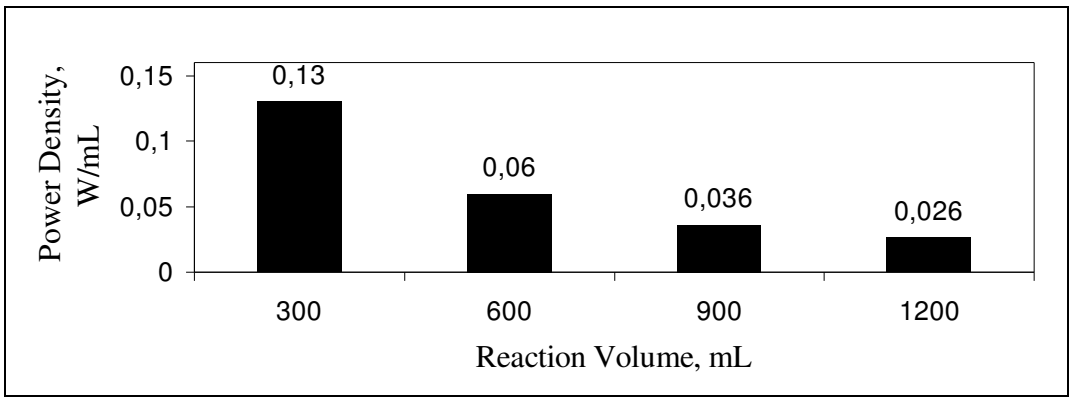

Figure 5.6. Representation of power density as a function of applied power

5.2. Bacterial Disinfection with Ultrasound

5.2.1. Aqueous Phase Disinfection with Power Ultrasound: Process Kinetics and Effect of Solid Catalysts

The study presented in this section was published in *Environmental Science and Technology,* 2001, 35 (9), 1885-1888 under the title "**Aqueous Phase Disinfection with Power Ultrasound: Process Kinetics and Effect of Solid Catalysts**". The following is a copy of the paper as published.

Introduction

Disinfection has become a challenging aspect of water treatment due to rapid elevation of health standards and the growing concern in pollution-free water resources. The most commonly practiced methods are those that involve chemical (e.g. chlorination and ozonation), and physical (e.g. treatment with heat and/or ultraviolet light at 254 nm) processes. Chlorination, as the most cost-effective of all, has been noted in recent years for its adverse health effects originated by residual chlorine, which reacts with natural organic matter to form carcinogenic by-products. Ozonation has lately emerged as a viable alternative by virtue of its non-residual effect, but more research is required to lower its operational costs and to protect the water from re-infection in the distribution system.

Decontamination of water bodies using ultrasonic techniques is a growing field, while the well known effectiveness of power ultrasound (20-100 kHz) for its surface cleaning action has been successfully utilized in some patented systems that find application in institutional and medical facilities for disinfecting non-disposable implements and accessories. Bacterial removal by these systems involves their dislocation from adhered surfaces and crevices, which are rather difficult to reach by conventional cleaning methods (Mason, 1999). Moreover, recent studies with aqueous systems have shown that power ultrasound is capable of inactivating bacteria, viruses and fungi in water, but long contact or high intensities are required for accomplishing high rates of kill (Scherb et al., 1991; Phull et al., 1997). It was further shown that bacterial survival under ultrasonic effects exhibits an exponential behavior, while the shear forces set up by cavitation bubbles are insufficient to

rupture the cells (unless by prolonged contact), although they disengage the more delicate attachment sites of the DNA to the membrane (Graham et al., 1980). The results of a novel study on the effects of discrete frequencies and dissolved gases have shown that germicidal effectiveness of ultrasound depends strongly on the frequency (highest at 205 kHz), but moderately on the power intensity and gas properties, being highest in argon-oxygen mixtures (Hua and Thompson 2000).

Most of the above effects are mechanical in origin, arising from cavitation events, which consist successively of the formation, growth and collapse of gas-filled microbubbles, during which temperatures and pressures of 5000^{o}C and 500-2000 atm are released (Mason, 1990; Dahlem et al., 1993). At these extreme conditions, gases and vapors of the surrounding liquid (entrapped in the bubbles) undergo pyrolytic destruction to dissociate into a variety of radicalar species (Crum, 1994; Serpone et al., 1994). Depending on the vibrational frequency (which dictates cavity lifetime and collapse duration), some of these radicals may migrate to the solution bulk to attack the cellular membrane for biocidal effects, while some may recombine to form molecular oxidants to act as secondary biocides. The fragmentation of water molecules during the collapse of cavity bubbles results in hydroxyl radicals, which upon recombination are converted to hydrogen peroxide. Hence, this and the uncombined radicals are believed to act as chemical biocides in infected waters, and power ultrasound is capable of enhancing their effects by breaking-up biological flocs and disrupting cell walls, leading to increased bacterial susceptibility and easier penetration of the biocide into the organism (Mason et al., 1993).

Due to long contact and large power requirements to achieve high rates of disinfection by ultrasound, current research on ultrasonic means of bacterial inactivation is focused on combining the system with chemical processes to enhance the germicidal action of biocides and to reduce chemical requirements. It was shown that the ozone requirements for constant kill rates of E.*Coli* were remarkably lowered by the use of power ultrasound in conjunction with ozonation, and the effect was attributed to increased ozone diffusion into the microbubbles to create a high gas-liquid surface area (Phull and Mason, 1999; Dahi and Lund, 1980). Recently, it was found that the degree of *E.Coli* destruction is doubled when chlorine treatment is conjugated with ultrasonic irradiation at 20 kHz (Phull et al., 1997). Moreover, some researchers have reported that sonolysis of UV-irradiated TiO_2 suspensions

in water with a 20 kHz unit enhanced the inactivation of *E.Coli* by a synergy in hydroxyl radical formation (Stevenson et al., 1997).

The efficiency of ultrasonic systems in aqueous solutions can be improved by the addition of impurities such as soluble gases and/or solid particles to reduce the cavitational threshold (Mason and Cordemans, 1998). The resulting effect is the formation of excess cavitational nuclei for a larger number and variety of collapse events. In a biphasic solid-liquid medium irradiated by power ultrasound, major mechanical effects are reduction of particle size leading to powder dispersion and increased surface area; and the formation of liquid jets at solid surfaces by the unsymmetrical inrush of the fluid to the voids (Phull et al., 1997; Mason et al., 1993). These jets not only provide surface cleaning, but also induce pitting and surface activation effects, and increase the rate of phase mixing and mass transfer (Mason and Cordemans, 1998; Hung and Hoffmann, 1998).

The study described herein was aimed to investigate and compare the effectiveness of power ultrasound in solute-liquid homogenous and solid-solute-liquid heterogeneous systems for inactivating bacterial survival. The method involved monitoring of total coliform bacteria during sonication of aqueous solutions of *E.Coli* in the absence and presence of ceramic, metallic zinc and activated carbon (AC) granules, respectively. Process kinetics and catalytic effects of test solids were established by non-linear regression analysis of residual coliform density with time.

Experimental

Set-up. The system consisted of a 20 kHz Bandelin Sonopuls HD2200 transducer, a 180 W horn type sonicator, and an 80 mL glass cell equipped with a water cooling jacket to maintain a constant liquid temperature. The horn was submerged 1.5 cm in the test solution, where the power was 0.674 W/mL as determined by calorimetry.

Preparation of the Stock Culture. A pure culture of E.*Coli* was grown in LB (Luria Bertani) medium, prepared by mixing 1 g of Tryptone (DIFCO), 0.5 g of Yeast Extract (DIFCO) and 1 g of NaCl (Merck) in 100 mL of ultra pure deionized water; followed by sterilization in autoclave for 1 h (APHA-AWWA-WPCF, 1989). A clean and healthy colony of *E.Coli* was

selected from the culture and placed in the growth medium in a closed container for 24 h to allow incubation at 37 ^{o}C in a shaking bath. The bacterial concentration in the medium at the end of the incubation period was approximately 10^{10} /mL in accordance with the "Membrane Filter Technique" of coliform count, based on the formation of colonies in standardized Endo-Broth growth medium (Sambrook et al., 1989). The test solutions were prepared by serial dilutions of this stock using ultra pure deionized water and a phosphate buffer to prevent cell damage by osmotic pressure. All reagents used during cultivation and analysis of bacterial count were of analytical grade, and materials such as petri dishes, petri pads and filter papers were of Millipore quality.

Sonication and Control Experiments. Test solutions of *E.Coli* after analysis of initial coliform density were irradiated for 20 min at constant temperature in the absence and presence of ceramic granules (irregular size) prepared in the laboratory, metallic zinc particles (0.6x0.25mm) of HACH, and granular activated carbon (0.84x0.25 mm) of AQUATECH, respectively. In heterogeneous samples, the mass concentration of the solids was 0.12 g/L in each run, irrespective of the solid type. Samples were withdrawn within short intervals in each set to monitor the change in coliform density with time. Each set was run three times to check repeatability and to report the results as arithmetic means of three independent measurements. Control experiments with each solid were run for 20 min in the absence of ultrasonic irradiation to detect if any reduction in bacterial density occurred by adsorption and/or other physicochemical processes.

Results and Discussion

Individual Effects of Ultrasound and the Test Solids. Comparative patterns of *E.Coli* survival during 20 min contact with power ultrasound and the test solids (controls) separately are presented in Figure 5.7. (The data points represent arithmetic means of three measurements from three independent runs of the same test with equal sampling intervals.) It was found that the concentration of coliform bacteria in all systems decreased with time, while ultimate reduction was achieved only with activated carbon and ultrasonic irradiation. The mechanism of removal in the control schemes (without ultrasound) involves the diffusion of bacterial colonies in the solid-liquid interface for sorption and/or adsorption on the solid surfaces. The strikingly larger efficiency of removal with AC than with the other

two solids is due to the "activated" surface of the former to favor adsorption processes, while the similar efficiency achieved with power ultrasound is a consequence of the mechanical effects brought about by cavitation phenomena.

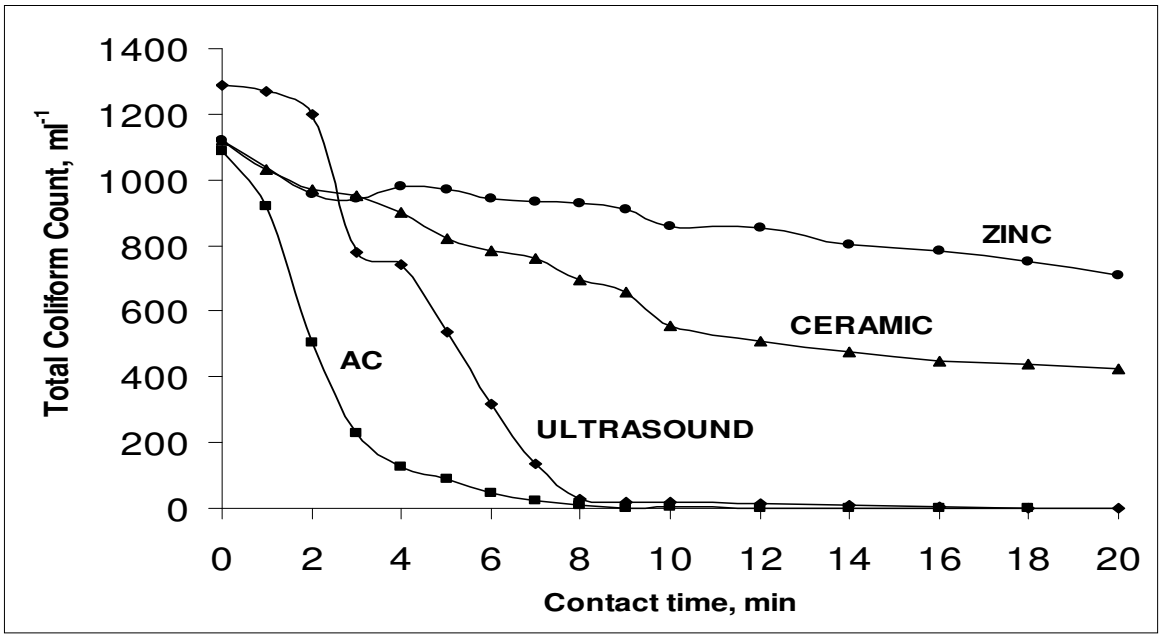

Figure 5.7. Individual effects of power ultrasound and the control solids on the survival pattern of *E. coli* during 20-min contact with each.

Combined Effects. Comparative rates of inactivation in the three heterogeneous systems upon combined effects of ultrasound and solid impurities are presented in Figure 5.8. It was found that all three solids induced catalytic effects in the ultrasonic inactivation of bacteria, the effects increasing in the order AC>ceramic>zinc. The acceleration or catalysis is due to the chain of events between increased cavitational nuclei and enhanced mechanical effects of ultrasound for attritioning, milling and dispensing solid particles, and activating their surfaces. The observed order on the other hand, is a consequence of the differences in surface and crystalline properties of the solids. Each solid exhibited a different degree of brittleness in the order: AC>ceramic>zinc, reproducing the catalytic order shown in Figure 5.8. Since brittleness is an indicator of the attritional capacity, diminution of AC particles by mechanical effects of ultrasound was largest, leading to the largest number of cavity nuclei, and largest effects of cavitational collapse. In fact, within the first minute of irradiation activated carbon granules were completely converted into powders, by which

surface/volume ratios are effectively enlarged. The disintegration of ceramic granules took a longer time, and powders appeared with increased contact, but they were not as fine as those of activated carbon. Particles of metallic zinc were the least brittle, and though dispensed into smaller size, they did not turn into powder form within the specified test period.

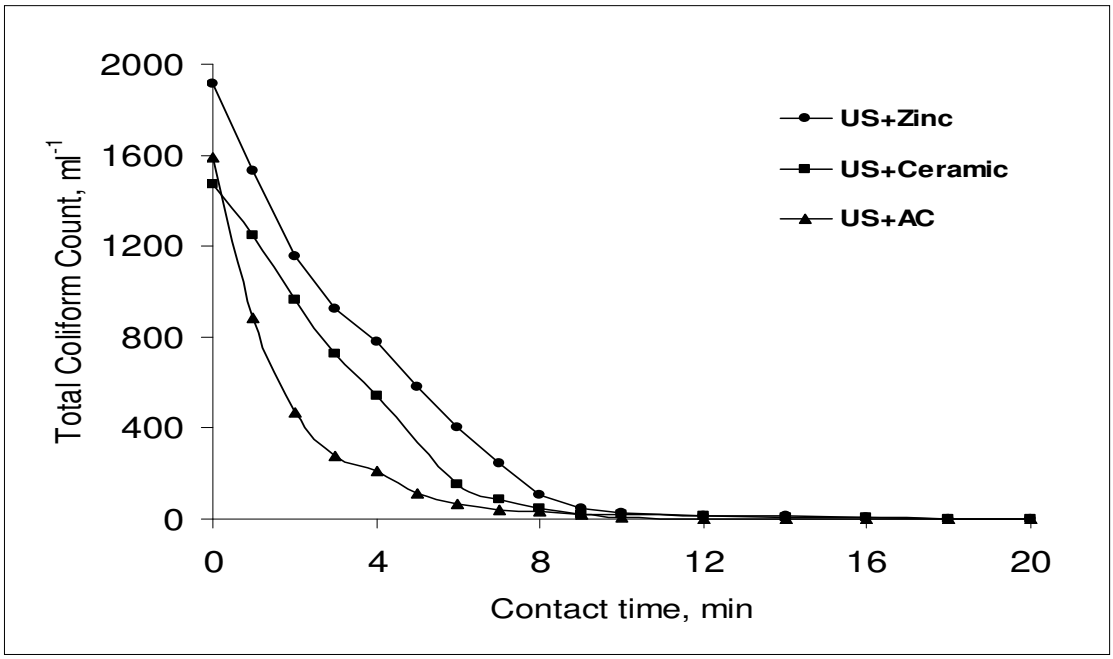

Figure 5.8. The relative profiles of *E. coli* survival upon the joint effects of power ultrasound and the test solids during 20-min contact

To investigate the contribution of adsorptive removal on the overall reduction of *E.Coli*, filtered suspensions of spent AC were washed and dried, and incubated in the nutrient agar for 24 hours. No bacterial growth was detected on the agar at the end of the incubation period, signifying that adsorption on carbon surface was not a significant removal pathway when bacteria are simultaneously exposed to ultrasonic irradiation. The test was repeated with the spent AC granules in one of the control experiments, where the ultrasonic power was off. In this case, incubation resulted in 70 per cent reactivation, showing that adsorption was the principal removal pathway in the absence of ultrasound. Hence, we concluded that in a combined medium of activated carbon and ultrasonic vibrations, surfaces of AC act mainly as sites for bubble formation, and bacterial cells are inactivated directly via cavitational effects. Even if some of the cells or colonies are attached on the solid-liquid interface to undergo adsorption, the lack of bacterial growth in suspensions of the spent

powders revealed that they are readily detached and destroyed by simultaneous effects of cavitation at the interfacial area or at solid surfaces.

Process Analysis**.** The bacterial survival-time data generated with the four test conditions using ultrasound were analyzed by non-linear regression techniques to establish the representative process kinetics. It was found that the concentration profile in both homogeneous and heterogeneous solutions is described by:

$$\ln N = a + bt^{n} \tag{5.7}$$

where: ***N*** is the total coliform number in unit volume, t is the contact time (min), and a, b, n are the model parameters. The predicted model is indeed the integrated form of a rate expression proposed for chlorination kinetics (Metcalf and Eddy, 1991):

$$\frac{dN}{dt} = kNt^{m} \tag{5.8}$$

where: dN/dt is the time rate of change in bacterial number per unit volume, k is the observed rate coefficient in $[\text{time}]^{-(m+1)}$, and m is an empirical constant. The integration of Equation 5.8 between the limits N_0 at t= 0 and N at t yields:

$$\ln N = \ln N_0 + \frac{k}{m+1} t^{m+1} \tag{5.9}$$

The predicted model in Equation (5.7) and the integrated expression in Equation (5.9) are identical so that the parameters a, b and n of the former are exchangeable with the constants of the latter, i.e. $\ln(N_0)$, $k/(m+1)$ and $m+1$, respectively. The similarity of the predicted model and that suggested for chlorination kinetics is of significance, for it suggests a similarity in the destruction mechanisms, as well. Thus, the formation of hydroxyl radicals and/or hydrogen peroxide upon cavitation effects should be accounted for in the overall destruction process.

The results of regression analysis and curve fitting are presented in Figure 5.9 in a panel chart. The model parameters *b* and *n* corresponding to each curve were substituted into k=*b*(m+1) and m=*n*-1, respectively to evaluate the kinetic coefficients, which are listed in Table 5.9, where the input of *E.Coli* is presented as part of the test condition to allow comparison with the predicted value associated with the model parameter "*a*". The values of "m" in Table 5.10 show that solids have the effect of reducing the order of the reaction with respect to time, and the process is turned to a pseudo-first order kinetic model in the presence of activated carbon, at which "m" is 0. The similarity of ceramic and zinc-catalyzed kinetics is in agreement with the survival profiles presented in Figure 2. The slightly larger rate coefficient with ceramic is due to its relatively higher particle diminution capacity, as discussed in the previous section. Since the overall reaction orders and the units of k were different in the other three cases, comparative evaluation of all process performances was made in accordance with the time requirements for 25%, 50%, 95% and 99.9% kill rates, as presented in Table 5.10.

Table 5.9. Model prediction of initial test conditions and coefficients of process kinetics.

Test Condition	Prediction of N_0 [(a)] {$\ln(N_0)= a$}	Kinetic Coefficients	
		k	**m**
Ultrasound: N_0=1290 /mL	1286.9 (±25.7) /mL	-0.035 $min^{-5/2}$	3/2
Ultrasound/Ceramic:N_0=1475 /mL	1450.1 (±25.9) /mL	-0.203 $min^{-3/2}$	1/2
Ultrasound/Zinc: N_0=1915 /mL	1790.1 (±69.7) /mL	-0.165 $min^{-3/2}$	1/2
Ultrasound/AC, N_0=1590 /mL	1571.8 (±40.0) /mL	-0.570 min^{-1}	0

[a]Numbers in parenthesis are 95% confidence intervals.

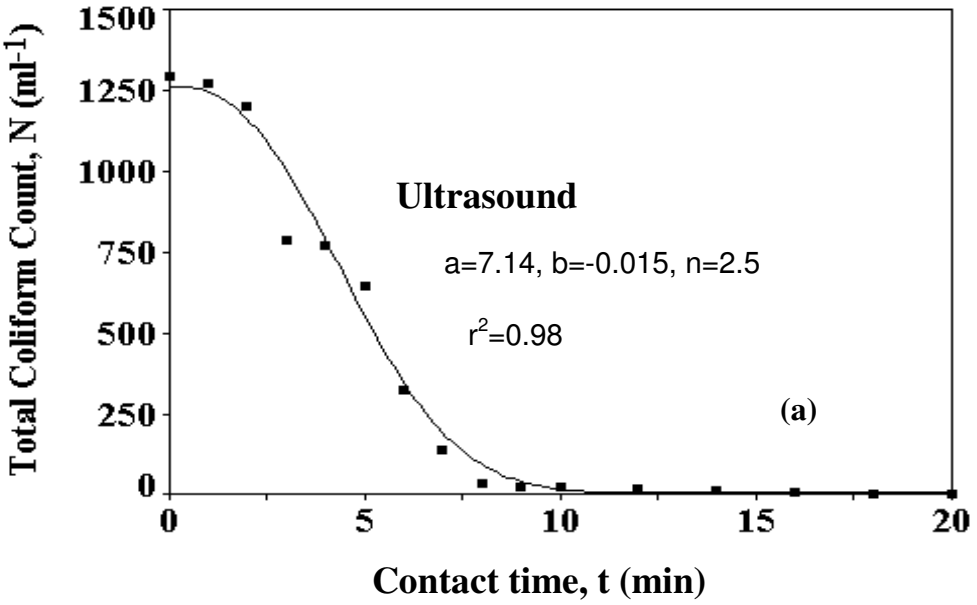

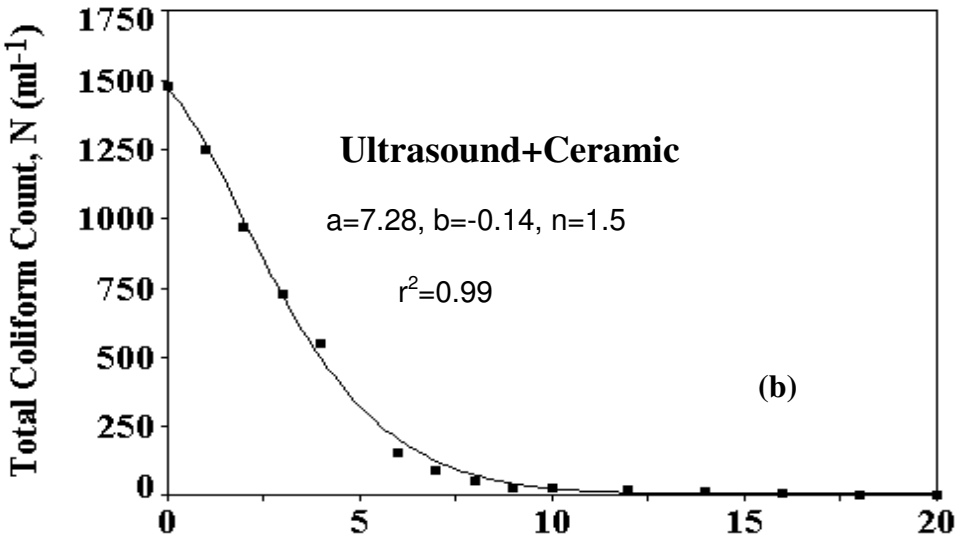

Figure 5.9. Comparative kinetics of bacterial destruction with
(a) ultrasound, (b) ultrasound + ceramic.

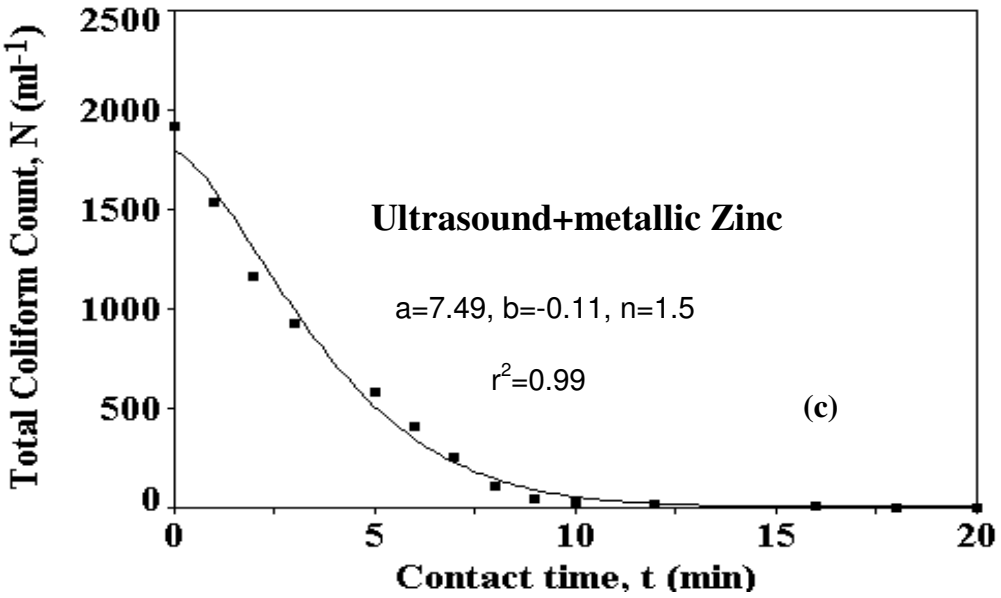

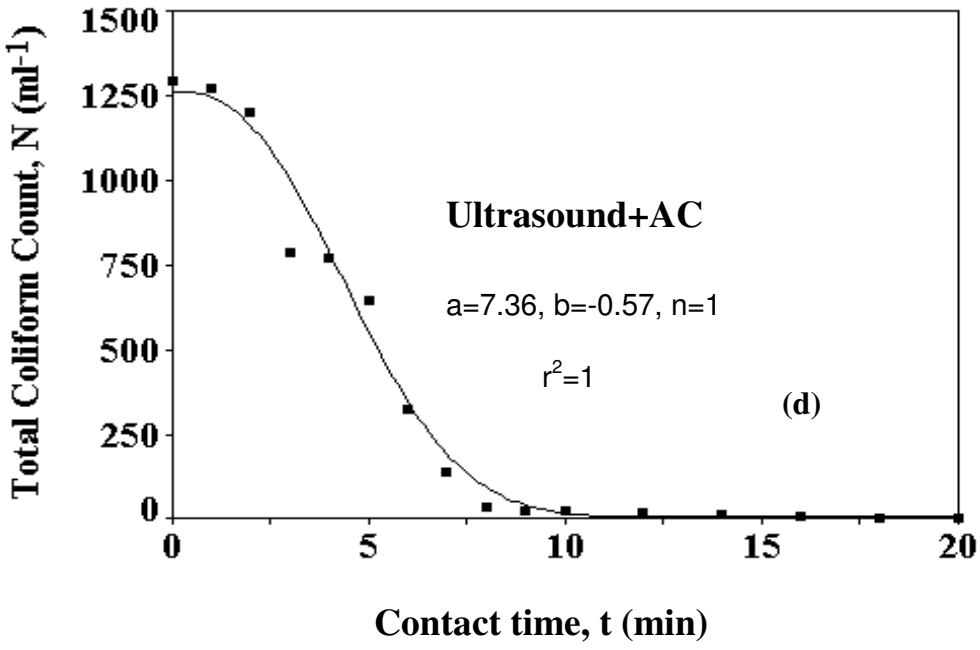

Figure 5.9. Comparative kinetics of bacterial destruction with
(c) ultrasound + zinc, and (d) ultrasound + activated carbon. Solid lines represent fitted curves to the model equation $\ln (N) = a + bt^n$, where t is the contact time; and a, b, and n are estimated values of model parameters.

The results show that the effect of solid catalysts is more pronounced at high concentrations of bacteria, as obvious from the relative time requirements for 25 % kill ratios. With prolonged sonication and lower bacterial concentrations, catalytic effects become less prominent, and process efficiencies approach that of individually applied ultrasonic irradiation. The declination of solid effects with time may be attributed to a variety of reasons. At high concentrations during early exposure, the probability of bacterial contact with the solid-liquid interface (where cavity formation is largest) is high too, but the chances get lower as the survival ratio is reduced.

At appreciably low concentrations, therefore, the rate of kill is limited by the number of cavity bubbles in the bulk solution: a condition, which is typical of non-catalyzed ultrasonic systems. In addition, catalytic effects may fade away by vibrational erosion of solid surfaces, the extent of which is related to the structure and surface properties of solid particles. Finally, it should be kept in mind that the rate of degassing in heterogeneous solutions is faster (than that in homogeneous solutions) due to larger number of cavitation events, which rapidly reduce the availability of dissolved gases during the formation stage.

Table 5.10. Comparative process performance for constant ratios of bacterial kill.

PROCESS	Kill time, min			
	25 %	50 %	95 %	99.9 %
Ultrasound	3.35	4.76	10.16	11.95
Ultrasound+Zinc	1.90	3.41	12.06	15.80
Ultasound+Ceramic	1.62	2.90	12.26	13.45
Ultrasound+AC	0.50	1.21	8.08	12.12

Since 100% bacterial removal in any system is not feasible, and it is possible to minimize the declination of solid effects (by proper selection of particle size and crystalline properties, and effective control of dissolved gases) we believe that ultrasonic technologies with heterogeneous catalysis will emerge as promising alternatives for disinfecting aqueous systems. Consequently, our current study is focused specifically on physical/chemical properties of solid surfaces, significance of particle size and density, effect of gas addition, and optimization of the process for large-scale applications.

5.3. Organic Matter Decay with Ultrasound: A Study with Phenols

5.3.1. Effects of Operating Conditions on Sonochemical Decomposition of Phenol

The study presented in this section has been recently submitted to *Journal of Hazardous Materials* under the title "**Effects of operating conditions on sonochemical decomposition of phenol**" and is currently under review.

Introduction

Phenols are widely consumed in the industry such as in preservers of paint, leather and textile goods, and in the production of resins, disinfectants, medicine, caprolactam and bisphenol A. Improper handling of these compounds and/or inappropriate disposal of their wastes into water is a major pollution, as many of phenolic compounds are resistant to conventional water treatment processes, and some are recognized as suspected carcinogens (Kim et al., 2002).

Methods of destroying phenolic wastes in water has been widely investigated and found that advanced oxidation processes (AOPs) are promising alternatives, owing to their potential to generate hydroxyl radicals in solution (Gogate et al., 2004; Kotronarou et al., 1991; Sivakumar et al., 2002; Espuglas et al., 2002). Among many tools of producing hydroxyl radicals in AOPs (e.g UV irradiation, ozonation, addition of hydrogen peroxide, Fenton's agent; and combinations thereof) ultrasound is a novel method, by which water molecules undergo molecular fragmentation to release hydroxyl and hydrogen radicals (Ince et al., 2001).

The underlying mechanism for this phenomenon is acoustic cavitation, which consists of the formation, growth and implosive collapse of gaseous cavity bubbles, resulting in local extremes of temperatures and pressures, at which molecules undergo pyrolysis (Mason, 1990). As some of these radicals escape into the aqueous phase, they readily attack organic molecules therein for oxidative destruction.

Sonochemical effects can be enhanced by increasing liquid defects in the water to favor cavitation, e.g. by inserting solid particles or by injecting a soluble gas in solution (Ince et al., 2001). In addition, sonochemical yields are related to the applied frequency, power and the reactor geometry. In general, frequency selection is based on the vapor pressure, solubility and octanol–water partition coefficient of the target chemical. Hydrophobic compounds with high vapor pressures tend to diffuse into the gaseous bubble interior, so that they may easily be destroyed in the bubble-liquid interface and/or the bubble itself. The most suitable frequencies for destroying such compounds lie between 20-100 kHz, by which long-lived "stable" cavities are generated (Fischer et al., 1986).

In contrast, hydrophilic compounds particularly at low concentrations tend to remain in the bulk liquid and their destruction is possible only by aqueous phase oxidation caused by the "unstable cavity" collapse (at 200-800 kHz), during which the probability of radical escape to the bulk liquid is high (Petrier et al., 1994; Petrier and Francony, 1997).

There are numerous studies on sono-degradation of phenol in water, focusing mainly on parametric effects. Basically, it has been shown that the most commonly used short frequency ultrasound (20 kHz) is ineffective, regardless of the accelerating conditions employed, while maximum effects are observed within the medium range (e.g. at 200 and 500 kHz) (Naffrechoux et al., 2000; Berlan et al., 1994; Popov et al., 2004; Hoffmann et al., 1996; Entezari et al., 2003). On the other hand, the short frequency 35 kHz was shown to provide adequate results when applied in the presence of Fenton type reagents (Entezari et al., 2003).

Recently, it has been reported that ultrasonic degradation of phenol could be improved by the addition of hydrogen scavengers such as CCl_4, which by reacting with hydrogen radicals (produced by water sonolysis) indirectly enhances the availability of uncombined hydroxyl radicals in solution (Zheng et al., 2005).

The purpose of this study was to investigate and compare the efficiency of phenol decomposition at 20, 300 and 520 kHz ultrasonic irradiation under either air or argon injection modes and to assess impacts of frequency, concentration, pH, and the saturating gas on process rate and product yield.

Experimental

Materials. Phenol was purchased from Riedel Häen (97% pure) in solid form, and was dissolved in deionized water. Potassium ferro cyanide ($K_3Fe(CN)_6$), 4-aminoantipyrine, ammonium chloride (NH_4Cl), ammonium hydroxide (NH_4OH), sulfuric acid, and all other reagents were obtained from Fluka and used as received.

Apparatus. Three different ultrasonic equipment with three distinct frequencies, power outputs and cell volumes were used throughout the study. The first one was a horn-type sonicator (tip diameter = 12 mm) connected to a 20 kHz Bandelin Sonopuls HD2200 generator with a capacity of 180 W. The tip of the horn was submersed into the liquid from the top of an 80 mL cylindrical glass reactor. The second one was made of a 300 kHz piezo-electric transducer located at the bottom of a 150 mL cell and connected to a generator with a maximum capacity of 25 W (UNDATIM ULTRASONICS). The third equipment consisted of a piezo-electric transducer emitting ultrasonic pressure at 520 kHz and mounted on a titanium plate at the bottom of a cylindrical pyrex reactor of 1200 mL with a generator capacity of 100 W (UNDATIM ULTRASONICS). In all systems, the cells were equipped with a water cooling jacket to maintain constant liquid temperature.

Analysis. Phenol was monitored spectrophotometrically by the aminoantipyrine method (APHA/AWWA/WPCP, 1992) using a UNICAM-Heλios, Alpha/Beta double beam spectrophotometer with an optical path length of 1 cm. The method is based on the reaction of phenol with 4-aminoantipyrine in the presence of potassium ferrocyanide at pH=7.9 to form a colored antipyrine complex (AMPH) as shown:

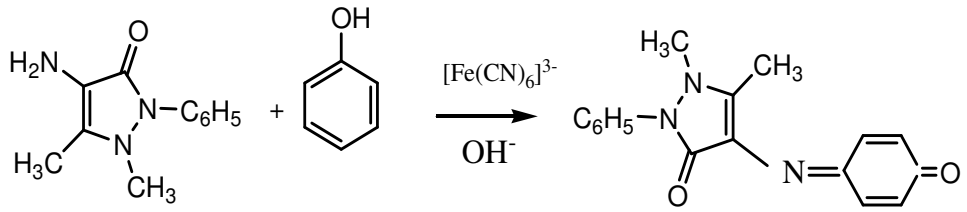

4-aminoantipyrine Phenol AMPH

Concentration of phenol in solutions of AMPH was estimated via a calibration curve (Appendix A.1.) generated from the absorption of the solutions in the visible band.

Hydrogen peroxide was monitored by the analytic procedure described by Klassen et al, 1994.

Procedure. A stock phenol solution of 0.5 M was made in deionized water and stored at 4° C in the dark. Test samples of 0.1 mM, 0.25 mM, 0.5 mM, 1 mM, 2 mM and 5 mM were prepared from the stock using deionized water. Sample volumes used in 20 kHz, 300 kHz and 520 kHz reactors were 80 mL, 100 mL and 300 mL, respectively. The test solutions were bubbled with air or argon for 30 min prior to sonication and the same gas was continually injected into the solution throughout 90 min exposure. Samples were withdrawn from the reactors every 10 min for duplicate analysis of the antipyrine complex by spectrometry.

Results and Discussion

Effect of frequency and initial concentration. The UV-visible spectrum of AMPH showed that it had two principle absorptions: one at the visible band (508 nm) corresponding to the phenolic chromophore, and the other at near UV (332 nm). Spectral changes in AMPH prepared by reacting the effluents of 300 kHz reactor during 90 min sonication of 5 mM phenol is presented in Figure 5.10. Note that sonication not only rendered decolorization (and decomposition) of the phenol complex but also induced UV absorption abatement.

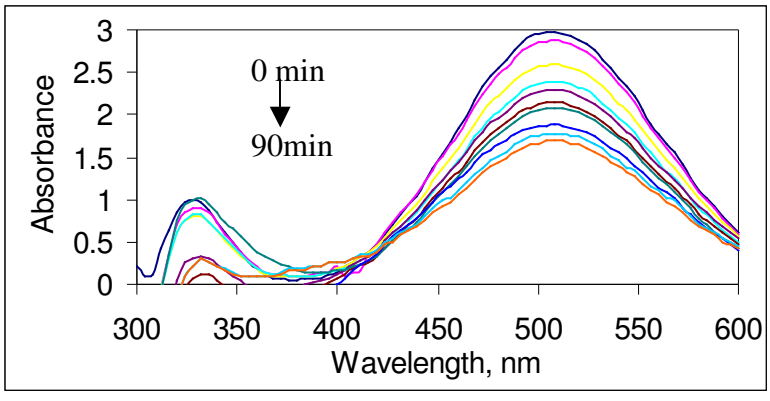

Figure 5.10. Changes in the spectrum of AMPH during sonication of 5 mM phenol for 0, 10, 20, 30, 40, 50, 60, 70, 80 and 90 min at 300 kHz and pH=2 during aeration.

The effect of frequency was tested by sonicating 5 mM solutions of phenol at 20, 300 and 520 kHz and monitoring its concentration in effluents collected at 10-min intervals during 90 min irradiation. The data revealed that the degradation process followed pseudo-first order reaction kinetics, and the rate constants were estimated accordingly using the integrated form of the related rate equation:

$$\frac{C}{C_0} = e^{-kt} \tag{5.10}$$

where C and C_0 are concentrations of phenol at time t and zero, and k is the pseudo-first order degradation rate coefficient.

Profiles of phenol removal at the test frequencies and values of k estimated by non-linear regression are presented in Figure 5.11.

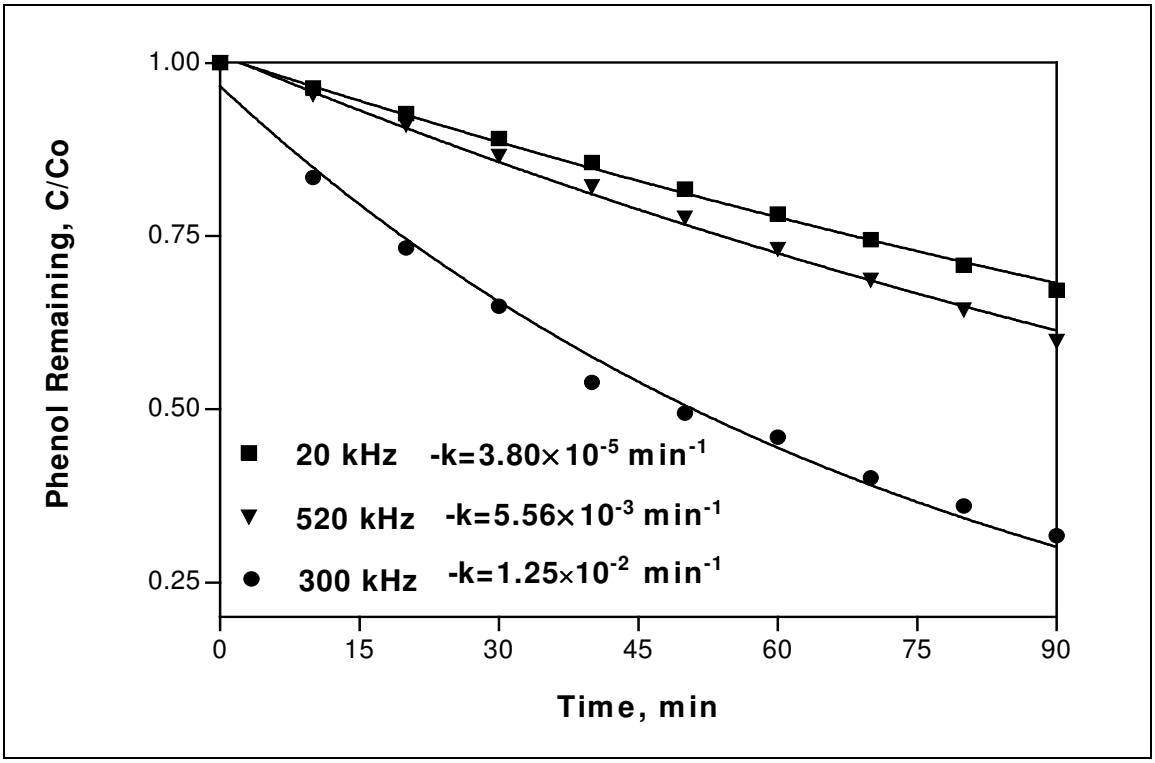

Figure 5.11. Comparative rates of phenol decomposition at 20, 300 and 520 kHz during 90 min sonication of 5.0 mM phenol at pH=2.0. The solid lines represent the fit of experimental data to Equation 5.4 with $0.98 \leq r^2 \leq 0.99$.

The fact that the degradation was remarkably slow at 20 kHz is consistent with the literature, and can be related to the low volatility of phenol (vapour pressure 0.41 mmHg at 25^{o}C) or its relative inability to diffuse into the gas phase for pyrolytic destruction. Higher efficiencies observed at 300 and 520 kHz indicate that ultrasonic degradation of phenol is governed by OH radical chemistry in the bulk liquid, as reported by others (Wu et al., 2001). The inability of 20 kHz to render aqueous phase oxidation is due to the fact that at such frequencies the time to reach the resonating radius of the bubble is long, and so is the bubble life time. Accordingly, radicals such as •OH that are produced during the long-lasting collapse process have sufficient time for combination in the gas phase (or at the interface) before they are ejected into the liquid bulk. On the other hand, at high frequency irradiation the duration of cavity collapse is much shorter so that a larger fraction of radical species will have the chance to escape into the bulk liquid.

The more rapid degradation at 300 kHz (than at 520 kHz) within the experimental conditions employed in this study is at a first glance inconsistent with the well-accepted hypothesis that radical production increases with increasing applied frequency (Weavers et al., 1998). In fact, short bubble life (short collapse duration) is favorable for radical production and the likelihood of their ejection out of the gas phase, but unfavorable for the "quality" or the violence of collapse (Colarusso and Serpone, 1996). In most cases, there exists an optimum frequency, at which the rate of radical production and the duration of cavity collapse provide the "best" conditions for the destruction of the targeted chemical. In our case 300 kHz is the optimum, because here longer lived bubble advantages (longer than those at 520 kHz) for more violently collapsing cavities seem to dominate over shorter lasting but less energetic cavity collapse (at 520 kHz) that allows larger spread of OH radicals into solution. To test the validity of this hypothesis, we monitored the concentration of H_2O_2 in deionized ultra-pure water as an indicator of the abundance of hydroxyl (and peroxy) radicals in the bulk liquid. We found that more OH radicals (and more ·OOH) were present in the bulk liquid during sonication at 300 kHz than at 520 or 20 kHz. The data are presented in Figure 5.12.

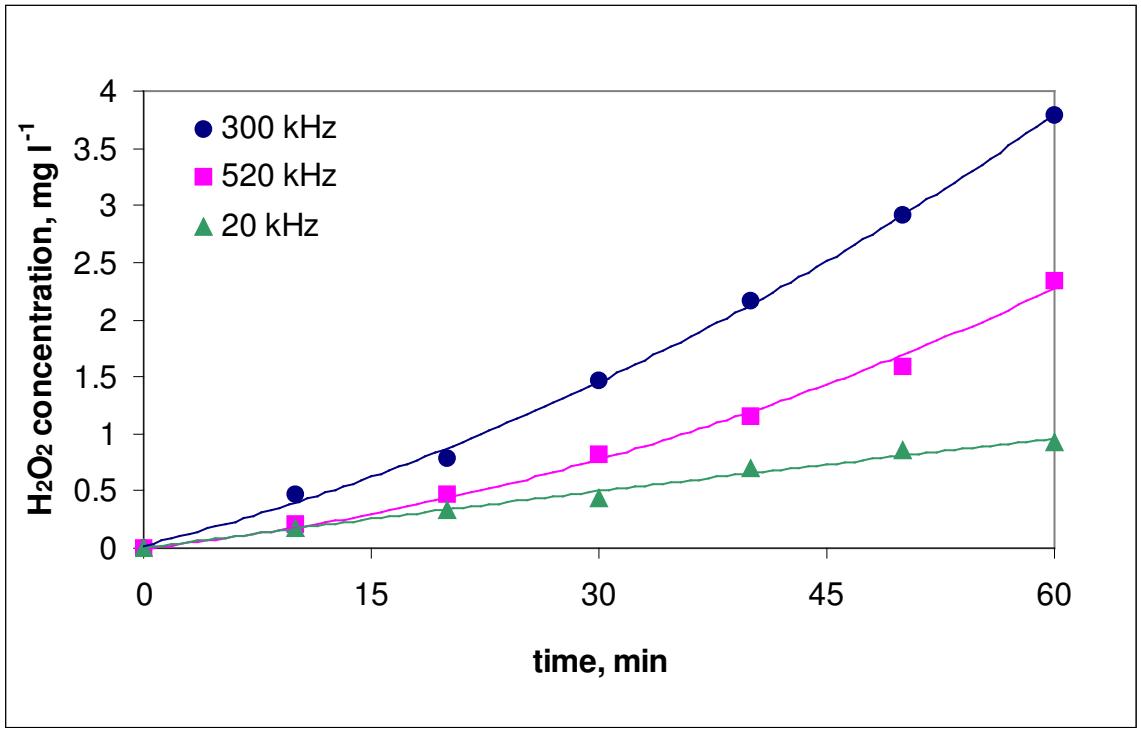

Figure 5.12. Net rate of H_2O_2 production during sonication of deionized water for 90 min by 20, 300 and 520 kHz ultrasound.

The relative efficiencies of the irradiation modes or the test frequencies were assessed also by comparing the reaction yields. Ultrasonic "yield" is defined as the change in chemical concentration in the experiment volume per power of the sonic energy deposited in that volume (Tauber, 2000):

$$G = \frac{\Delta C \times V}{P_d} \qquad (5.11)$$

where: G = the product yield (mol/W)

ΔC= the change in the concentration of the test chemical (M)

V= the volume of solution (L)

P_d = the sonic energy deposited in a given volume (W)

Values of P_d in each test system were estimated by the calorimetric method (Margulis and Margulis, 2003) and the yields as listed in Table 5.11 were calculated for 5

mM phenol exposed to 90 min irradiation. Note that the reason for different input powers and different solution volumes in each scheme is that the systems are operated at their previously optimized values.

The values of G in Table 5.3 show again that frequency efficiencies for phenol destruction within our experimental conditions are in the order 300 kHz >520 kHz >20 kHz. Note, however, that if the systems are compared for power transfer efficiencies ($E=P_d/P_a$), the order is: 520 kHz > 20 kHz > 300 kHz, which makes one expect higher yields from irradiation at 520 kHz and 20 kHz than what were observed. However, despite the fact that the efficiency of power transfer from the source to the medium is an important parameter in the overall performance of an ultrasonic system, factors such as reactor geometry, solution volume, and transducer location must be as important, while the crucial parameter is the applied frequency and its suitability to the target compound.

Table 5.11. Relative power inputs and the product yields observed for 5 mM phenol exposed to 90 min sonication at pH=2.0 during air injection.

Frequency, kHz	20	300	520
Power applied (P_a), W	54.0	25	40
Power deposited (P_d), W	37.25	18.99	39.14
Solution Volume, L	0.08	0.10	0.30
ΔC, mole/L	1.64	3.41	2.01
$G\times10^{-3}$, mole /W	3.52	17.96	15.41

The effect of initial phenol concentration was tested by sonicating 0.25, 0.50, 1.0, 2.0 and 5.0 mM phenol solutions during air injection at constant pH (2.0), followed by estimating the product yields and the pseudo-first order rate coefficients, which are presented in Figure 5.13 and Figure 5.14, respectively.

It was found that at very low concentrations of phenol, the yields were also very low even at high frequency irradiation. The noticeable enhancement in G as C_0 was increased to 5 mM implies the probability of other destructive mechanisms or other reaction media than aqueous phase oxidation or the solution bulk, such as the bubble sheath, where a fraction of phenol may exist upon diffusive transfer and sorption at the interface.

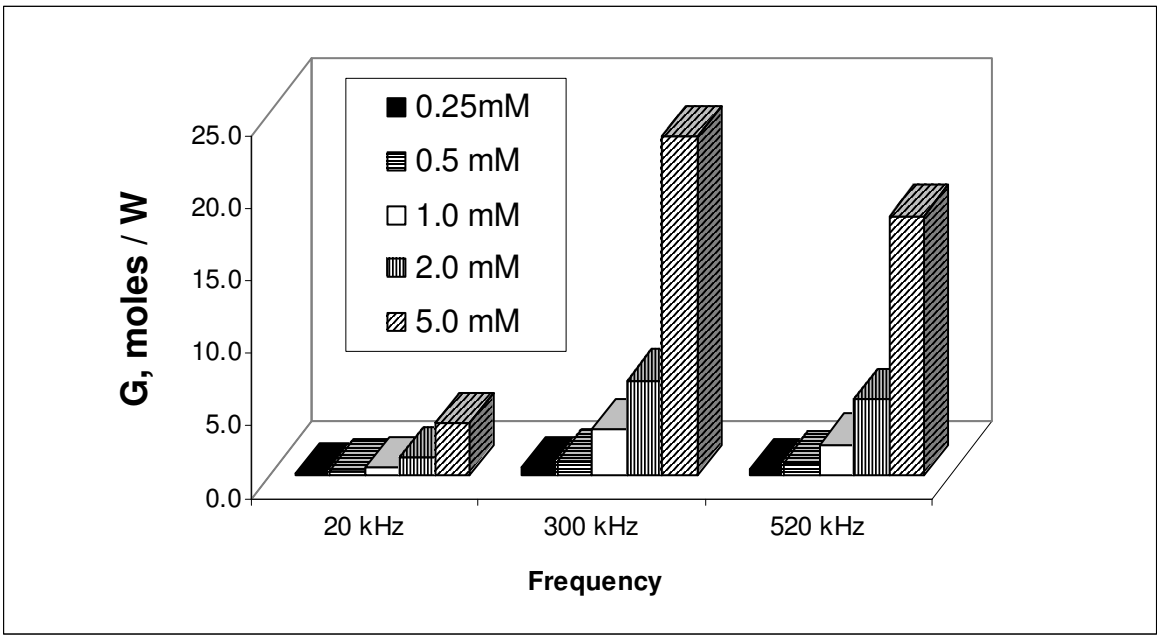

Figure 5.13. Variation of G with initial phenol concentration and the applied frequency. (Operating conditions are pH=2.0 and continuous air injection).

The increase in phenol decomposition rate with initial concentration (Figure 5.13) verifies that at high concentrations of low volatility solutes, an additional destructive pathway exists, as was demonstrated in the literature by the formation of pyrolysis products along with hydroxylated intermediates (Serpone et al., 1994). The probable site for thermal decomposition of concentrated non-volatile solutes is the interfacial bubble sheath, at which solutes may accumulate via diffusive sorption during the formation and growth of acoustic cavities. The adsorptive tendency of highly concentrated non-volatile solutes on non-polar surfaces of cavity bubbles was verified by the exhibition of saturation type kinetics of Langmuirian behavior, which is commonly proposed for describing photocatalytic processes (Ince et al., 2001).

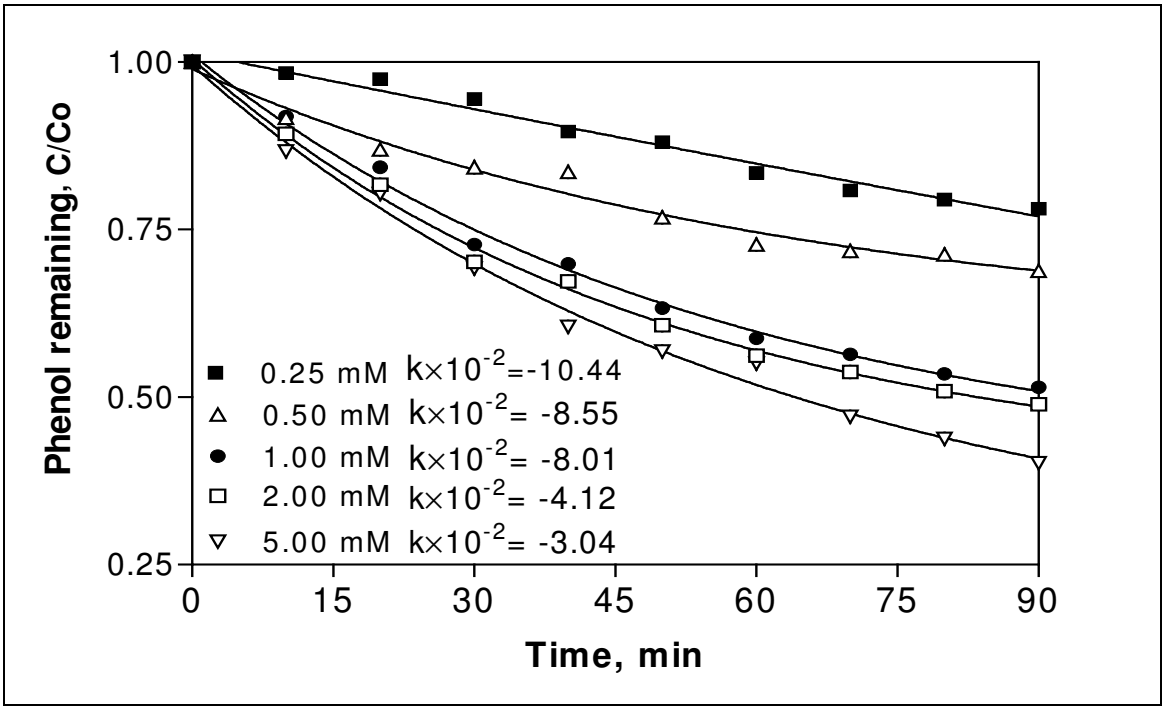

Figure 5.14. Variation of phenol decomposition rate by initial phenol concentration. Operating conditions were: frequency=300 kHz, pH=2.0, injection gas: air.

Effects of pH and the sparge gas. In aqueous solutions of phenol the degree of ionization from molecular state to the phenolate ion increases as pH is raised, and at pH>pK_a (=10) phenolate ion is the major species, which due to repulsive forces are unable to approach the negatively charged cavity bubbles or even the bubble-liquid interface, where uncombined OH radical concentration is at a maximum (Petrier and Francony, 1997). As pH is lowered and the fraction of molecular phenol increases, the probability of solutes approaching the interfacial area also increases, resulting in enhanced rates of phenol removal. This is demonstrated by the rate profiles in Figure 5.15 plotted for five different values of pH.

The impact of sparge gas was tested by injecting individually a monatomic (argon) and a diatomic gas (air) at 1.5 L/min to buffered and non-buffered solutions of phenol at various concentrations during irradiation at 300 and 520 kHz. Despite the well-accepted knowledge that the presence of monatomic gases in sonicated liquids are more

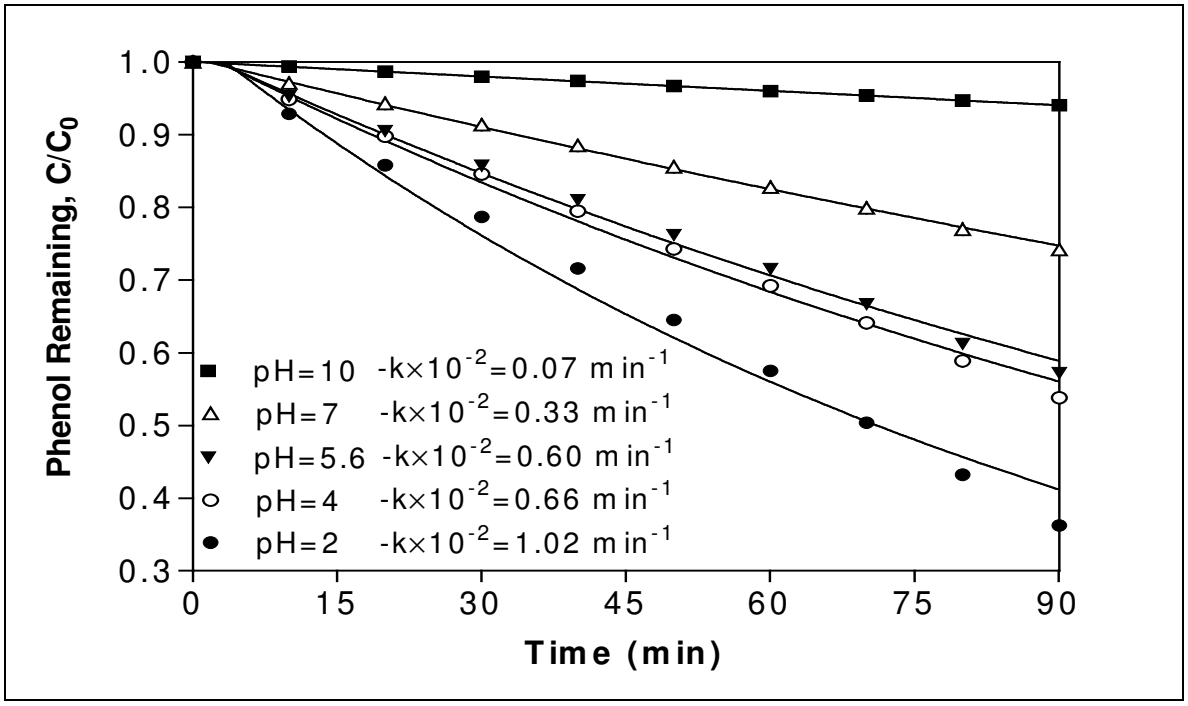

Figure 5.15. Impact of pH on the rate of phenol removal during irradiation by 300 kHz. (Initial phenol concentration= 5.0 mM)

Table 5.12. Variation of sonochemical yield with the sparge gas.

Phenol Input	G (moles removed/W)							
	300 kHz				520 kHz			
	pH=5.6		pH=2.0		pH=5.6		pH=2.0	
	AIR	ARGON	AIR	ARGON	AIR	ARGON	AIR	ARGON
0.25 mM	0.28	0.33	0.66	0.37	0.22	0.19	0.42	0.22
0.50 mM	1.05	0.68	1.32	1.06	0.74	0.63	1.00	0.70
1.00 mM	5.14	1.97	4.06	3.30	1.93	1.70	2.46	2.36
2.00 mM	12.39	4.29	8.46	6.95	5.01	3.64	6.02	5.61
5.00 mM	16.88	16.10	23.40	20.35	13.70	11.50	17.90	16.05

favorable than iatomic ases in terms of the utput temperatures generated at collapse (as a consequence of their higher polytrophic gas ratios:1.33 to 1.67 vs. 1.36-1.40) (Suslick, 1990), we found higher sonochemical yields under the influence of air than that of argon. Estimates of the "product yield" G for different experimental conditions are listed in Table 5.12.

Larger yields in the presence of air despite its lower polytrophic gas ratio is due to the reactions of nitrogen with molecular oxygen to yield nitric acid and radical species such as •OH, $•NO_2$ and $•NO_3$ that accelerate the oxidation process. Chemical reactions that take place during air injection into a sonoreactor are as follows (Ullerstam et al., 2000):

$$H_2O +))) \rightarrow \ •OH + •H \quad (5.12)$$

$$•OH + •H \rightarrow H_2O \quad (5.13)$$

$$2•OH \rightarrow H_2O + O \quad (5.14)$$

$$2•OH \rightarrow H_2O_2 \quad (5.15)$$

$$2N_2 + O_2 \rightarrow 2N_2O \quad (5.16)$$

$$2N_2O + H_2O \rightarrow 2HNO_2 + 2N_2 \quad (5.17)$$

$$•H + N_2O \rightarrow N_2 + •OH \quad (5.18)$$

$$•OH + N_2O \rightarrow 2NO + •H \quad (5.19)$$

$$HNO_2 + H_2O_2 \rightarrow HNO_3 + H_2O \quad (5.20)$$

$$HNO_3 +))) \rightarrow •OH + •NO_2 \quad (5.21)$$

$$HNO_3 +))) \rightarrow •H + •NO_3 \quad (5.22)$$

While the formation of nitrous and nitric acids (Reactions 5.17, 5.20) favor the decomposition process via pH reduction, generation of excess •OH and radicals such as nitrite and nitrate, which are comparably strong oxidants of organic compounds ($k_{•Nox}=10^7$; $k_{•OH}=10^{12}$ L/ mol.sec (Gogate et al., 2003) accelerates the oxidation process.

Conclusions

Ultrasonic decomposition efficiency of phenol is significantly related to the applied frequency (300 kHz>520 kHz>20 kHz), solution pH (acidic>neutral>alkaline), initial concentration (5mM>2 mM>1 mM>0.5 mM, etc) and the injected gas quality (air>argon). Frequency effects are due to the resonating bubble size and the nature of bubble collapse in addition to the physical-chemical properties of phenol, while pH and concentration effects rise because of enhanced probability of solute approach to the cavity sheath, where radical species are at a maximum. More effective decomposition in the presence of air despite its lower polytrophic gas ratio is a consequence of the reactions of nitrogen in ultrasonic media to produce additional radicals.

5.3.2. Analysis of Reactor Effluents in System II

5.3.2.1. Total Organic Carbon (TOC) Analysis. The overall degradation of phenol was assessed by the degree of mineralization in solution during 90 min sonication of phenol. The data as Total Organic Carbon (TOC) and phenol against time are plotted in Figure. 5.16.

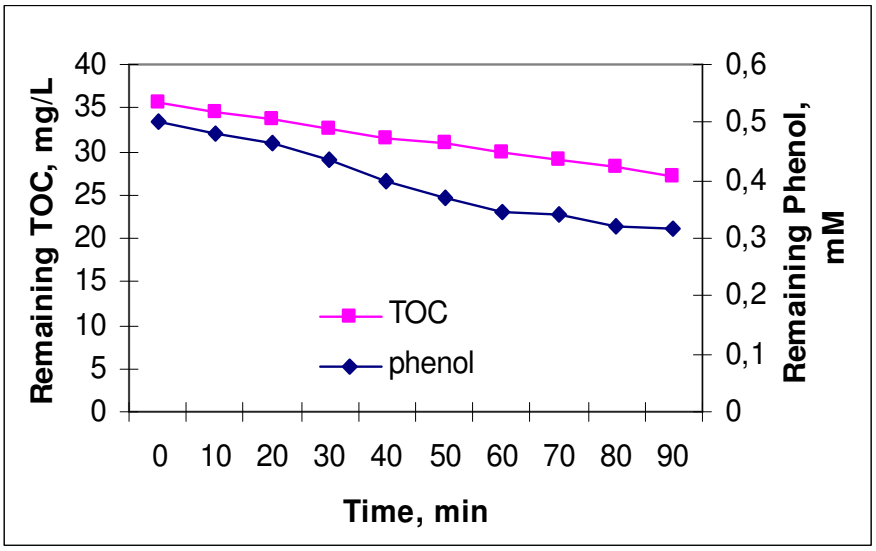

Figure 5.16. Total mineralization during sonochemical degradation of 0.5 mM phenol in System II.

The figure shows that while about 40% of phenol is removed within 90 min contact, total mineralization is only 23%, implying the formation of intermediate oxidation by-products, which have not been totally oxidized and therefore exhibit as TOC in the effluent. This finding is consistent with previous studies, which reported that much longer contact is required for remarkable degrees of mineralization by ultrasound (Ince and Tezcanli, 2001).

5.3.2.2. Gas Chromatographic (GC) Analysis. Although ultrasonic irradiation at 300 kHz yielded maximum phenol degradation under optimized conditions, the overall degradation or reduction in TOC was insufficient as was presented above. This indicates that the apparent phenol removal was a consequence of its conversion to some intermediate oxidation by-products. Identification of these by-products was made by GC analysis of the reactor effluents at 0, 10, 30, 45, 60, 75, 90 and 120 min sonication time.

GC was calibrated using 5 different concentrations of phenol and the peak before sonication was observed at a retention time (RT) of 8.710 ± 0.007 min. As presented in Appendix A.2. New peaks in varying RT and peak areas were observed after various times of contact with ultrasound, as presented in Figure 5.18 a,b,c,d,e,f,g.

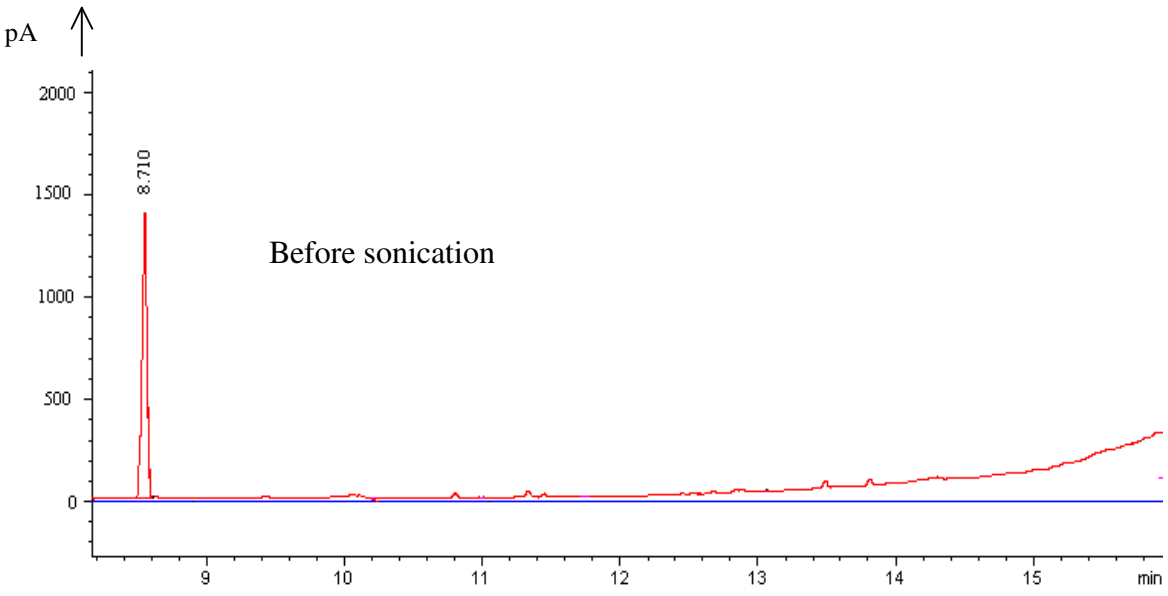

Figure 5.17. GC chromatogram of non-sonicated phenol solution

The peak observed in Figure 5.18 (a) corresponding to 10 min sonication was detected at a retention time of 12.121 min; those in 5.17 (b) were at 13.111 min and 14.670 min. As these new compounds could not be definitely identified at the absence of certified standard solutions, they were tentatively proposed through comparison with reported findings in the literature.

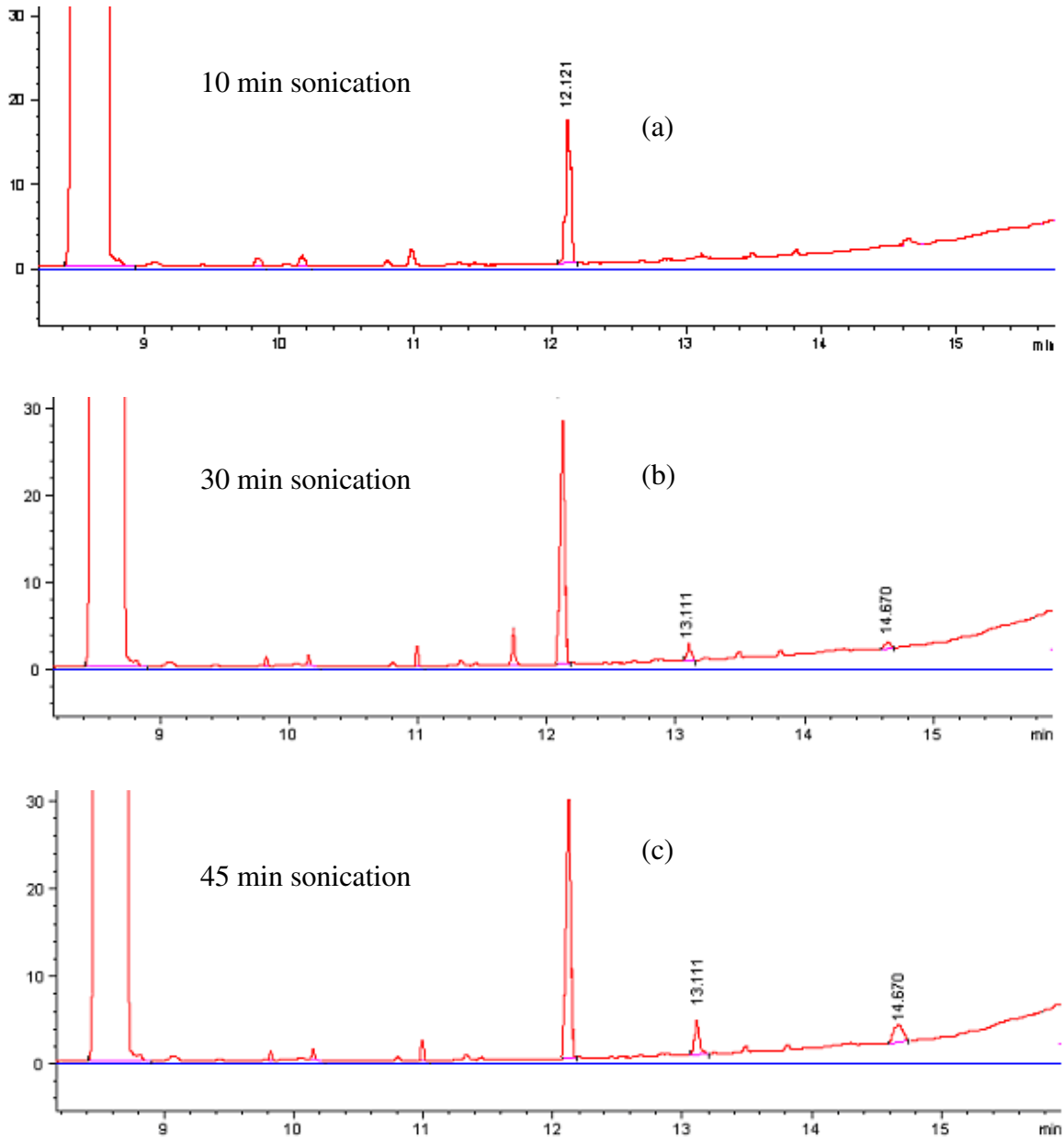

Figure 5.18. GC chromatograms of sonicated phenol solutions at (a)10 min, (b) 30 min, (c) 45 min sonication times.

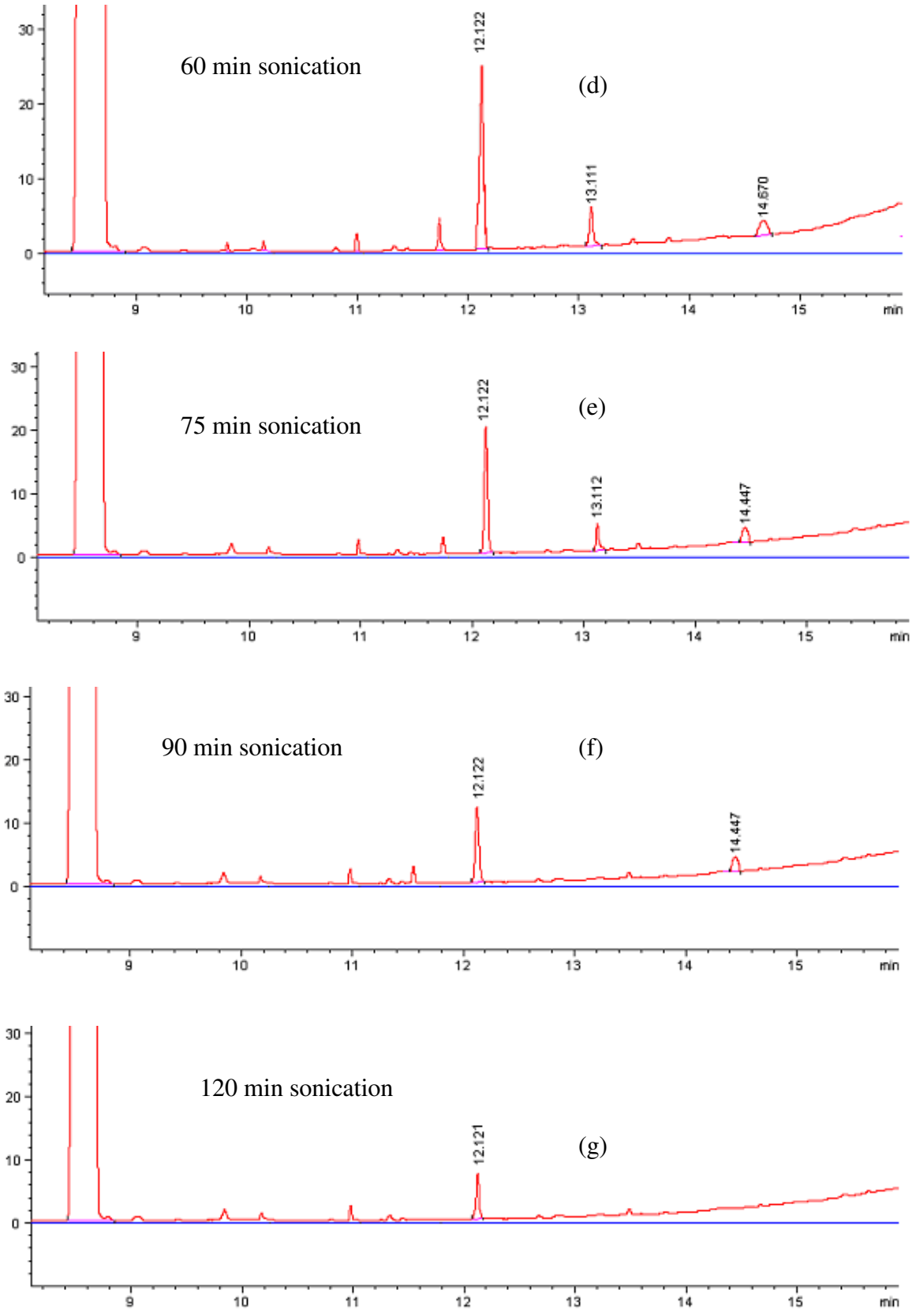

Figure 5.18 (continued). GC chromatograms of sonicated phenol solutions at (d) 60 min, (e) 75 min, (f) 90min, (f)120 min sonication times.

A summary of peak properties in the chromatograms shown in Figures 5.17 and 5.18 a-g are presented in Table 5.13.

Table 5.13. Summary of peak properties in chromatograms presented in Figures 5.17-5.18.

time, min	RT_1, min	$Peak_1$, Area	RT_2, min	$Peak_2$, Area	RT_3, min	$Peak_3$, Area	RT_4, min	$Peak_4$, Area
0	8.710	1353.000	12.121	0.000	-	0.000	-	0.000
10	8.711	1176.243	12.121	14.409	-	0.000	-	0.000
30	8.711	993.535	12.122	25.937	13.111	2.882	14.678	1.441
45	8.717	855.286	12.122	28.818	13.111	5.764	14.670	4.323
60	8.711	680.062	12.122	25.937	13.112	7.205	14.670	5.764
75	8.709	605.752	12.122	20.173	13.112	2.882	14.447	5.764
90	8.708	495.370	12.122	12.968	-	0.000	14.447	4.323
120	8.711	319.875	12.121	5.215	-	0.000	-	-

The oxidation reaction and intermediates of phenol during sonication as proposed in the literature are as follows (Berlan et al.,1994):

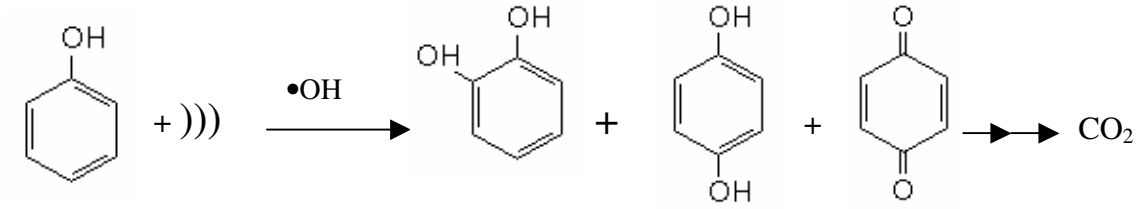

Phenol Catechol Hydroquinone p-benzoquinone

The chromatograms observed in this study are consistent with the literature showing the formation of catechol, hydroquinone and p-benzoquinone at the following retention times: Catechol **(CC)**, RT = 12.121 min ; Hydroquinone **(HQ)**, RT = 13.111 min; Benzoquinone (**BQ)**, RT = 14.670 min. Moreover, it is possible to determine the fractional occupancies of each compound during the contact time by using the peak areas in the chromatograms. The results are listed in Table 5.14.

Table 5.14. Distribution of phenol and its by-products during 120 min sonication

time, min	% phenol	% CC	% HQ	% BQ
0	100.0	-	-	-
10	86.9	50.0	-	-
30	73.4	90.0	40.0	25.0
45	63.2	100.0	80.0	75.0
60	50.3	90.0	100.0	100.0
75	44.8	70.0	40.0	100.0
90	36.6	45.0	0.0	75.0
120	23.6	18.1	0.0	0.0

The relative distribution of phenol and the oxidation by-products are plotted against time in Figure 5.19. Note that catechol reaches a maximum concentration at 45 min of sonication, after which it begins to decline and is completely removed at 120 min of contact. Hydroquinone and benzoquinone show similar patterns: hydroquinone is formed at the 30th min, reaches a maximum at 60 min and vanishes completely at 120 min; while benzoquinone also appears at 30th, reaches a maximum at 60 min, but vanishes more slowly being totally removed only after 150 min of contact (not shown).

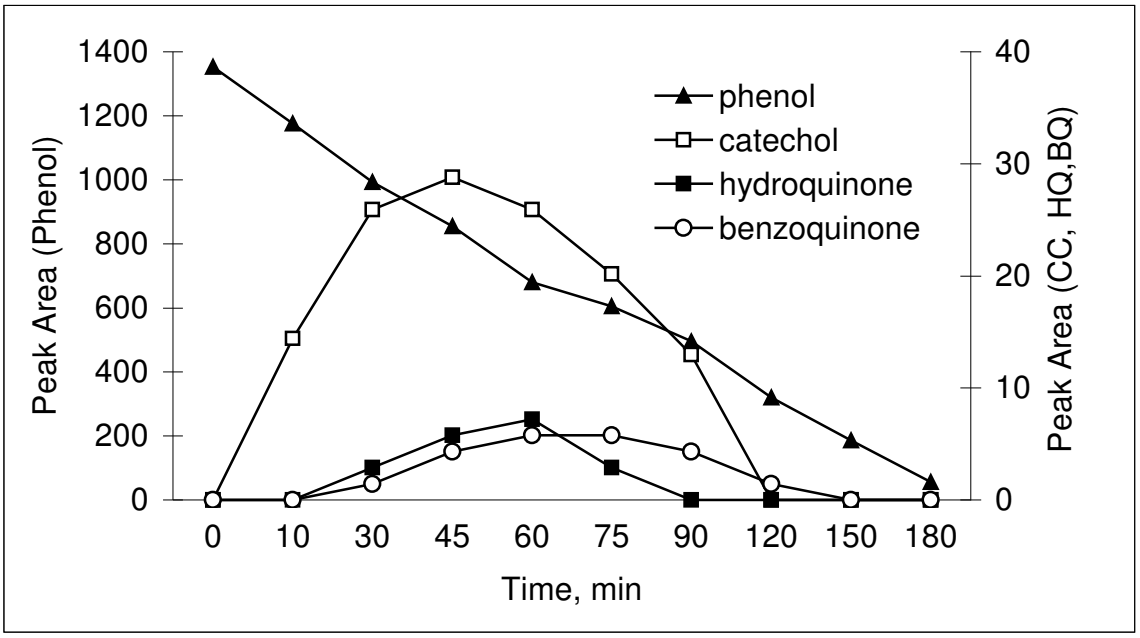

Figure 5.19. Intermediate compounds formed during sonication of 1 mM phenol in System II.

5.3.2.3. Toxicity Analysis. The toxic effect of phenol on living cells can be explained by free radical mechanisms, whereby the loss of hydrogen from the OH group results in the formation of a phenolate radical, which while migrating through the cell eventually removes a hydrogen atom from the DNA molecule (Graham et al., 1980).

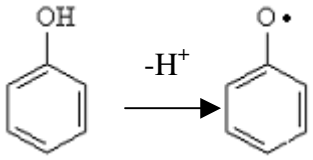

(5.23)

Phenol Phenolate radical

The details of Microtox Toxicity Protocol were given in section 4.2.2.3., where the indicator was EC_{50}; 50 per cent reduction in the light transmitting capacity of *V. fisheri.* For convenience and ease of interpretation, values of observed EC_{50} were converted to a relative toxicity index, TU, as defined by Equation 5.24.

$$TU = \frac{1}{EC_{50}} \tag{5.24}$$

The variation in TU and phenol concentration of sonicated effluents with time are plotted in Figure 5.20.

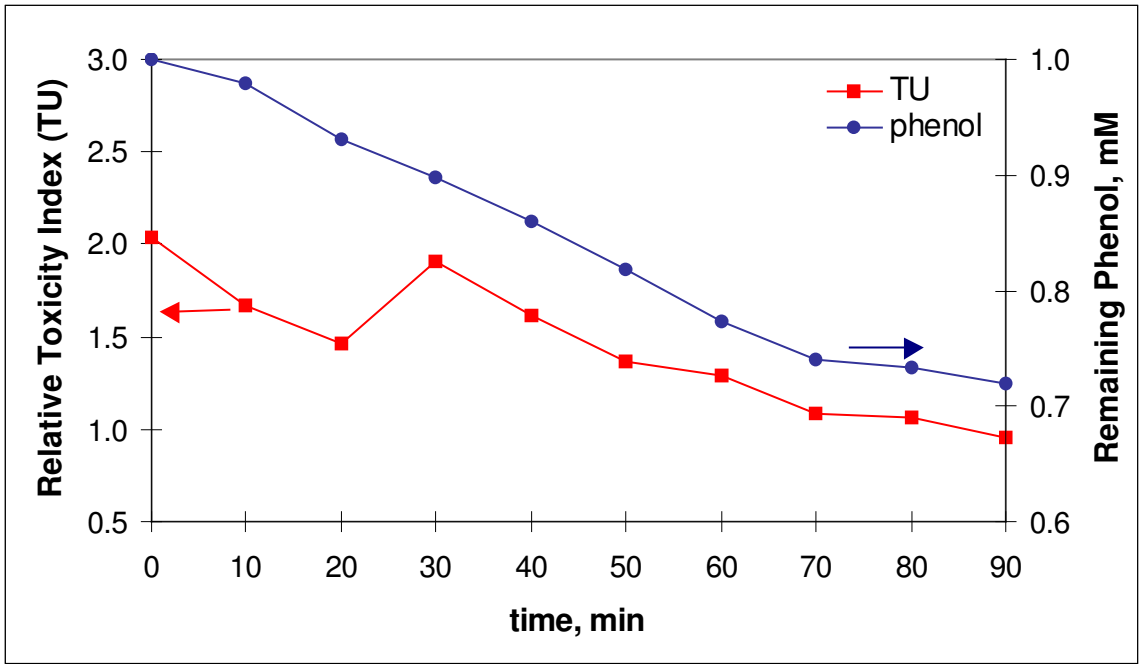

Figure 5.20. Microtox Toxicity and correlation with remaining phenol during 90 min sonication of 1 mM phenol in System II

The rapid detoxification observed during the first 20 min is due to the decay of phenol, while the sudden increase between t=20-30 min is a consequence of the formation and accumulation of catechol as was confirmed by GC analysis. Toxicity thereafter steadily declined, owing to the rapid decay of catechol and indicating the relatively lower toxicities of hydroquinone and benzoquinone. Total phenol removal and total detoxification in 90 min were 29% and 25%, respectively.

To assess relative efficiencies of System II and System I for toxicity reduction, phenol was exposed to sonication in System I at exactly the same conditions and reactor effluents were monitored for phenol and Microtox Toxicity within 10-min intervals. The data are plotted in Figure 5.21.

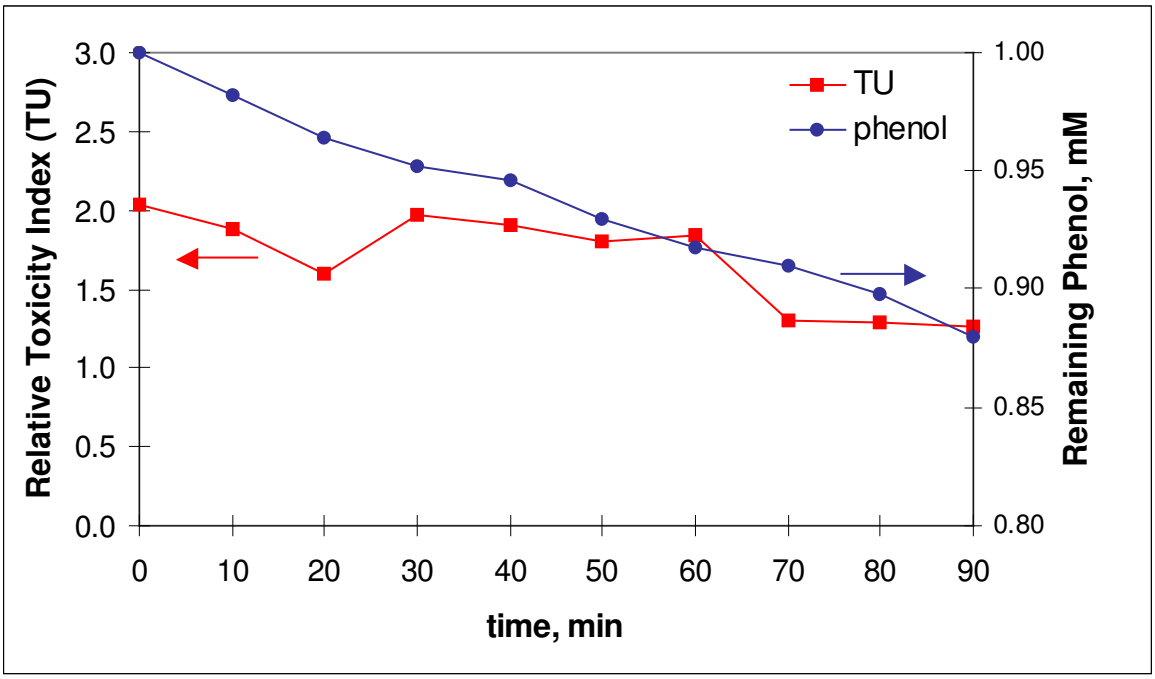

Figure 5.21. Microtox Toxicity and correlation with remaining phenol during 90 min sonication of 1 mM phenol in System I.

It was found that the effluent toxicity during 20 kHz irradiation declined with initial contact with ultrasound, reached the first minimum at t =25 min, increased suddenly to a value close to the initial and remained constant till after a contact of 60 min. The initial increase signals the larger toxicity of the first intermediate (CC) than that of phenol; the steadiness shows that it was the predominant product within 20-60 minute of sonication; and the sharp decline beyond 60 min and the following steadiness show the decay of CC and the formation of less toxic HQ and BQ. Total phenol removal and total detoxification in 90 min were 14 per cent and 11 per cent, respectively.

The difference in the detoxification pattern in this system from that in System II is due to the difference in the applied frequency, which dictates the availability of •OH radicals in solution, as was discussed in detail in section 5.3 with comparison and evaluation of frequency effects. Relative efficiencies of System I and System II for toxicity reduction and phenol decay are plotted in Figure 5.22 as bars.

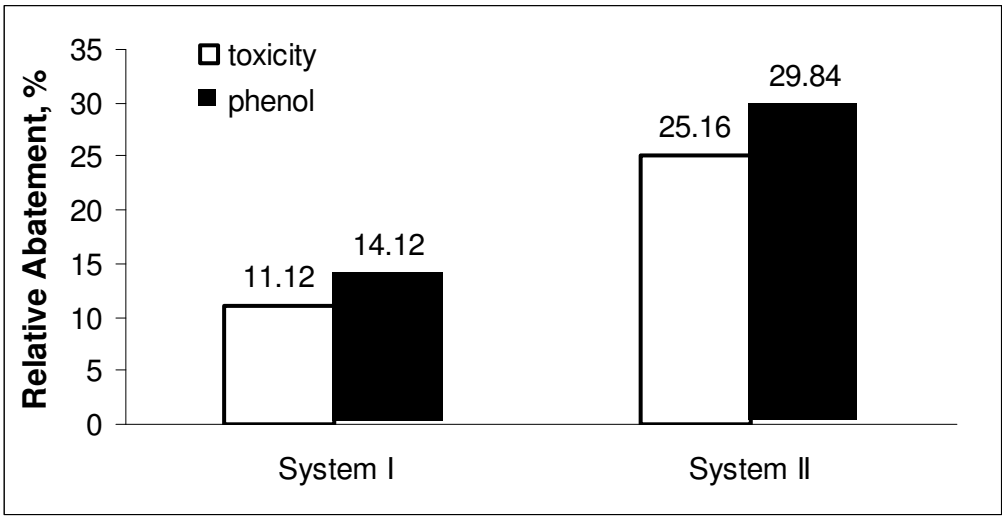

Figure 5.22 Relative Detoxification and Phenol Removal in System I and System II

5.4. Combined Ultrasound/Ozone/UV Systems and Comparison with Individual Operations

We reported that the decay of phenol by ultrasound followed 1st order rate law:

$$\frac{dC}{dt} = -k'C \tag{5.25}$$

where:

C= the concentration of phenol at time t

k'= pseudo first order rate coefficient, 1/min

t = reaction time, min

Integration of Equation 5.25. yields:

$$\frac{C}{C_0} = e^{-k't} \tag{5.26}$$

where:

C_0 = the concentration of phenol at time t.

A plot of C/C_0 vs. time for 2.5 mM phenol sonicated in System II for 200 min and the fit of the data to Equation 5.26 is presented in Fig. 5.23.

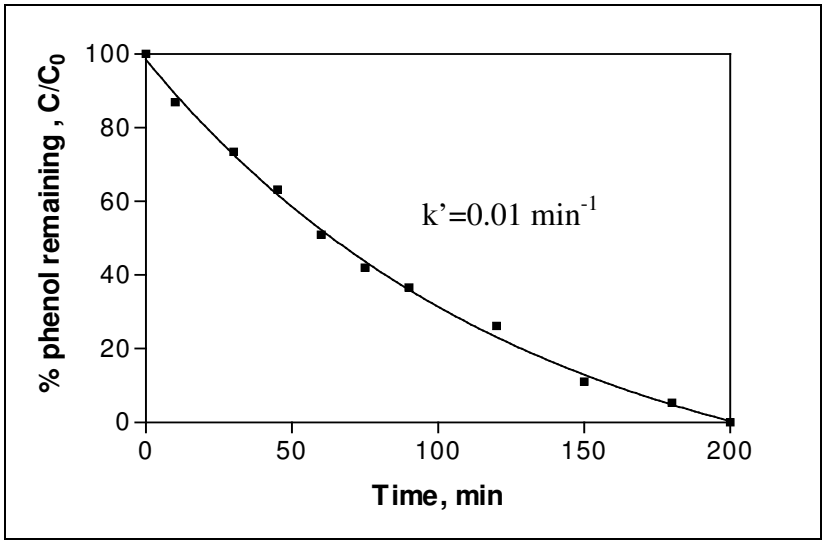

Figure 5.23. Completion of the degradation of 2.5 mM phenol at pH=2 in System II

The figure shows that more than twice the optimum contact time (90 min) is necessary to removal all phenol from solution (It was shown in previous sections that total removal in 90 min contact was 68.2 per cent). Since this is not economic, we attempted to integrate our system with ozone and/or UV radiation to improve the efficiency of the degradation process. To isolate the effects, we first investigated individual efficiencies of ozonation and UV irradiation.

5.4.1. Degradation of Phenol by Ozone

Ozonation of water in the presence of ultraviolet light at 254 nm, results in the generation of hydroxyl radicals as active oxidative species:

$$O_3 + h\nu \rightarrow O_2 + O(^1D) \quad (5.27)$$

$$O(^1D) + H_2O \rightarrow \bullet OH + \bullet OH \quad (5.28)$$

$$O_3 + H_2O \rightarrow \rightarrow H_2O_2 + O_2 \quad (5.29)$$

$$O_3\bullet^- + H_2O \rightarrow \bullet OH + HO^- + O_2\bullet \quad (5.30)$$

Hence, ozonation of phenolic solutions is a powerful method of phenol removal. The important point of interest is the selection of optimum ozone flow and the pH, because the process rate is limited by the rate of transfer in solution and the pH.

5.4.1. Selection of pH

To select the optimum pH in ozone applications, we applied ozone in phenolic solutions at three different pH; 2.0, 5.6 and 10.0. In figure 5.24, the pseudo first order rate coefficients were estimated as 0.0221/min, 0.0243/min, 0.0284/min for pH=2.0, 5.6 and 10.0, respectively. O_3 is most effective at pH=10, due to its decomposition at alkaline solutions to yield peroxy and hydroxyl radicals. Hence, the optimum pH was selected as 10.0.

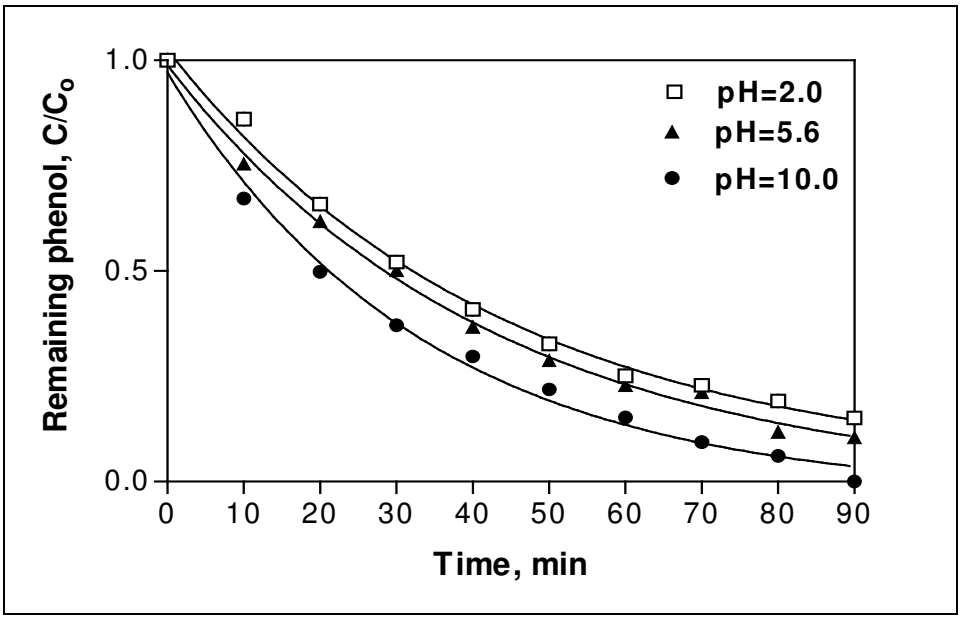

Figure 5.24. The impact of pH on the degradation of phenol during 90 min ozonation of 2.5 mM phenol in System II at pH=2.0, 5.6 and 10.0.

5.4.2. Selection of Ozone Input

To select the optimum ozone input, we injected different amounts of ozone in solution and monitored the decay of phenol in the absence of ultrasound during 90 min ozonation. Profiles of phenol degradation by increasing inputs of ozone (pH=10) are presented in Figure 5.25.

The pseudo-first order rate coefficients were estimated as 0.0284/min, 0.0326/min, and 0.0413/min for 2, 4 and 6 mg/L ozone inputs, respectively. Despite the fact that the

rate of degradation was slowest at 2 mg/L of ozone (0.75 L/min), it was much faster than the rate observed by sonication alone, as was discussed in previous sections (k'_{us} =1.0 x 10^{-2} /min). Hence, we selected 2 mg/L as the operating ozone input into combined operations.

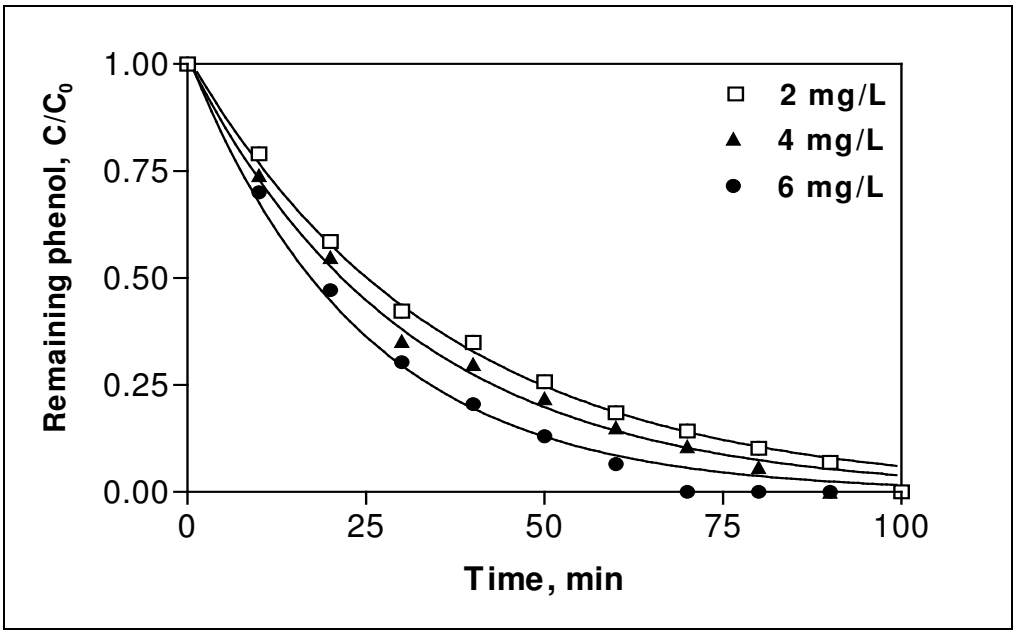

Figure 5.25. The impact of ozone input on the degradation of phenol during 90 minute ozonation of 2.5 mM phenol in System II at pH=10.

5.4.2. Degradation of Phenol by Ultrasound/Ozone Combination

The rate limiting parameter in degradation of organic compounds by ozone is the mass transfer rate of ozone in solution. It is expected that application of ultrasound simultaneously with ozone, will enhance the rate of organic matter decay in a synergistic manner, due to enhanced mass transfer of ozone by mechanical effects of ultrasound, and the formation of excess hydroxyl radicals upon thermal decomposition of ozone in the gas phase. The reactions that occur in the US/O_3 combined system in addition to those given in (5.27-5.30) are as the following:

$$H_2O +))) \longrightarrow \bullet OH + \bullet H \quad (5.31)$$

$$O_{3\,(g)} +))) \longrightarrow O_{2\,(g)} + O(^3P)_{(g)} \quad (5.32)$$

$$O(^3P)_{(g)} + H_2O_{(g)} +))) \longrightarrow 2\bullet OH_{(g)} \quad (5.33)$$

As was indicated in previous chapters, some of the hydroxyl radicals formed by sonolysis recombine at the cooler bubble-liquid interface to yield water and hydrogen peroxide, others react with gaseous substrates inside the collapsing bubbles, and under proper conditions some diffuse into the bulk liquid to activate aqueous phase oxidation reactions (Ince et al., 2001; Serpone et al. 1994; Kang and Hoffmann, 1998; Weavers et al., 1998).

Depending on their solubility and vapor pressures, organic solutes during combined ozonation and sonolysis may be destroyed by (i) direct thermal decomposition, (ii) ●OH-mediated advanced oxidation in the bulk liquid, (iii) chemical oxidation with ozone and hydrogen peroxide, (iv) thermal and radicalar decomposition in the bubble-liquid interface, and/or (v) combination of all (Ince et al, 2001).

5.4.2.1. Effect of pH. It was found that the degradation by combined operation was largely related to the solution pH as was the case with individual applications. The profiles of phenol degradation by combined sonolysis and ozonation at varying pH is presented in Figure 5.26.

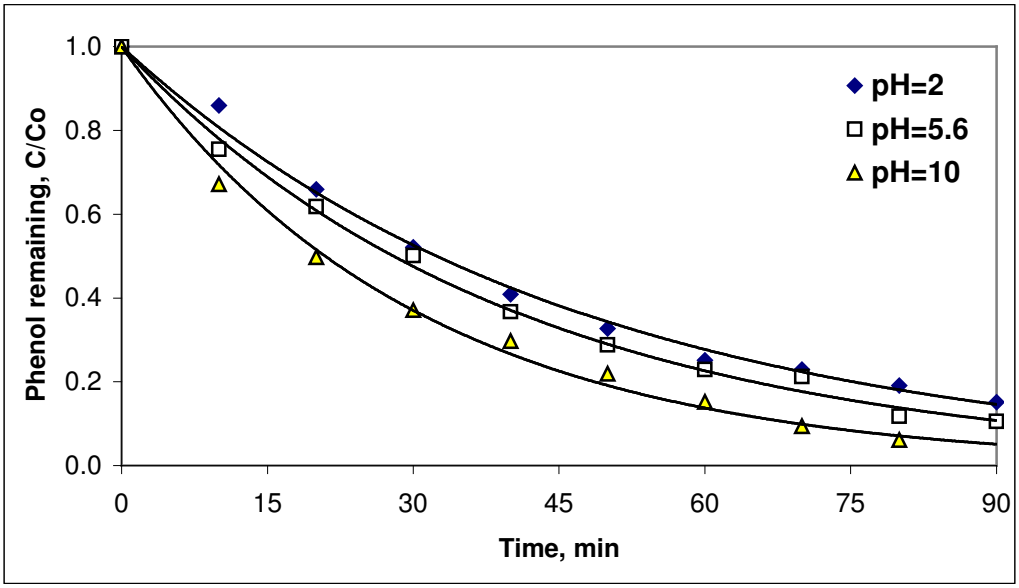

Figure 5.26. Degradation of 2.5 mM phenol at pH 2.0, 5.6 and 10 by combined sonolysis (300 kHz) and ozonation (2 mg/L) .

5.4.2.2. Comparison of Single and Combined Operations. To assess the relative performances of individual and combined systems, the degradation of phenol in each system was monitored at equivalent conditions. Comparative rates of phenol degradation by single and combined US/O_3 operations and the estimated rate coefficients are presented in Figure 5.27 and Table 5.15, respectively.

Table 5.15. Variations in k' by the operated system and pH

k' x 10^{-2}, 1/min			
pH	O_3	US	O_3 /US
2.0	1.52 ±0.05	1.07±0.03	2.21 ± 0.06
5.6	1.80 ±0.03	0.58 ±0.01	2.43 ± 0.06
10.0	2.79 ±0.12	0.08 ±0.002	3.26 ± 0.14

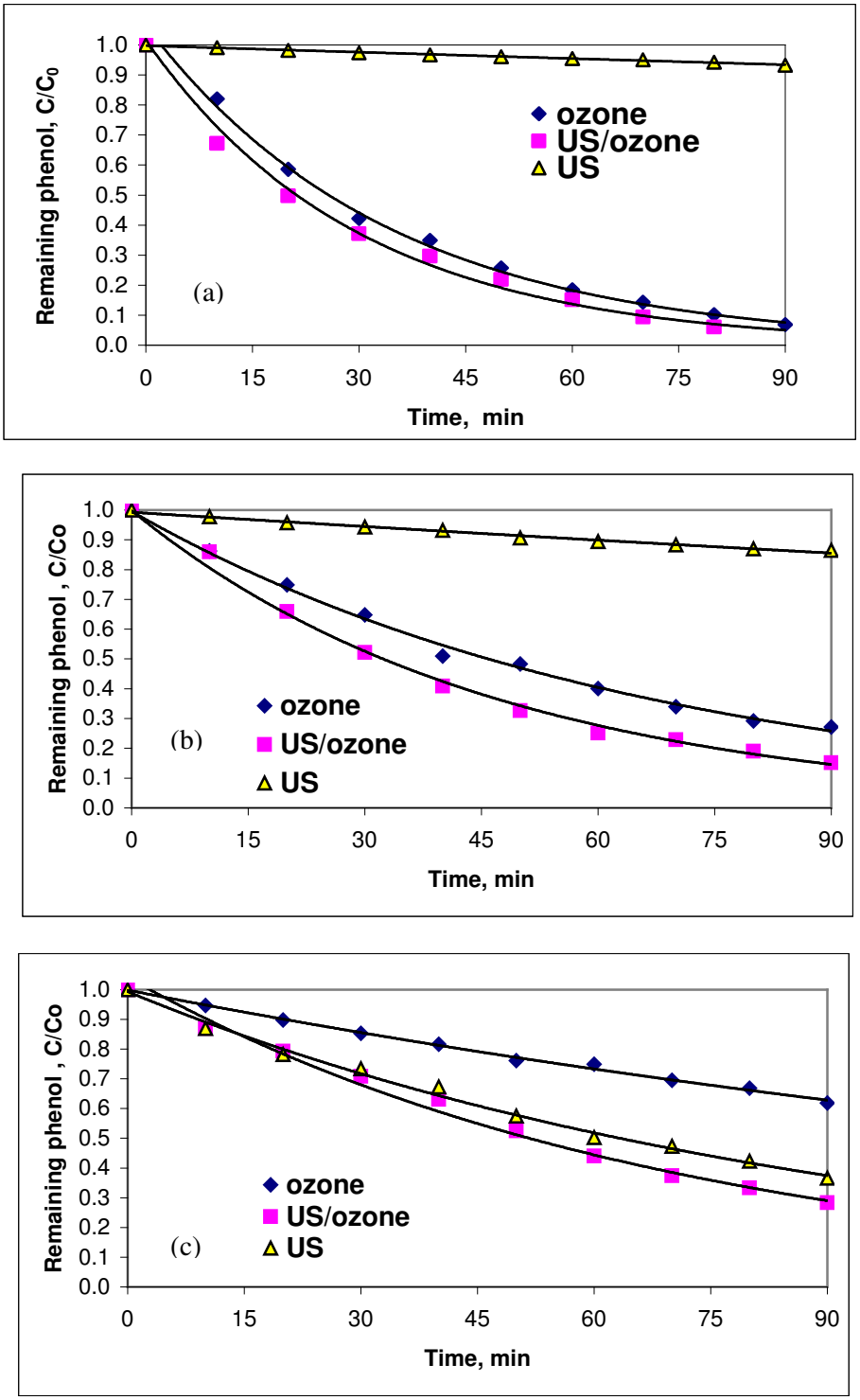

Figure 5.27. Comparative rates of phenol (C_0=2.5 mM) decay by US, Ozone and US/Ozone operations at three different pH values. (a) pH=10.0, (b) pH=5.6, (c) pH=2.0.

The negligible rate of decay by US at pH=10 is due to the formation of phenolate ion, which is much more hydrophobic than molecular phenol. This means that the probability of the anion to approach the bubble-liquid interface is very low, so that all the decomposition must take place in the bulk solution. On the other hand, O_3 is most effective at pH=10, due to its aqueous phase decomposition at alkaline solutions to yield peroxy and hydroxyl radicals. It is notable that the enhancement in the rate of degradation by combining US and O_3 is different at each pH level:

- at pH=2, the observed rate constant (2.21×10^{-2}/min) is less than the sum of individual rate constants (2.59×10^{-2}/min). This shows that the enhancement in the mass transfer rate of O_3 by ultrasound does not induce an additive effect on the rate of decay, implying the inefficiency of direct ozone reactions with phenol.

- at pH=10, we observe a synergy because the observed rate constant (3.26×10^{-2} /min) is much larger than the sum of individual constants (2.87×10^{-2}/min). Thus there are two mechanisms here: One is enhanced rate of aqueous decomposition of O_3 to result in enhanced peroxy and hydroxyl radicals in solution, and the other is excess hydroxyl radical ejection to the bulk liquid or the gas-liquid interface upon thermal decomposition of O_3 in the gas phase during bubble collapse.

- at pH=5.6, or in between 10 and 2, the effect is just additive as was expected.

5.4.3. Degradation of Phenol by Ultrasound/UV Combination

Integrating US systems with UV irradiation is expected to provide a synergy, due to the formation of excess ●OH by photolysis of US-induced hydrogen peroxide. The results of single UV, US and combined UV/US tests with phenol are presented in Figure 5.28.

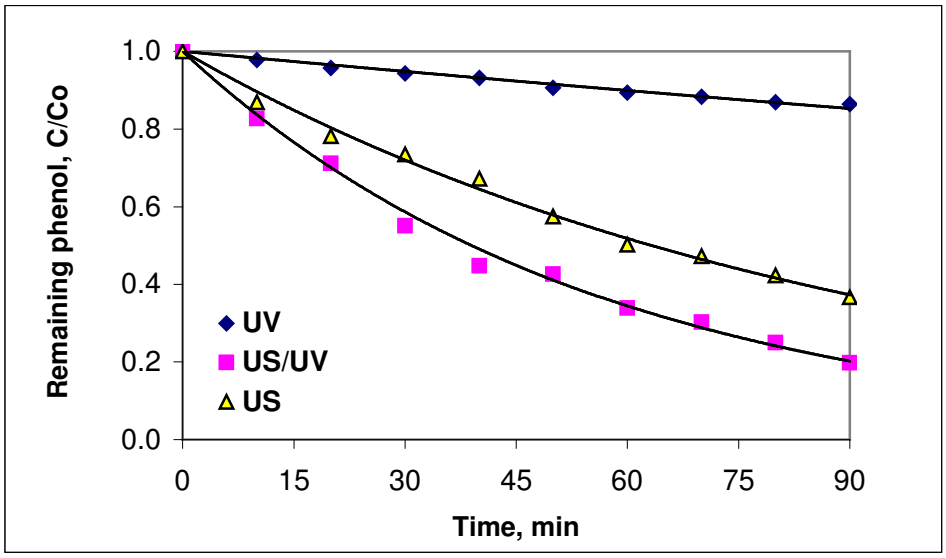

Figure 5.28. Comparative rates of phenol (C_0=2.5 mM) decay in 90 min by UV irradiation (254 nm), sonolysis (300 kHz) and US/UV operation, at pH=2.

It was found that photolytic decomposition of phenol was negligible and independent on pH (k'=0.018, 0.020 and 0.020/min at pH= 2.0, 5.6 and 10.0, respectively). On the other hand, sonolytic degradation at pH=2.0 in the presence of UV irradiation was found to be nearly twice faster than that by sonolysis alone (k'_{US} = 1.0 x 10^{-2}/min; $k'_{US/UV}$ = 1.8 x 10^{-2}/min). This is mainly due to excess hydroxyl radical generation by photolysis of ultrasound-generated H_2O_2 and partly to the possible generation of ozone above the surface of the solution by the UV lamp.

$$H_2O_2 \xrightarrow{h\nu} 2\bullet OH \qquad (5.34)$$

The concentration of H_2O_2 was monitored during 90 min sonolysis of deionized water in the presence and absence of UV irradiation to justify the above reasoning on the

production and photolysis of H_2O_2. The data are presented in Figure 5.29, where we can see that H_2O_2 accumulates during sonolysis alone, while in the presence of UV irradiation it declines after 30 min of contact, upon photolysis.

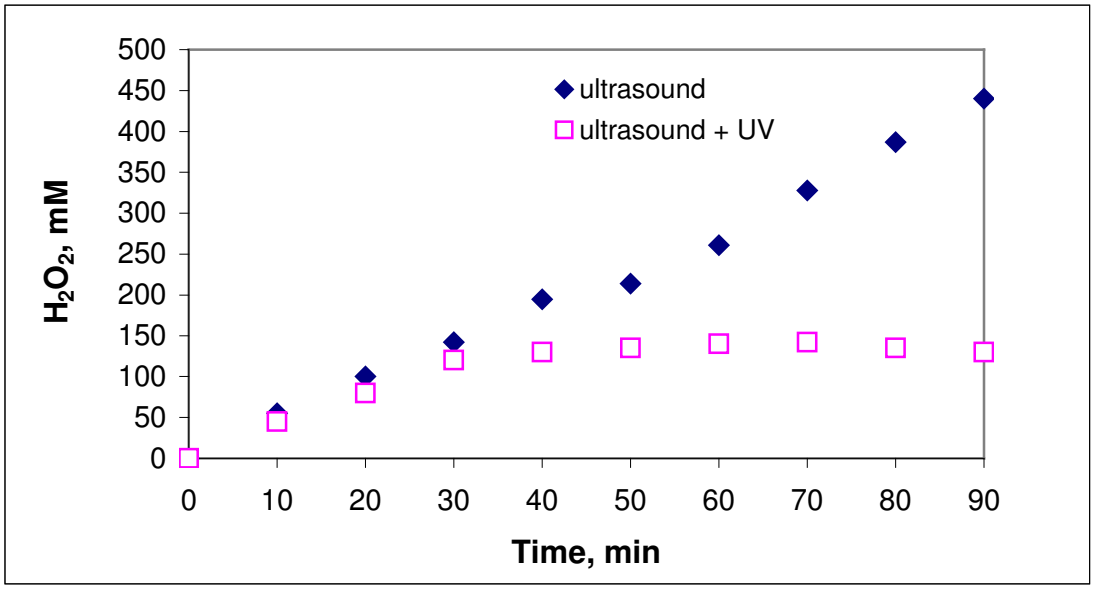

Figure 5.29. Net rate of H_2O_2 formation in sonolysis of deionized water in the presence and absence of UV irradiation.

5.4.3.1.Effect of pH. The effect of pH was investigated by running the operation at four different pH values, followed by estimating the pseudo-first order rate coefficients. The results are presented in Figure 5.30. Similar to what we observed at sonolysis alone, the rate in combined US/UV operation is decelerated by pH elevations. However, the effect was found less significant in the presence of UV than in its absence, as presented in a comparative bar chart in Figure 5.31.

It is notable that although the rate of phenol decay at pH=10 is extremely slow by sonolysis, it is 7 times faster when sonolysis is conducted with UV irradiation. As pH is lowered to 5.6 and 4.0, enhancement by UV is only 2-fold, owing to the fact that at these pH levels ultrasound is quite effective. At pH=2.0, where ultrasound had maximum efficiency, the enhancement by UV was only 0.8-fold.

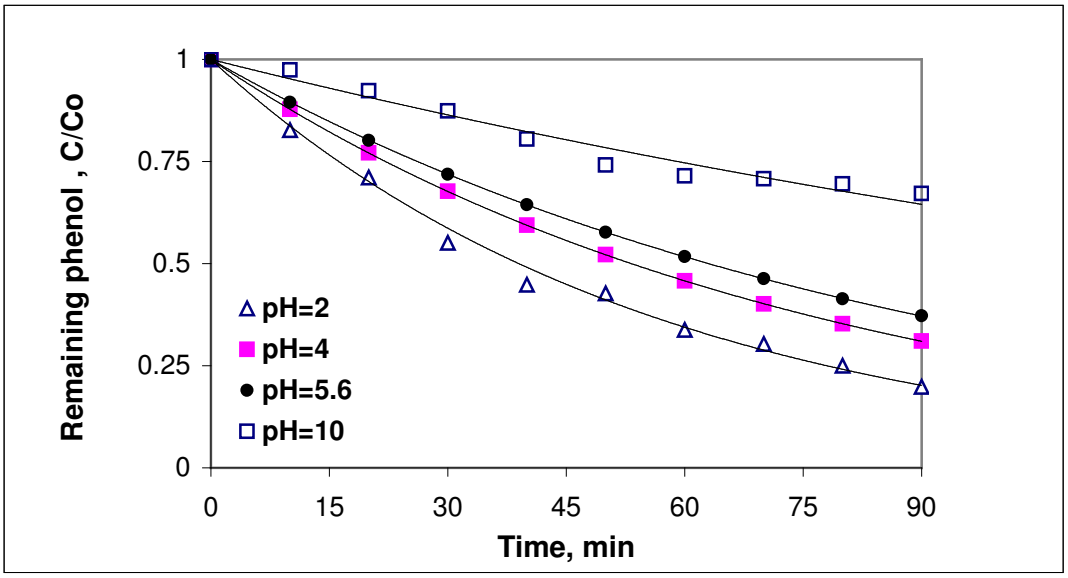

Figure 5.30. Impact of pH on the rate of phenol decay by UV/US combination.

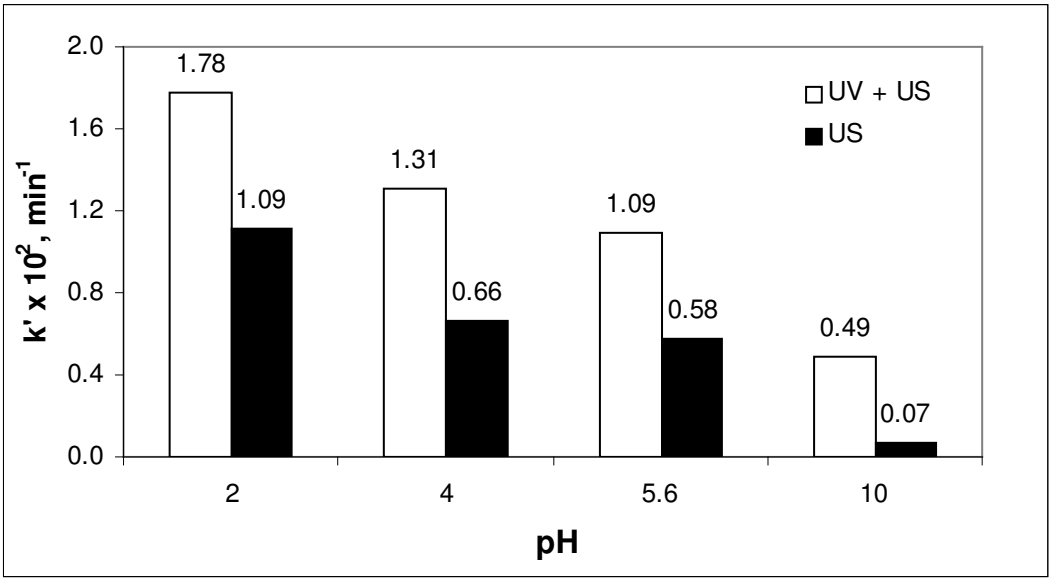

Figure 5.31. Comparative response of phenol decay coefficient k' to pH raise in US and US/UV operations.

5.4.4. Degradation of Phenol by Ultrasound/Ozone/UV Combination

Combined operation of ultrasound, ozone and UV light was the most effective system as was expected, but the effect was more positive than what we expected. For summarizing and making an overall assessment of all test systems, the decay pattern of phenol initially at 2.5 mM and exposed separately to all systems at pH=2 and pH=10 for 90 min are presented in Figure 5.32 and Figure 5.33, respectively.

.

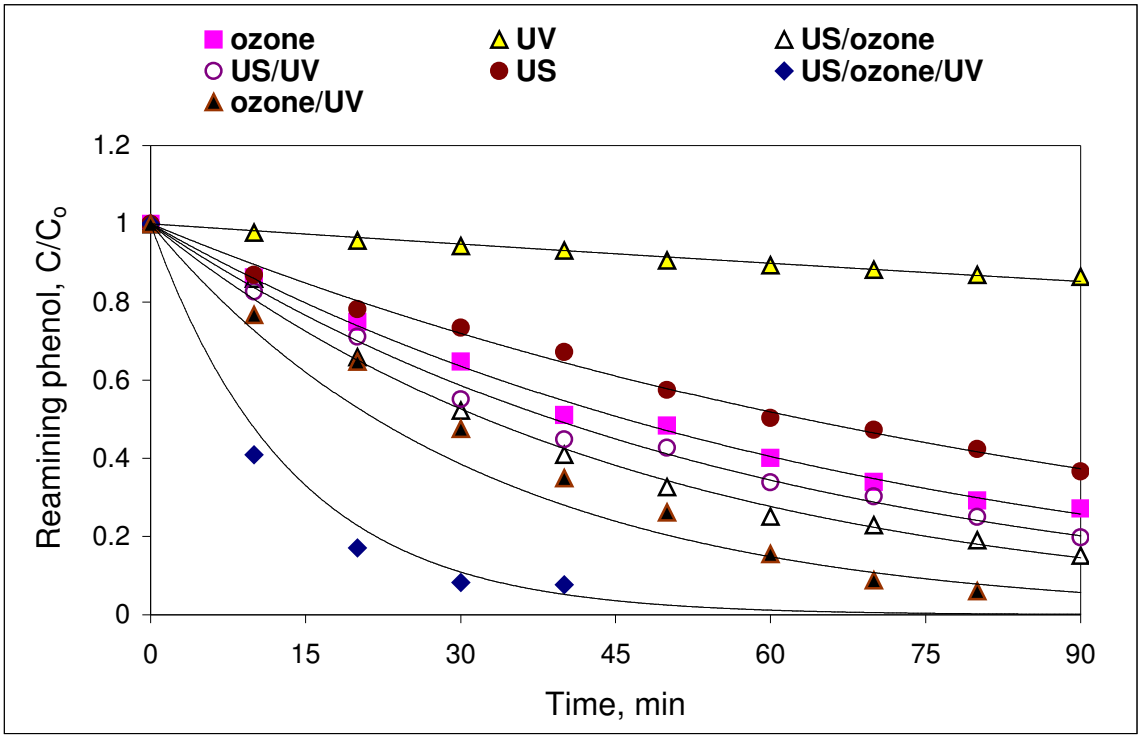

Figure 5.32. Comparative profiles of phenol degradation in the test systems at pH=2.

The estimated rate coefficients for each system are summarized in Table 5.16 for pH=2.0 and pH=10.0. As a conclusion, system efficiencies with respect to the solution pH are as follows:

pH=2.0: US /UV/ O_3 >> O_3/UV > US/O_3 >US/UV > O_3 > US>UV.

pH=10.0: US /UV/ O_3 > O_3/UV > O_3 > US/O_3 > US/UV >UV>US.

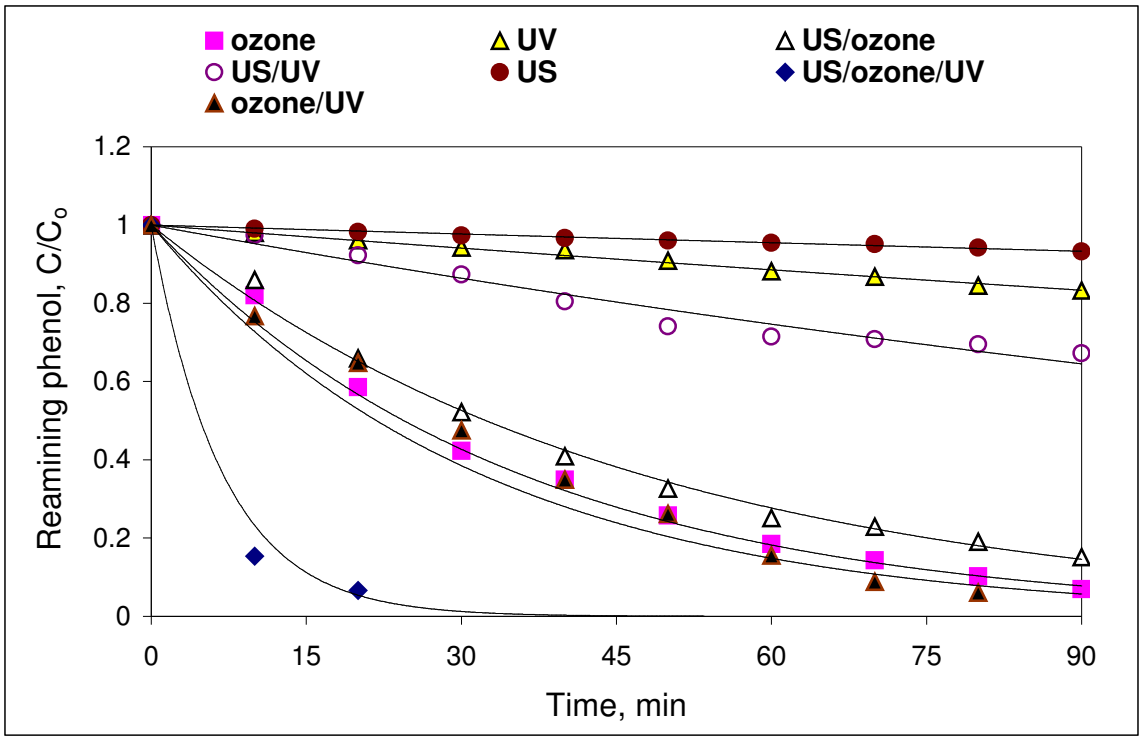

Figure 5.33. Comparative profiles of phenol degradation in the test systems at pH=10.

Table 5.16. Pseudo-first order rate coefficients of phenol (C_0=2.5 mM) degradation at pH=2.0 and pH=10.0 in single and combined systems.

	k' x 10^{-2} /min	
SYSTEM	pH=2.0	pH=10.0
UV irradiation (254 nm)	0.002 ± 0.0005	0.21 ± 6 x10^{-5}
US (300 kHz)	1.07 ± 0.03	0.08 ± 4 x10^{-5}
O_3 (2 mg/L)	1.52 ± 0.04	2.79 ± 0.08
US/UV	1.79 ± 0.05	0.50 ± 0.03
US/O_3	2.21 ± 0.06	3.26 ± 0.14
UV/O_3	2.88 ± 0.19	8.69 ± 0.54
US/UV/O_3	8.65 ± 0.32	17.93 ± 0.84

6. CONCLUDING REMARKS AND RECOMMENDATIONS FOR FUTURE WORK

The study presented herein consisted of

(1) a thorough literature survey on ultrasonic processes and their applicability to environmental decontamination;
(2) experimentation and kinetic modeling of inactivation of *E. coli* by power ultrasound at 20 kHz;
(3) investigation of ultrasonic destruction of phenol by irradiation at short (20 kHz) and medium frequency (300 kHz, 520 kHz) ultrasound to assess and optimize operating parameters. Investigation of the effects of combinations of ultrasound with ozone and UV radiation on the rate of phenol decay.

Although conclusions were presented at the end of each discussion, a summary of the key remarks are provided in the following.

Ultrasonic Disinfection. The rate of *E.coli* kill by 20 kHz ultrasound was significantly accelerated by the addition of solids in the reactor, or generation of a heterogeneous medium and the relative affectivity of the test solids was as: activated carbon>ceramic>metallic zinc. The kinetic model developed using the experimental data showed similarity to models describing chlorination kinetics, implying that the mechanism of destruction is governed by oxidation rather than mechanical effects. It was further found that catalytic effects faded with increased sonication time and/or reduced number of bacteria, to be attributed to: (i) decreased probability of bacterial contact with the solid-liquid interface; (ii) erosion of solid surfaces by vibrational effects; and (iii) reduced cavity formation due to degassing effects of ultrasound.

Ultrasonic Destruction of Phenol. The efficiency of destruction was largely dependent on the applied frequency, the relative effectiveness following the order: 300 kHz>520 kHz>20 kHz. The decomposition rate was accelerated by lowering the pH, increasing the input phenol concentration, and injecting bubbles of air into the solution. Frequency effects were

attributed to the resonating bubble size and the nature of bubble collapse in addition to the physical-chemical properties of phenol; while pH and concentration effects were related to enhanced probability of solute approach to the cavity sheath, where radical species are at maximum. More effective decomposition in the presence of air despite its lower polytrophic gas ratio was attributed to the reactions of nitrogen in ultrasonic media to produce additional radicals that participate in the oxidation process.

Combined Processes. Individual effects of ultrasound (US) and ozone (O_3) were compared with combined operations such as US/O_3, US/UV and US/UV/O_3. It was found that sonication was efficient at low pH, while ozonation required elevated pH for maximum efficiency. Combined US/O_3 operation rendered a synergy in phenol decomposition, which was attributed to: a) excess hydroxyl radicals formed upon thermal decomposition of ozone in the gas phase, and b) increased mass transfer of ozone in solution by mechanical effects of ultrasound. UV irradiation alone was found totally ineffective, while combined US/UV operation produced a synergy in the overall degradation of phenol. This was attributed to the photolysis of US-generated H_2O_2 to produce excess hydroxyl radicals in solution. The effectiveness of combined applications was in the order: (i) acidic and slightly acidic pH: US/O_3/UV>US/O_3>US/UV> O_3>US>UV; (ii) highly alkaline pH: US/O_3/UV>US/O_3>O_3> US/UV>US >UV. The larger effectiveness of O_3 than US/UV at alkaline pH (pH=10.0) was explained by the aqueous phase decomposition of ozone to HOO and OH radicals.

Suggestions and recommendations for future work may be summarized as the following:

(1) Exposure of chlorinated phenols and other phenolic compounds to the same systems to assess substituent effects.
(2) Exposure of bio-treated effluents containing phenolic residuals to assess matrix effects.
(3) Addition of solid particles in the reactors to assess catalytic effects.
(4) Development of a mathematical model to explain organic matter decay by ultrasound.
(5) Operation of pulsed sonolysis at 20 kHz and sonolysis at higher frequencies to assess the improvement in bacterial kill rates.

REFERENCES

Adewuyi, Y. G., 2001. Sonochemistry: Environmental Science and Engineering Applications, Industrial and Engineering Chemistry Research, 40, 4681-4715.

Agency for Toxic Substances and Disease Registry (ATSDR), Department of Health and Human Services, Public Health Service, 1998. Toxicological Profile for phenol, Atlanta, GA: U.S. (http://www.atsdr.cdc.gov/toxprofiles/tp115.html)

Alegria, E., Lion, Y., Kondo, T., Riesz, P., 1989. Sonolysis of Aqueous Surfactant Solutions-Probing the Interfacial Region of Cavitation Bubbles by Spin Trapping, Journal of Physical Chemistry, 93, 4908-4913.

Alnaizy, R., Akgerman, A., 2000. Advanced Oxidation of Phenolic Compounds, Advances in Environmental Research, 4, 233-244.

Amoore, E., Hautala, E., 1983. Odor as an Aid to Chemical Safety: Odor Thresholds Compared with Threshold Limit Values and Volatilities for 214 Industrial Chemicals in Air and Water Dilution, Journal of Applied Toxicology, 3, 272-290.

APHA/AWWA/WPCP, 1992. Standard Methods for the Examination of Water and Wastewater, 17th Edition, American Public Health Association, Washington DC.

Barbier, P. F., Petrier, C., 1996. Study at 20 kHz and 500 kHz of the Ultrasound- Ozone Advanced Oxidation System: 4-Nitrophenol Degradation, Journal of Advanced Oxidation Technologies, 1, 154-159.

Berlan, J., Trabelsi, F., Delmas, H., Wilhelm, A. M., Petrignani, J. F., 1994. Oxidative Degradation of Phenol in Aqueous Media Using Ultrasound, Ultrasonics Sonochemistry, 1, 97-102.

Bevilaqua, J.V., Cammarota, M.C., Freire, D.M.G., Sant'Anna Jr., G.L., 2002. Phenol Removal Through Combined Biological and Enzymatic Treatments, Brazilian Journal of Chemical Engineering, 19 (2).

Bull, R. J., Birnbaum, L. S., Cantor, K. P., Rose, J. B., Butterworth, B. E., Pegram, R., Tuomisto, J., 1995. Water Chlorination: Essential Process or Cancer Hazard?, Fundamentals of Applied Toxicology, 28(2), 155-166.

Cahn, R. P., Li, N. N., 1974. Separation Of Phenol From Waste Water by the Liquid Membrane Technique Separation, Science, 9, 505-519.

Chen, Y.C., Smirniotis, P., 2002. Enhancement of Photocatalytic Degradation of Phenol and Chlorophenols by Ultrasound, Industrial and Engineering Chemistry Research, 41, 5958-5965.

Colarusso, P., Serpone, N., 1996. Sonochemistry Effects of Ultrasound on Homogeneous Chemical Reactions and in Environmental Detoxification, Research on Chemical Intermediates, 22(1), 61-89.

Cost, M., Mills, G., Glisson, P., Lakin, J., 1993. Sonochemical Degradation of p-Nitrophenol in the Presence of Chemical Components in Natural Waters, Chemosphere, 27, 1737-1743.

Crum, L. A., 1994. Sonoluminescence, Sonochemistry and Sonophysics, Journal of the Acoustical Society of America, 95, 559-562.

Dahlem, O., Demaiffe, V., Halloin, V., Reisse, J., 1998. Direct Sonication System Suitable for Medium-Scale Sonochemical Reactors, American Institute of Chemical Engineers Journal, 44, 2724-2730.

David, L., Sedlak, A., Andren, W., 1991. Oxidation of Chlorobenzene with Fenton's Reagent, Environmental Science and Technology, 25, 777-782.

de Visscher, A., van Langenhove, H., 1998. Sonochemistry of Organic Compounds in Homogeneous Aqueous Oxidising Systems, Ultrasonics Sonochemistry, 5, 87-92.

Drijvers, D., van Langenhove, H., Beckers, M., 1999. Decomposition of Phenol and Trichloroethylene by the Ultrasound/H_2O_2/CuO Process, Water Research, 33(5), 1187-1194.

Entezari, M. H., Petrier, C., Devidal, P., 2003. Sonochemical Degradation of Phenol in Water: A Comparison of Classical Equipment With a New Cylindrical Reactor, Ultrasonics Sonochemistry, 10, 103-108.

Entezari, M. H., Petrier, C., 2005. A Combination of Ultrasound and Oxidative Enzyme: Sono-enzyme Degradation of Phenols in a Mixture, Ultrasonics Sonochemistry, 12, 283-288.

Espuglas, S., Yue, P.L., Perez, M.I., 1994. Degradation of 4-chlorophenol by Photolytic Oxidation, Water Research, 28, 1323-1328.

Fischer, C. H., Hart, E. J., Henglein, A., 1986. Ultrasonic Irradiation of Water in the Presence of Oxygen 18, $^{18}O_2$: Isotope Exchange and Isotopic Distribution of Hydrogen Peroxide, Journal of Physical Chemistry, 90, 1954-1956.

Glaze, W.H., Peyton, G. R., Lins, S., Huang, F. Y., Burleson, J. L., 1982. Destruction of Pollutants in Water with Ozone in Combination with Ultraviolet Radiation, Environmental Science and Technology, 16, 454-461.

Glaze, W. H., Kang, J. W., Chapin, D. H., 1987. The Chemistry of Water Treatment Processes involving Ozone, Hydrogen Peroxide and Ultraviolet Radiation, Ozone Science and Engineering., 9, 335-352.

Gogate, P. R., 2003. Sonochemical Reactors for Waste Water Treatment: Comparison Using Formic Acid Degradation As a Model Reaction, Advances in Environmental Research, 7, 283-299.

Gogate, P. R., Pandit, A. B., 2004. A Review of Imperative Technologies for Wastewater Treatment I: Oxidation Technologies at Ambient Conditions, Advances in Environmental Research, 8, 501-551.

Graham, E., Hedges, M., Leeman, S., Vaughan, P., 1980. Cavitational Bio-effects at 1.5 MHz, Ultrasonics, 18, 224-228.

Gurol, M. D., Vatistas, R., 1987. Oxidation of Phenolic Compounds by Ozone and Ozone-UV Radiation: A Comparative Study, Water Research, 21, 895-900.

Hart, E.J., Henglein, A., 1985. Free Radical and Free Atom Reactions in the Sonolysis of Aqueous Iodide and Formate Solutions, Journal of Physical Chemistry, 89 (20),4342-4347.

Hau, H., Chen, Y., Wu, M., Wang, M., Yin, Y., Lü, Z., 2004. Sonochemistry of Degrading p-Chlorophenol in Water by High Frequency Ultrasound, Ultrasonics Sonochemistry, 11, 43-46.

Henglein, A., 1987. Sonochemistry: Historical Developments and Modern Aspects, Ultrasonics, 25(1), 6-16.

Hoffmann, M. R., Martin, S. T., Choi, W., Bahnemann, D. W., 1995. Environmental Applications of Semiconductor Photocatalysis, Chemical Review, 95, 69-96.

Hua, I., Höchemer, R. H., Hoffmann, M. R., 1995. Sonolytic Hydrolysis of p-Nitrophenyl Acetate: The Role of Supercritical Water, Journal of Physical Chemistry, 99, 2335-2342.

Hua, I., Hoffmann, M. R., 1997. Optimization of Ultrasonic Irradiation as an Advanced Oxidation Technology, Environmental Science and Technology, 31, 2237-2243.

Hua I., Thompson, J.E., 2000. Inactivation of Escherichia Coli by Sonication at Discrete Ultrasonic Frequencies, Water Research, Volume 34, 15, 3888-3893.

Hung, H. M., Hoffmann, M. R., 1998. Kinetics and Mechanisms of the Enhanced Reductive Degradation of CCl_4 by Elemental Iron in the Presence of Ultrasound, Environmental Science and Technology, 32, 3011-3016.

Ince, N. H., 1998. Light-enhanced Chemical Oxidation for Tertiary Treatment of Municipal Landfill Leachate, Water Environment Research, 70, 1161-1169.

Ince, N. H., Tezcanli, G., 2001. Reactive Dyestuff Degradation by Combined Sonolysis and Ozonation, Dyes and Pigments, 49, 145-153.

Ince, N.H., Tezcanli, G., Belen, R.K., Apikyan, I.G., 2001. Ultrasound as a Catalyzer of Aqueous Reaction Systems: the State of the Art and Environmental Applications, Applied Catalysis B: Environmental, 29, 167-176.

Kang, J. W., Hoffmann, M. R., 1998. Kinetics and Mechanisms of the Sonolytic Destruction of Methyl-tert-Buthyl Ether by Ultrasonic Irradiation in the Presence of Ozone, Environmental Science and Technology, 32(20), 3194-3199.

Kim, J. H., Oh, K. K., Lee, S. T., Kim, S. W., Hong, S. I., 2002. Biodegradation of Phenol and Chlorophenols with Defined Mixed Culture in Shake-Flasks and a Packed Bed Reactor, Process Biochemistry, 37, 1367-1373.

Klassen, N. V., Marchington, D., McGowan, H. C. E., 1994. H_2O_2 Determination by the I_3^- Method and by the $KMnO_4$ Titration, Analytical Chemistry, 66, 2921-2925.

Kotronarou, A., Mills, G., Hoffmann, M. R., 1991. Ultrasonic Irradiation of p-Nitrophenol in Aqueous Solution, Journal of Physical Chemistry, 95, 3630-3638.

Ku, Y., Chen, K. Y., Lee, K. K., 1997. Ultrasonic Destruction of 2-Chlorophenol in Aqueous Solution, Water Research, 31, 929-935.

Kumar, S., Upadhyay, S. N., Upadhyay, D., 1987. Removal of Phenols by Adsorption on Fly Ash, Journal of Chemical Technology and Biotechnology, 37, 281-290

Lazarova, V., Savoye, P., Janex, M. L., Blatchley, E. R. III., Pommepuy, M., 1999. Advanced Wastewater Disinfection Technologies: State of the Art and Perspectives, Water Science and Technology, 40, 203-213.

Leighton, T. G., 1994. The Acoustic Bubble, Academic Press, Harcourt Brace & Company, London.

Legrini, O., Oliveros, E., Braun, A. M., 1993. Photochemical Processes for Water Treatment, Chemical Review, 93, 671-698.

Lepoint, T., Mullie, F., 1994. What Exactly is a Cavitation Chemistry, Ultrasonics Sonochemistry, 1, 13-22.

Lin, J. G. and Ma, Y. S., 1999. Magnitude of Effect of Reaction Parameters on 2-chlorophenol Decomposition by Ultrasonic Process, Journal of Hazardous Materials, 66, 291-305.

Makino, K., Mossoba, M. M., Riesz, P., 1982. Chemical Effects of Ultrasound on Aqueous Solutions, Journal of American Chemistry Society, 104 (12), 3537-3539.

Margulis, M., 1995. Sonochemistry and Cavitation; OPA (Amsterdam) B. V. Gordon and Breach Science Publ.: New York.

Margulis, M. A., Margulis, I. M., 2003. Calorimetric Method for Measurement of Acoustic Power Absorbed in a Volume of a Liquid, Ultrasonics Sonochemistry, 10 , 343-345.

Mason, T. J., Lorimer, J. P., Walton, D. J., 1990. Sonoelectrochemisry, Ultrasonics, 28, 333-337.

Mason, T. J., Lorimer, J. P., Bates, D. M., Zhao, Y., 1994. Dosimetry in Sonochemistry: The Use of Aqueous Terephthalate Ion as a Fluorescence Monitor, Ultrasonics Sonochemistry, 1(2), 91-95.

Mason, T. J., Cordemans, E. D., 1998. Practical Consideration for Process Optimization, J. L. Luche (Ed), Synthetic Organic Sonochemistry, 301-331, Plenum Press, New York.

Mason, T. J., 1999. Sonochemistry, Oxford University Press Inc., New York.

Meulemans, C. C. E., 1987. Basic Principles of UV-Disinfection of Water, Ozone Science and Engineering, 9, 299-314, 1987.

Microbics Co., 1992. Microtox Manual, Carlsbad, CA.

Morris, J. C., 1975. The Chemistry of Aqueous Chlorine in Relation to Water Chlorination, Proceedings of the Conference on the Environmental Impact of Water Chlorination, Oak Ridge, Tennessee, 6-8 October 1975, 1, 27-41.

Naffrechoux, E., Chanoux, S., Petrier, C., Suptil, J., 2000. Sonochemical and Photochemical Oxidation of Organic Matter, Ultrasonics Sonochemistry, 7, 255-259.

Nagata, Y., Nakagawa, M., Okuno, H., Mizukoshi, Y., Yim, B., Maeda, Y., 2000. Sonochemical Degradation of Chlorophenols in Water , Ultrasonics Sonochemistry 7, 115-120.

Negishi, K., 1961. Experimental Studies on Sonoluminescence and Ultrasonic Cavitation, Journal of Physical Society of Japan, 16, 1450-1454.

Neppiras, E. A., 1980. Acoustic Cavitation Thresholds and Cyclic Processes, Ultrasonics, 18, 201-209.

Noltingk, B. E., Neppiras, E. A., 1950. Cavitation Induced by Ultrasonics, Proceedings of Physical Society, B63, 674-678.

O'Shea, K. E., Kalen, D. V., Cooper, W. J., Garcia, I., Aguilar, M., 1998. Degradation of Chemical Warfare Agent Stimulants in Aqueous Solutions by Cobalt-60 Gamma

Irradiation: Similarities with TiO_2 Photocatalysis. In Environmental Applications of Ionizing Radiation, W. J. Cooper, R. D. Curry, K. E. O'Shea (Eds), John Wiley & Sons, Inc., New York.

Papadaki, M., Emery, R. J., Abu-Hassan, M. A., Bustos, A. D., Metcalfe, I. S., Mantzavinos, D., 2004. Sonocatalytic Oxidation Processes for the Removal of Contaminants Containing Aromatic Rings from Aqueous Effluents, Separation Purification Technologies, 34, 35-42.

Pelczar, M. J., Jr, Chan, E. C. S., Microbiology, 5th Ed., Mc. Graw-Hill, New York, 1986.

Peller, J., Wiest, O., Kamat, P. V., 2001. Sonolysis of 2,4-Dichlorophenoxyacetic Acid in Aqueous Solutions. Evidence for •OH-Radical-Mediated Degradation , Journal of Physical Chemistry A, 105 (13), 3176 –3181.

Petrier, C., Micolle, M., Merlin, G., Luche, J. L., Reverdy, G., 1992. Characteristics of Pentachlorophenate Degradation in Aqueous Solution by Means of Ultrasound, Environmental Science and Technology, 26 (8), 1639-1642.

Petrier, C., Lamy, M. F., Francony, A., Benahcene, A., David, B., 1994. Sonochemical Degradation of Phenol in Dilute Aqueous Solutions: Comparison of the Reaction Rates at 20 and 487 kHz, Journal of Physical Chemistry, 98, 10514-10520.

Petrier, C., Francony, A., 1997. Ultrasonic Waste-Water Treatment: Incidence of Ultrasonic Frequency on the Rate of Phenol and Carbon Tetrachloride Degradation, Ultrasonics Sonochemistry. 4, 295-300.

Petrier, C., Jiang, Y., Lamy, M. F., 1998. Ultrasound and Environment: Sonochemical Destruction of Chloroaromatic Derivatives, Environmental Science and Technology, 32, 1316-1318.

Petrier, C., Casadonte, D., 2001. The Sonochemical Degradation of Aromatic and Chloroaromatic Contaminants, Advances in Sonochemistry, 6, 91-109.

Phull, S. S., Newman, A. P., Lorimer, J. P., Pollet, B., Mason,T. J., 1997. The Development and Evaluation of Ultrasound in the Biocidal Treatment of Water, Ultrasonics Sonochemistry, 4, 157-164.

Plewa , M. J., Wagner, E. D., Jazwirska, P.E., Richardson, S., Chen P., Bruckemcauge, A., 2004. Halonitromethane Drinking Water Disinfection By-products: Chemical Characterization and Mammalian Cell Cytotoxicity and Genotoxicity, Environmental Science and Technology, 38, 62-68.

Popov, P., Getoff, N., Grodkowski, J., Zimek, Z., Chmilevski, A. G., 2004. Steady-State Radiolysis and Product Analysis of Aqueous Diphenyloxide in the Presence of Air and N_2O, Radiation Physics and Chemistry, 69, 39-44.

Prado, J., Arantegui, J., Chamarro, E., Esplugas, S., 1994. Degradation of 2,4-D by Ozone and Light. Ozone Science and Engineering, 16, 235-245.

Qualls, R. D., Johnson, J. D., 1983. Bioassay and Dose Measurement in UV Disinfection, Applied Environmental Microbiology, 45, 872–877.

Reisse, J., 1995. Measurements of Gas Bubble Sizes Using High Frequency Ultrasound Imaging, Proceedings of the 15th International Congress on Acoustics, Trondheim, Norway, August 1995, 5, 409-412.

Riesz, P., Kondo, T., Krishna, C. M., 1990. Sonochemistry of Volatile and Nonvolatile Solutes in Aqueous Solutions, Ultrasonics, 28 (5), 295-303.

Riesz, P., Mason T. J. (Eds), 1991. Advances in Sonochemistry, JAI Press London Vol. 2, 23.

Rivas, F. J., Kolaczkowski, S. T., Beltran , F. J., McLurgh, D. B., 1995. Hydrogen peroxide Promoted Wet Air Oxidation of Phenol: Influence of Operating Conditions and

Homogeneous Metal Catalysts, Journal of Chemical Technology and Biotechnology, 74, 390-398.

Rothmann, N., Bechtold, W. E., Yin, S. N., Dosemeci, M., Li, G. L., Wang, Y. Z., Griffith, W. C., Smith, M. T., Hayes, R. B., 1998. Urinary Excretion of Phenol, Catechol, Hydroquinone, and Muconic Acid by Workers Occupationally Exposed to Benzene, Occupational Environmental Medication, 55, 705-711.

Ruppert, G., Bauer, R., Heisler, G., 1993. The Photo-Fenton Reaction-An Effective Photochemical Wastewater Treatment Process, Journal of Photochemistry and Photobiology A-Chemistry, 73, 75-78.

Sambrook, J., Fritsch, E. F., Maniatis, T., 1989. Molecular Cloning: A Laboratory Manual, 2nd Edition, Cold Spring Harbor, N.Y.

Scherb, G., Weigel, R., and O'Brien, W. D., 1991. Use of High Intensity Ultrasound for Disinfection, Applied and Environmental Microbiology, 57, 2079-2082.

Schuets, M. N., Vroom, D. A., 1998. The Use of High Power, Low-Energy Electron Beams for Environmental Remediation. In Environmental Applications of Ionizing Radiation, W. J. Cooper, R. D. Curry, K. E. O'Shea (Eds), John Wiley & Sons, Inc., New York..

Seghal, C., Yu, T. J., Sutherland, R. G., Verrall, R., 1982. Use of 2,2-Diphenyl-1-picrylhydrazyl to Investigate the Chemical Behavior of Free Radicals Induced by Ultrasonic Cavitation, Journal of Physical Chemistry, 86, 2982- 2986.

Serpone, N., Terzian, R., Colarusso, P., Minero, C.,1992. Sonochemical Oxidation of Phenol and Three of its Intermediate Products in Aqueous Media: Catechol Hydroquinone, and Benzoquinone, Kinetic and Mechanistic Aspects, Research on Chemical Intermediates, 18, 183–202.

Serpone, N., Terzian, R., Hidaka, H., Pelizetti, E., 1994. Ultrasonic Induced Dehalogenation and Oxidation of 2-, 3-, and 4-Chlorophenol in Air-Equilibrated Aqueous Media. Similarities with Irradiated Semiconductor Particulates**,** Journal of Physical Chemistry, 98, 2634-2640.

Singh, N. P., Graham, M. M., Singh, V., Khan, A. 1995. Induction of DNA Single-strand Breaks in Human Lymphocytes by Low Doses of ?-rays, International Journal of Radiation Biology, 68, 563 – 569.

Staehelin, J., Hoigne, J., 1982. Decomposition of Ozone in Water: Rate of Initiation by Hydroxide Ions and Hydrogen Peroxide, Environmental Science and Technology, 16, 676-681.

Suslick, K. S., Hammerton, D. A., Cline, Jr., R. E., 1986. Sonochemical Hot Spot, Journal of American Chemical Society, 108, 5641-5642.

Suslick, K. S., 1990. Sonochemistry, Science, 247, 1439-1445.

Suslick, K. S., 1994. The Chemistry of Ultrasound, http://www.scs.uiuc.edu//~suslick/britannica.html.

Tauber, A., Schuchmann, H. P., von Sonntag, C., 2000. Sonolysis of Aqueous 4-Nitrophenol at Low and High pH, Ultrasonics Sonochemistry, 7, 45-52.

Teo, K. C., Xu, Y., Yang, C., 2001. Sonochemical Degradation for Toxic Halogenated Organic Compounds, Ultrasonics Sonochemistry, 8, 241-246.

Tezcanli, G., 1998. Reuse of Textile Dyebaths by Treatment with Advanced Oxidation, M.S. Thesis, Bogazici University.

Tiehm, A., Neis, U., 2005. Ultrasonic Dehalogenation and Toxicity Reduction of Trichlorophenol, Ultrasonics Sonochemistry, 12, 121-125.

Thompson, J. A., Blatchley, E. R., 2000. Gamma irradiation for inactivation of C. parvum, E. coli, and Coliphage MS-2, Journal of Environmental Engineering, 126, 761-768

Tukac, V., Hanuka, J., 1995. Purification of Phenolic Waste Waters by Catalytic Oxidation, Collection of Czechoslovak Chemical Communications, 60, 482-488.

U.S. Environmental Protection Agency, Semivolatile Organic Compounds by Gas Chromatography / Mass Spectrometry (GC/MS) Method 8270D. www.epa.gov/SW-846/pdfs/8270d.pdf. (accessed January 2005a).

U.S. Environmental Protection Agency, Appendix A to Part 136 Methods for Organic Chemical Analysis of Municipal and Industrial Wastewater Method 604 -Phenols, www.epa.gov/waterscience/methods/guide/604.pdf. (accessed January 2005b).

Ullerstam, M., Langer, S., Ljunstrom, E., 2000. Gas Phase Rate Coefficients and Activation Energies for the Reaction of Butanal and 2-methyl-propane with Nitrate Radicals, International Journal of Chemical Kinetics, 32, 294-303.

Vinodgopal, K., Kamat, P. V., 1998. Hydroxyl-Radical-Mediated Oxidation: A Common Pathway in the Photocatalytic, Radiolytic and Sonolytic Degradation of Textile Dyes. In Environmental Applications of Ionizing Radiation, W. J. Cooper, R. D. Curry, E. O'Shea (Eds), John Wiley and Sons Inc., New York.

Weavers, L. K., Ling, F. H., Hoffmann, M. R., 1998. Aromatic Compound Degradation in Water Using a Combination of Sonolysis and Ozonolysis, Environmental Science and Technology, 32, 2727-2733.

Wegelin, M., Canonica, S., Mechsner, K., Fleischmann, T., Pesaro, F., Metzler, A., 1994. Solar Water Disinfection: Scope of the Process and Analysis of Radiation Experiments, Aqua, 43, 154-169.

Weir, B. A., Sundstrom, D. W., 1993. Destruction of Trichloroethylene by UV Light Catalysed Oxidation with Hydrogen Peroxide, Chemosphere, 27, 1279-1291.

Weissler, A., Cooper, H. W., Snyder, S., 1950. Chemical Effect of Ultrasonic Waves: Oxidation of Potassium Iodine Solution by Carbon Tetrachloride, Journal of American Chemical Society, 72, 1769-1772.

Wolfe, R. L., Ward, N. R., Olson, B. H., 1984. Inorganic Chloramines as Drinking Water Disinfectants: A Review, Journal of American Water Works Association, 76, 74-88.

Wu, C., Liu, X., Wei, D., Fan, J., Wang, L., 2001. Photosonochemical Degradation of Phenol in Water, Water Research, 35, 3927-3933.

APPENDIX A

CALIBRATION CURVES FOR THE ANALYTICAL METHODS

A.1. Calibration curve of phenol for spectrophotometric analysis

A calibration curve was prepared by aminoantipyrine method and all the samples were analysed for phenol concentration using this calibration curve (Figure A.1).

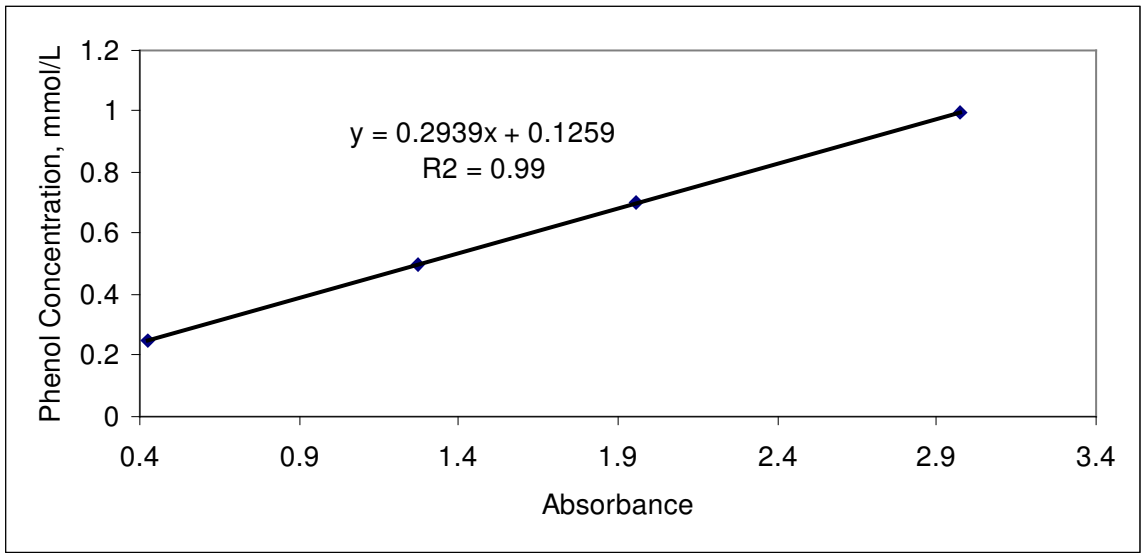

Figure A.1. Calibration curve of phenol for spectrophotometric analysis

A.2. Calibration curve of phenol for GC analysis

A series of phenol solutions were injected to the GC, to achieve a calibration curve and it was utilized for the quantification of phenol as presented in Table A.1 and Figure A.2.

Table A.1. Detected peak heights and areas for the injected phenol solutions with concentrations between 5-200 mg/L during calibration of Gas Chromatograph.

Phenol Concentration, mg/L	Phenol Concentration, mM	Retention Time, min	Peak Area, pA.sec
5	0.053	8.496	67.50572
10	0.106	8.501	144.92491
20	0.213	8.504	290.60361
50	0.530	8.512	711.03174
100	1.064	8.529	1439.97827
150	1.596	8.544	2187.43823
200	2.128	8.558	2864.46045

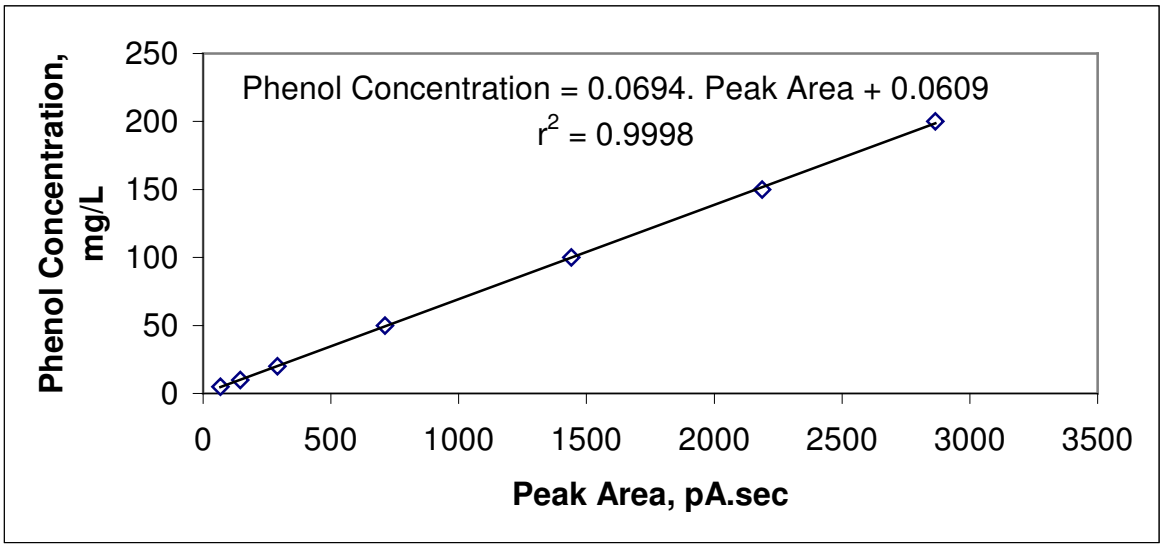

Figure A.2. Calibration curve of phenol for GC analysis